

**DESIGN AND PRODUCTION OF LIGHT-WEIGHT  
PRESSURE RESISTANT COMPOSITE TANK  
MATERIALS AND SYSTEMS FOR HYDROGEN  
STORAGE**

A Thesis Submitted to  
the Graduate School of Engineering and Sciences of  
İzmir Institute of Technology  
in Partial Fulfillment of the Requirements for the Degree of  
**DOCTOR OF PHILOSOPHY**  
**in Mechanical Engineering**

by  
**Osman KARTAV**

**July 2020**  
**İZMİR**

## **ACKNOWLEDGMENTS**

First of all, I would like to express my sincere gratitude to my supervisor and mentor Prof. Dr. Metin TANOĞLU not only for his tremendous academic support, patience, and motivation but also for giving me so many significant opportunities during my thesis. I feel honored to be supervised by him.

I would like to thank Assoc. Prof. Dr. H. Seçil ARTEM, she is also one of my PhD thesis committee members, for her guidance, support, and encouragement during my education life, our project, and my thesis. Her support and kindness are greatly appreciated. Also, another PhD thesis committee members Assoc. Prof. Dr. Engin AKTAŞ for his useful comments, guidance, support, encouragement, and motivation.

I am really thankful to my friend and labmates Serkan KANGAL, Yusuf Can UZ Mehmet Deniz GÜNEŞ, Bertan BEYLERGİL, Mustafa AYDIN, Seçkin MARTİN, Hikmet Sinan ÜSTÜN, Hatice SANDALLI, Ceren TÜRKDOĞAN, Gözde ESENOĞLU, Zeynep AY, Mehmet Ziya OKUR.

I would like to thank my wife Ezgi ABATAY KARTAV, for her support, continuous advice, motivation, and love in all my life and believing in me.

Lastly, I offer my sincere thanks to parents Kadriye and Hüseyin KARTAV and my sister and her husband Hilal and Uğur ÇİZMECİOĞLU for their love, motivation, and support during my study.

Besides, this dissertation was supported by TÜBİTAK via project number 215M182.

## ABSTRACT

### DESIGN AND PRODUCTION OF LIGHT-WEIGHT PRESSURE RESISTANT COMPOSITE TANK MATERIALS AND SYSTEMS FOR HYDROGEN STORAGE

This thesis focuses on the development of high-pressure resistant composite tanks for hydrogen storage. For this aim, composite tanks with aluminum liners were designed and manufactured by filament winding technique with various lay-up configurations and tested. The main objective of this study was to develop composite tanks with 700 bar working pressure and 1400 bar burst pressure. Furthermore, composite doily layers were incorporated into the filament winding technique and inserted at the front and end dome sections of the composite tanks to improve the burst pressure performance of the composite tanks and to develop the manufacturing process. Before the manufacturing process, the winding simulations were completed using CADWIND™ CAM software. The manufactured composite tanks were hydrostatically loaded with increasing internal pressure up to the burst pressure. During loading, the deformations over the composite tanks and liners were measured locally using strain gauges. Besides, composite plates were manufactured by filament winding technique to determine the mechanical and the thermo-mechanical properties, and the fiber mass fractions of composite sections were determined. Additionally, a preliminary study was carried out to investigate the effect of hybrid fiber usage on the burst pressure performance of steel liner based composite tanks. The effect of filament winding parameters on the burst pressure performance of composite tanks was investigated experimentally.

The aimed burst pressure value of more than 1400 bar was obtained in this study for aluminum liner-based carbon fiber reinforced composite tanks. Also, a desired safe burst mode that is expected to occur in the mid-region of the composite tanks was successfully obtained. This study may be useful for the development of composite tanks for high-pressure hydrogen storage especially for the automotive industry and can be helpful to decrease the usage of fossil fuels.

## ÖZET

### HİDROJEN DEPOLANMASI AMAÇLI YÜKSEK BASINCA DAYANIKLI HAFİF KOMPOZİT TANK MALZEMELERİNİN VE SİSTEMLERİNİN TASARLANMASI VE ÜRETİMİ

Bu tez, hidrojen depolanması amaçlı yüksek basınçda dayanıklı kompozit tankların geliştirilmesine odaklanmaktadır. Bu amaçla, aluminyum iç gömleğe sahip kompozit tanklar tasarlanmış ve çeşitli katman dizilimleri ile filament sarma yöntemi ile üretilmiş ve test edilmiştir. Bu çalışmanın ana amacı, 700 bar çalışma basıncına ve 1400 bar patlama basıncına sahip kompozit tankların geliştirmesidir. Üstelik, kompozit tankların patlama basıncı performansını iyileştirmek ve üretim yöntemini geliştirmek için kompozit takviye tabakaları filament sarma tekniğine dahil edilerek ön ve arka dom kısımlarına yerleştirilmiştir. Üretim prosesinden önce, sarım simülasyonları CADWIND™ CAM yazılımı kullanılarak tamamlanmıştır. Üretilen kompozit tanklara, patlama basıncı noktasına kadar artan hidrostatik yük uygulanmıştır. Yükleme sırasında kompozit tanklarda ve iç gömleklerde oluşan lokal deformasyonlar gerinim pulları kullanılarak ölçülmüştür. Ayrıca, kompozit kısmın mekanik ve termo-mekanik özelliklerini ve fiber ağırlık oranını belirlemek için filament sarma yöntemi ile kompozit plakalar üretilmiştir. Ek olarak, hibrit fiber kullanımının çelik iç gömleğe sahip kompozit tankların patlama basıncı performansına olan etkisinin incelenmesi için bir ön çalışma gerçekleştirilmiştir. Filament sarma parametrelerinin kompozit tankların patlama basıncına olan etkileri deneySEL olarak incelenmiştir.

Bu çalışmada aluminyum iç gömlek esaslı karbon fiber takviyeli kompozit tanklar için hedeflenen 1400 bar üstü patlama basıncı elde edilmiştir. Ayrıca kompozit tankların orta bölgesinde olması gereken güvenli patlama moduna istenilen şekilde başarıyla ulaşılmıştır. Bu çalışma, özellikle otomotiv endüstrisi için yüksek basınç hidrojen depolama amaçlı kompozit tankların gelişimde ve katı yakıt kullanımının azaltılmasında yararlı olabilir.

# TABLE OF CONTENTS

LIST OF FIGURES.....	vii
LIST OF TABLES .....	vii
CHAPTER 1. INTRODUCTION .....	1
1.1. Introduction .....	1
1.2. Aim of the Study.....	3
1.3. Novelty of the Thesis .....	4
1.4. Thesis Outline.....	5
CHAPTER 2. BACKGROUND AND LITERATURE SURVEY.....	7
2.1. Composite Materials .....	7
2.1.1. Definition of Composite Materials.....	7
2.1.2. Classification of Composite Materials .....	8
2.1.3. Manufacturing Techniques for FRP Composites .....	10
2.1.4. Applications of Composite Materials.....	15
2.2. Hydrogen .....	19
2.2.1. Hydrogen as an alternative energy carrier.....	19
2.2.2. Hydrogen Storage Techniques.....	21
2.3. Composite High-Pressure Tanks .....	23
2.3.1. Applications of Composite Tanks.....	23
2.3.2. Classification of Composite Tanks .....	24
2.3.3. Manufacturing of Composite Tanks by Filament Winding Technique.....	25
2.3.4. Performance of Composite Tanks.....	27
CHAPTER 3 EXPERIMENTAL.....	46
3.1. Materials.....	46
3.2. Determining the Mechanical Properties of Composite Section and Liner .....	48
3.3. Determining the Fiber Mass Fractions of Composite Sections .....	50
3.4. Determining the Thermomechanical Properties of Composite Sections.....	52
3.5. Filament Winding Simulations.....	52
3.5.1. Mandrel Definitions .....	53
3.5.2. Winding Parameters Definitions.....	54
3.5.2.1. Winding Parameters Definitions for Steel Composite Tanks ...	54

3.5.2.2. Winding Parameters Definitions for Al Based Composite Tanks .....	58
3.6. Manufacturing of Composite Tanks .....	60
3.6.1. Manufacturing of Steel based Composite Tanks .....	63
3.6.2. Manufacturing of Al based Composite Tanks .....	66
3.7. Burst Pressure Testing.....	71
3.7.1. Burst Pressure Testing of Steel based Composite Tanks .....	71
3.7.2. Burst Pressure Testing of Al based Composite Tanks .....	73
CHAPTER 4. RESULTS AND DISCUSSION.....	76
4.1. Tensile Test Results of Liner and Composite Sections.....	76
4.2. Fiber Mass Fractions of Composites.....	78
4.3. Dynamic Mechanic Analysis (DMA) of Composites .....	78
4.4. Burst Pressure Performance of Steel Based Composite Tanks .....	79
4.5. Burst Pressure Performance of Aluminum Based Composite Tanks ...	85
CHAPTER 5. EFFECT OF WINDING PARAMETERS ON THE PERFORMANCE OF COMPOSITE TANKS .....	97
5.1. Manufacturing of Composite Tanks .....	97
5.2. Results of Burst Pressure Test .....	99
CHAPTER 6. CONCLUDING REMARKS .....	102
6.1. Future Studies .....	105
REFERENCES.....	107
APPENDIX A PRODUCED G-CODES FOR FILAMENT WINDING.....	115

## LIST OF FIGURES

<u>Figure</u>	<u>Page</u>
Figure 1.1. Hydrogen Energy Usage Areas .....	1
Figure 1.2. Placement of a Type III hydrogen tank in a vehicle.....	2
Figure 2.1. Classsification of composite materials .....	8
Figure 2.2. (a) Composite pipe as an example of PMCs (b) some engine parts as an example of MMCs and and (c) brake system an example of CMCs .....	9
Figure 2.3. Classification of Composite Manufacturing Technique .....	10
Figure 2.4. Hand lay-up technique for composite manufacturing .....	11
Figure 2.5. Filament winding technique for composite manufacturing .....	12
Figure 2.6. Vacuum bag molding technique for composite manufacturing .....	12
Figure 2.7. Vacuum infusion technique for composite manufacturing .....	13
Figure 2.8. Resin transfer molding technique for composite manufacturing .....	14
Figure 2.9. Pultrusion technique for composite manufacturing.....	14
Figure 2.10. Lightweight CFRP automotive body parts (a) hood (b) tub chassis (c) door trim .....	16
Figure 2.11. Composite material usage in Boeing 787 airplane.....	17
Figure 2.12. Composite propeller used in marine industry .....	18
Figure 2.13. Lightweight bicycle made of composite material. ....	18
Figure 2.14. Global greenhouse emissions. ....	19
Figure 2. 15. Powertrain of a FCEVs .....	20
Figure 2.16. A fuel cell bus used in public transportation.....	21
Figure 2. 17. Classification of hydrogen storage techniques.....	22
Figure 2.18. Classification of hydrogen storage techniques .....	23
Figure 2.19. Classification of composite storage tanks.....	24
Figure 2.20. Winding types for filament winding (a) Hoop winding, (b) Helical winding (c) Polar winding and (d) Non-geodesic winding. ....	27
Figure 2.21. A specimen prepared for burst pressure testing .....	28
Figure 2.22. Pressure vs. hoop strain curves of DIC and strain gauges measurements: (a) carbon/vinylester specimen; (b) carbon/epoxy specimen .....	29

<u>Figure</u>	<u>Page</u>
Figure 2.23. Experimentally measured burst pressure of composite tanks .....	30
Figure 2.24. The number of tangent points used for optimization.....	31
Figure 2.25. Composite tanks after burst test .....	34
Figure 2.26. The manufactured composite spherical tank.....	35
Figure 2.27. The geometry of aluminum liner with unequal dome section.....	36
Figure 2.28. (a) Composite tank and (b) fragments after failure .....	37
Figure 2.29. Manufacturing of composite plate by filament winding technique .....	39
Figure 2.30. Stress-strain behavior of carbon/epoxy and glass/epoxy composites.....	40
Figure 2.31. Integrated doily layers the numeric model.....	41
Figure 2.32. Layer orientations of composite tank .....	42
Figure 2.33. Stress distribution of geodesic dome section at failure pressure.....	43
Figure 2.34. Burst pressure at different locations of the composite tank, MPa.....	44
Figure 2.35. Stresses of all the components in the composite tank, MPa .....	45
Figure 3.1. The drawing of the steel liner (dimensions are in mm) .....	47
Figure 3.2. The geometry of the aluminum liner (dimensions are in mm) .....	47
Figure 3.3. (a) Tensile test specimen cut from liner (b) Specimen placement at the test set up.....	48
Figure 3.4. (a) Glass fiber/epoxy (b) Carbon fiber/epoxy plates manufacturing .....	49
Figure 3.5. Carbon/epoxy tensile test specimen during tensile testing. ....	50
Figure 3.6. Carbon/epoxy specimen in an acid solution during the matrix digestion test.....	51
Figure 3.7. TA <sup>TM</sup> Q800 DMA test equipment. ....	52
Figure 3.8. Steel liner defined as a mandrel in the CADWIND software .....	53
Figure 3.9. Aluminum liner defined as a mandrel in the CADWIND software .....	54
Figure 3.10. Glass fiber and epoxy material properties defined to the software .....	55
Figure 3.11. Defined winding parameters to the software and angle variations.....	56
Figure 3.12. Fully covered (a) front dome section (b) back dome section with angle variations. ....	57
Figure 3.13. Defined winding parameters to the software for Al-based composite tank .....	58
Figure 3.14. Calculation results of helical layer winding for one composite layer .....	59

<u>Figure</u>	<u>Page</u>
Figure 3.15. Fully covered (a) front dome section (b) back dome section of Al based composite tanks.....	60
Figure 3.16. Filament winding machine used for composite tank manufacturing.....	61
Figure 3.17. Fiber tensioner system for filament winding manufacturing.....	61
Figure 3.18. Resin bath for filament winding manufacturing.....	62
Figure 3.19. Curing oven with rotating shaft.....	62
Figure 3.20. The filament winding of (a) a helical layer and (b) a hoop layer over the steel liner.....	64
Figure 3.21. A hybrid steel liner based composite tank after curing. ....	65
Figure 3.22. A helical layer winding over the aluminum liner. ....	66
Figure 3.23. Section of firstly manufactured aluminum liners. ....	67
Figure 3.24. Section of final manufactured liners. ....	68
Figure 3.25. Doily layers during the filament winding process.....	69
Figure 3.26. Inside wall control of a composite tank by snake cam. ....	71
Figure 3.27. (a) technical drawing and (b) photograph of adapter for steel-based tank.....	72
Figure 3.28. (a) schematic of strain gages positions (b) a test ready composite tank (c) test set-up for steel-based composite tank.....	73
Figure 3.29. (a) Strain gage positions, (b) burst pressure testing ready specimen, (c) specimen in the burst testing chamber.....	75
Figure 4.1. Experimental average tensile stress-strain curve of aluminum liner.....	76
Figure 4.2. Failure modes of (a) aluminum liner and (b) carbon/epoxy specimen.....	77
Figure 4.3. (a) steel liner, (b) glass fiber, (c) hybrid fiber tanks after hydrostatic burst pressure testing. ....	80
Figure 4.4. Comparison of axial strain values of composite tanks at the front (L1) cylindrical section.....	81
Figure 4.5. Comparison of radial strain values of composite tanks at the front (T1) cylindrical section.....	82
Figure 4.6. Comparison of axial strain values of composite tanks at the central (L2) cylindrical section.....	82

<u>Figure</u>	<u>Page</u>
Figure 4.7. Comparison of radial strain values of composite tanks at the central (T2) cylindrical section.....	83
Figure 4.8. Comparison of axial strain values of composite tanks at the central (L3) cylindrical section.....	83
Figure 4.9. Comparison of radial strain values of composite tanks at the back central (T3) cylindrical section.....	84
Figure 4.10. (a) Aluminum liner failure, (b) Composite tank front dome failure, (c) cylindrical failure, (d) Back dome failure .....	89
Figure 4.11. Polyurethane layer after failure (a) Top view, (b) Side view.....	90
Figure 4.12. Local axial strain (L1, L2 and L3) vs. pressure values of Al Liner. ....	91
Figure 4.13. Local radial strain (T1, T2 and T3) vs. pressure values of Al Liner. ....	91
Figure 4.14. Axial and radial strain (L2 and T2) vs. pressure values of Tank 18.....	92
Figure 4.15. Axial and radial strain (L2 and T2) vs. pressure values of Tank 19 .....	92
Figure 4.16. Axial and radial strain (L2 and T2) vs. pressure values of Tank 20 .....	92
Figure 4.17. Axial and radial strain (L2 and T2) vs. pressure values of Tank 26.....	93
Figure 4.18. Axial and radial strain (L2 and T2) vs. pressure values of Tank 27.....	94
Figure 4.19. Axial and radial strain (L2 and T2) vs. pressure values of Tank 32.....	94
Figure 4.20. Axial and radial strain (L2 and T2) vs. pressure values of Tank 33.....	95
Figure 4.21. Axial and radial strain (L2 and T2) vs. pressure values of Tank 34.....	95
Figure 4.22. Axial and radial strain (L2 and T2) vs. pressure values of Tank 35 .....	96
Figure 5.1. Defined Friction Factor Value.....	98
Figure 5.2. Fiber tensioner system .....	99
Figure 5.3. Composite Tanks After Failure .....	101

## LIST OF TABLES

<u>Table</u>	<u>Page</u>
Table 2.1. Summary of the FCEVs currently in available.....	21
Table 3.1. Mechanical properties of the fibers and the matrix .....	46
Table 3.2. Orientations and properties of the manufactured steel liner based composite tanks .....	65
Table 3.3. Orientations and properties of the manufactured Aluminum liner based composite tanks .....	69
Table 4.1. Experimentally found mechanical properties of the Al Liner .....	76
Table 4.2. Tensile test results of glass fiber/epoxy and carbon fiber/epoxy plates.....	77
Table 4.3. Fiber mass fractions of glass fiber/epoxy and carbon fiber/epoxy plates.....	78
Table 4.4. DMA results of manufactured composite specimens. ....	78
Table 4.5. Burst pressure results of manufactured steel based composite tanks.. .....	79
Table 4.6. Burst pressure results of manufactured aluminum based composite tanks....	86
Table 4.7. Mass comparisions of aluminum and steel based tanks.....	96
Table 5.1. Manufactured composite tanks with different winding properties.....	98
Table 5.2. Burst Pressure Results of Manufactured Composite Tanks.....	100

# CHAPTER 1

## INTRODUCTION

### 1.1. Introduction

Today, approximately 25% of the world CO<sub>2</sub> emissions are attributable to the transportation system. According to current trends, the number of cars may double until 2050 because of the increasing population and income<sup>1</sup>. The decarbonization of the transport system is one of the most important factor for reducing climate change.

Hydrogen is regarded as the new energy source for the next century due to zero greenhouse gasses emission, high energy efficiency and its abundance in nature. Especially since the year 2000, there are important milestones in technologies for the use of hydrogen energy and developed products are in usage. For example, hydrogen is used as an energy source for public and personal transportation, in hospitals, public buildings and remote areas from settlements as shown in Figure 1.1<sup>2</sup>.



Figure 1.1. Hydrogen Energy Usage Areas

There are generally three ways to store hydrogen which are: (i) Storage in solid material, (ii) Storage as cryogenic liquid, (iii) Compressed gaseous storage in pressurized tank. However, compressed gaseous storage in pressurized tank technique is the most popular and effective way since the filling process is faster and more economical<sup>3</sup>.

In mobile applications, Type 3 (metallic lined fully overwrapped with composite layers) and Type 4 (polymer lined fully overwrapped with composite layers) tanks are designed and used. The working pressures of Type 3 and Type 4 composite tanks are generally 350 bars however, by storing hydrogen at 700 bars the same weight can be provided with lower volume. Therefore, it can be more suitable for new generation automobiles which have smaller dimensions <sup>4</sup>. In Figure 1.2, the placement of a Type III hydrogen tank in a vehicle is shown.



Figure 1.2. Placement of a Type III hydrogen tank in a vehicle

The working pressures of composite high pressure tanks are generally 350 bar for automotive applications. However, new generation hydrogen vehicles require approximately 4 kg of hydrogen gas for 400 km continuous operation range which needs about 22.5 L internal volume. This value is considerably high for the new generation of hydrogen vehicles and this volume can be reduced by storing hydrogen at higher pressures (700 bar). The most important performance criterion for a composite storage tank is the burst pressure test. According to ISO 15869:2009, which is a standard for hydrogen storage tanks for mobile applications, there should not be any failure up to two times of working pressure. Therefore, in order to reach 700 bar working pressure, the composite tank must have a burst pressure of a minimum 1400 bar. To reach these 1400 bar burst pressure value, the liners can be reinforced helical, hoop and doily composite layers by filament winding methods. Hydrogen storage in composite pressure tanks has some advantages as compared to other hydrogen storage techniques such as <sup>4-6</sup>:

- Lower cost
- Technical simplicity
- Rapid filling and unloading

- Storage at room temperature

Some advantages of this approach as compared metallic vessels are as follows;

- **High strength to weight ratio**
- Weight reduction of up to 75%
- Corrosion resistance
- Fatigue resistance

Although composite tanks have higher manufacturing costs as compared to metallic vessels, it is possible to store more amount hydrogen at the same weight of vessels. Also, doily layers can be used during the filament winding process. In this way, the number of helical layers can be decreased and manufacturing time and manufacturing cost of composite tanks can be reduced.

## **1.2. Aim of the Study**

The main objective of this study is to design, produce and manufacture composite pressure tanks that have 700 bar working pressure and minimum 1400 bar burst pressure value for hydrogen storage. Also, hybridization affects on the the burst pressure of steel liner based composite tanks were investigated. Another important aim of this study is to improve the performance of the tanks by using doily layers.

Another critical purpose of this study are as follows;

- Utilize the filament winding process for manufacturing the steel and aluminum-based composite tanks for high-pressure storage.
- Determining the mechanical properties of the liners and the composite sections.
- Determining the thermo-mechanical properties of composite sections.
- Investigate the effect of the number of helical, hoop and doily layers on the burst performance of the composite tanks.
- Measure the local strain values of the composite tanks and liners during the burst pressure test.

- Obtain the failure modes of the composite tanks and liners after the pressure test.
- Investigate the effect of fiber tension during the filament winding process on the burst pressure of composite tanks.
- Investigate the effect of friction factor used for winding simulation software during the filament winding process on the burst pressure of composite tanks.
- Utilizing the doily layers to the aluminum-based composite tanks and observe its effects on the burst pressure performance and failure modes of composite tanks.

### **1.3. Novelty of the Thesis**

In this thesis, composite tanks for hydrogen storage with 700 bar working pressure and minimum 1400 bar burst pressure were designed, manufactured and tested. Effect of number of helical, hoop and doily layers on the performance of the composite tanks were investigated experimentally. To our knowledge, there are only a few studies reported in the literature on the investigation of the effect of the number of helical, hoop and doily layers on the burst pressure of composite tanks manufactured by the filament winding method. Also, an experimental investigation of the effect of the number of doily layers on the burst performance of the tanks is a unique contribution to the literature since there is no work published which investigates the effect of the number of front and back dome doily layers experimentally. Furthermore, polyurethane-based resin system coverage inside aluminum liner and determining the effect of this coverage is another unique contribution to the literature.

Also, in this study mechanical and thermomechanical properties of steel and aluminum liners and composite sections were determined. For this aim a specific aluminum plate was designed and attached to the filament winding machine. Then composite unidirectional plates were manufactured by filament winding method. Tensile and dynamic mechanic analysis test specimens produced by these plates and tests were carried out. Therefore, this study gives a contribution to the literature about the mechanical characterization of filament wound composites.

Furthermore, this thesis contributes to the literature about developing the manufacturing technique. The aluminum liners were manufactured with deep drawing and spinning techniques and they have a specific geometry. Because of their specific geometry, obtaining full coverage by composite helical layers and reaching the burst pressure of more than 1400 bar is another unique contribution to the literature.

Additionally, the effect of filament winding parameters such as fiber tension and friction factor during winding on the burst pressure performance of composite tanks were investigated experimentally. These parameters are directly affecting the helical layer winding angle, winding pattern, amount of fiber usage and coverage of the liner by composite section. The effects of these parameters were determined in this thesis experimentally. Thus, this study can be helpful for other researches and give them some ideas for their design about the effect of filament winding parameters on the performance of filament wound composite materials.

#### **1.4. Thesis Outline**

In Chapter I, the importance of hydrogen, hydrogen storage techniques and the benefits of composite tanks were discussed briefly. After this brief background information, the objectives of this thesis were listed. Furthermore, at the end of the chapter novelty of the thesis was mentioned.

In Chapter II, general information about composite materials was given by considering the definition and classification of them. Additionally, manufacturing techniques and applications of fiber-reinforced composite materials were mentioned. These general overviews of composite materials can be helpful for researchers who are unfamiliar with these studies. The importance of hydrogen and hydrogen storage techniques were also given. Besides, the usage and applications of composite tanks at industrial applications were analyzed. Types of composite tanks and their advantages and disadvantages were discussed. Filament winding manufacturing techniques for composite tanks production were expressed. The working principle and parameters effected filament winding technique were discussed with studies presented in the literature. Studies published in the literature about the performance development and characterization of composite tanks were investigated in detail and summarized in this chapter. Therefore,

this chapter is not only helpful to figure out general concepts and studies presented in the literature, but also to catch the gaps in the literature.

In Chapter III, the experimental techniques used in this thesis were given in detail. Materials, machines, and other apparatus used during the study were mentioned. Tensile testing for mechanical characterization, matrix digestion and burn out method for determining fiber volume fraction was described. Dynamic mechanic analysis (DMA) for determining the thermomechanical properties of composites was expressed also in this chapter. To simulate the filament winding technique, CADWIND CAM software was used and details of this simulation were showed. Chapter III, also contains a detailed description of the filament winding method used for manufacturing composite tanks in these thesis. Furthermore, burst pressure testing of liners and composite tanks were mentioned.

With Chapter IV, results of the tensile characterization of liners and composite sections were given. Also, the thermomechanical properties of the composite section were determined. Burst pressure results of steel-based composite tanks were given and the effect of hybridization on the burst pressure performance of composite tanks was discussed. Effect of number of helical, hoop and doily layers on the burst pressure performance of aluminum-based composite tanks were investigated. Also, the influence of polyurethane coverage inside aluminum liners was discussed.

In Chapter V, the effect of winding parameters on the burst pressure performance of composite tanks was investigated experimentally. The effect of winding tension during the manufacturing process and effect of friction factor values used during simulation and winding process was investigated individually. This chapter also contains the burst pressure tests of these composite tanks. Chapter V is also important for filling the gaps in the literature and can be helpful for other researchers for selecting filament winding parameters.

Chapter VI contains concluding remarks and future works were also given.

## CHAPTER 2

### BACKGROUND AND LITERATURE SURVEY

#### 2.1. Composite Materials

##### 2.1.1. Definition of Composite Materials

A composite material, as it can be understood from its name, is a combination of two or more different materials. These component materials have significantly unique physical and chemical properties however when these materials combined, the generated material has completely different properties as compared to its component materials<sup>7-8</sup>.

Composite material is a mixture of a base material and filler material. Base material is also known as matrix material and it covers the filler material. Filler material can be found as particle, powder or fiber form<sup>9-10</sup>. Filler or reinforcement materials are stiffer and stronger than matrix material therefore they carry the applied load to the material. The definition of composite material is well understood by investigating the naturally occurred composites material such as wood. Wood consists of cellulose molecules as reinforcement material and polymer lignin as a matrix material<sup>11</sup>.

The usage of composite materials goes back to ancient times when Egyptians and Mesopotamian settlers used a combination of mud and straw to reinforce their buildings around 1500 B.C. Mongolians used first composite weapons in the history and their composite bow consists of wood, bone and animal glue. After the invention of plastics in the early 1900s, the modern era of composites began. Plastics are not strong enough for specific applications and plastics are combined with glass fiber. Therefore, stronger and stiffer material obtained as compared to plastic also it is lightweight. During World War II, there was a need for lightweight and strong material for military applications and composite materials was a solution for this need. During the 1970s, plastics resins were improved as matrix material and aramid and carbon fibers started to use and composite materials became a rival for steel in the industrial applications. The development studies

of composite material are continuing today, especially increasing its part of the clean energy area<sup>12</sup>.

### 2.1.2. Classification of Composite Materials

Composite materials can be categorized by the type of constituents as shown in Figure 2.1.

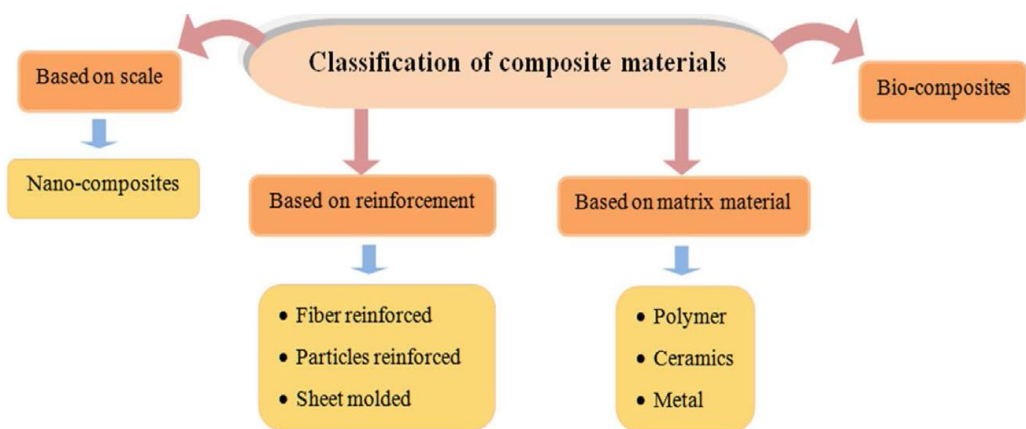


Figure 2.1. Classssification of composite materials

(Source: Rajak et al., 2019)

Firstly, composite can be classified according to their matrix type. Composites can have three different types of matrix material which are; Polymer matrix composites (PMCs), Ceramic matrix composites (CMCs) and Metal matrix composites (MMCs). For PMCs, thermosetting plastics or thermoplastics are the matrix material of PMCs and these thermoset and thermoplastic matrices generally reinforced by glass, carbon and aramid fibers<sup>14-16</sup>. Thermosets and thermoplastic matrices both have advantages and disadvantages according to their application areas. Thermosets have higher strength and resistance to elevated temperatures. Thermoplastics can be reshaped and recyclable however thermosets can not be reformed or recyclable after they cured and solidified<sup>17</sup>. PMCs are a popular type of composites because of their different type of fabrication techniques and low cost<sup>18</sup>. For CMCs, there is a ceramic matrix structure and carbon, silicon carbide (SiC), aluminum oxide (Al<sub>2</sub>O<sub>3</sub>), silicon nitride (SiN) fibers are generally used as reinforcement material. In MMCs the matrix material can be aluminum,

magnesium, copper or titanium and reinforcements can be ceramics or a metallic structure. MMCs are widely used in automotive and aerospace industries because of their superior properties such as high strength, low weight and high wear resistance<sup>19</sup>. In Figure 2.2 examples for PMCs, CMCs and MMCs are given<sup>20-22</sup>.



(a)



(b)



(c)

Figure 2.2. (a) Composite pipe as an example of PMCs (b) some engine parts as an example of MMCs and (c) brake system an example of CMCs.

Another classification type of composites is based on reinforcement type. Reinforcements can be called as fiber, particle and sheet. In fiber-reinforced plastic (FRP) composite materials, carbon, glass, aramid and basalt fibers are the most widely used fiber types since they have some superior properties such as; high strength and stiffness, resistance to corrosion and fatigue<sup>23,24</sup>. Also, natural fibers take attention nowadays since they can be found at lower prices and they are eco-friendly. In particle type reinforcement, the main aim is increasing the wear resistance not strength. The particle reinforced composites are used widely in wear resistance required applications. Particle reinforced composites are cheaper and easier to manufacture as compared to fiber-reinforced composites<sup>25</sup>. Sheet based composites are composed of a glass fiber reinforcement and unsaturated resins as a matrix to produce a high strength molding composite. These composites are suitable for large structural applications<sup>26</sup>. Composite material also can be

classified based on their scale. Nanocomposites and bio-composites are examples of this classification.

### 2.1.3. Manufacturing Techniques for FRP Composites

Composites can be fabricated with different manufacturing techniques. These techniques are selected according to the type matrix or fiber material used. Some of the composite manufacturing techniques are given in Figure 2.3.

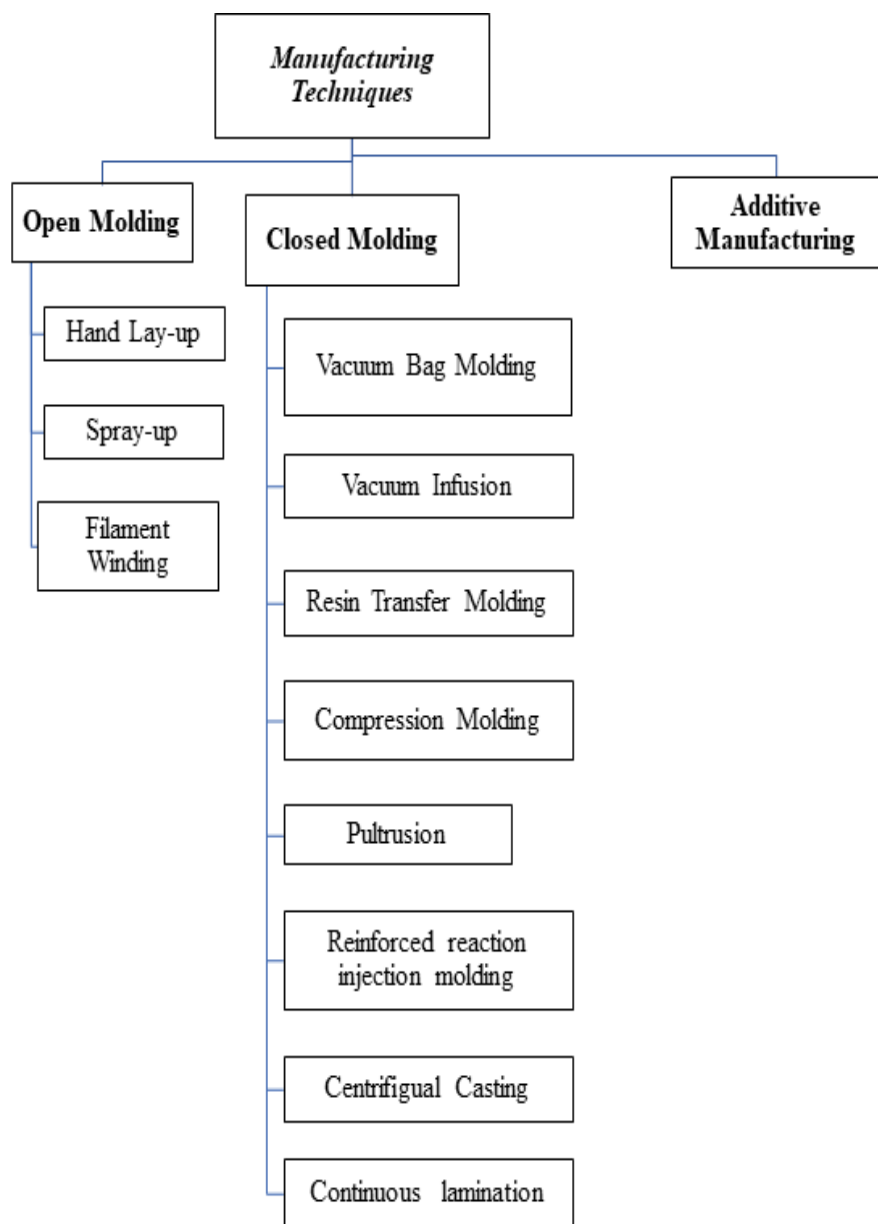


Figure 2.3. Classification of Composite Manufacturing Technique.

Hand lay-up, spray-up and filament winding technique can be called an open molding technique. Hand lay-up is the most basic and known composite manufacturing process as it requires a minimum amount of equipment. In this process, fiber reinforcement which can be woven, non-woven, or unidirectional (UD) fabrics are manually wetted with a resin system and placed an open mold system properly<sup>27,28</sup>. To prevent air between the fabrics, brushes and rotating rollers are used. The schematic of the hand lay-up technique is displayed in Figure 2.4 <sup>29</sup>.

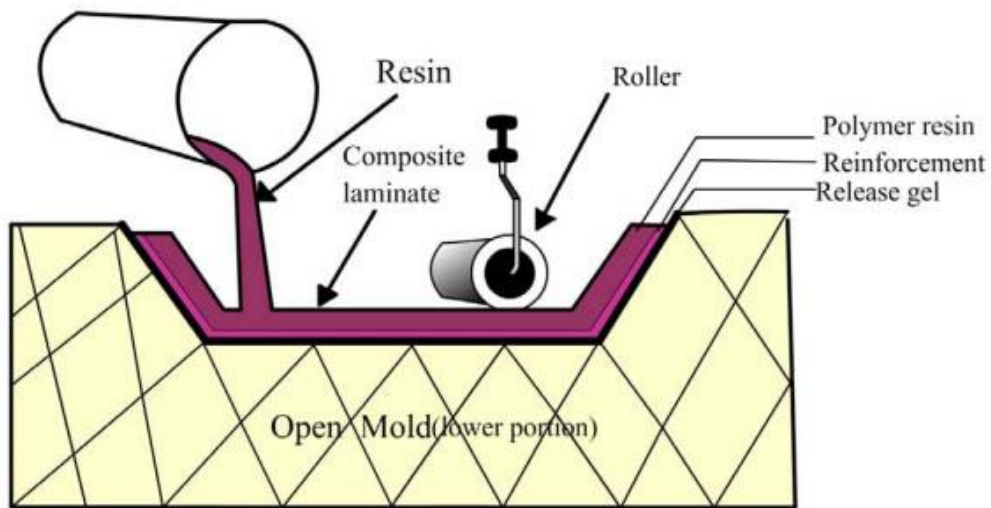


Figure 2.4. Hand lay-up technique for composite manufacturing <sup>29</sup>

(Source: Eppcomposites)

In the spray-up technique, short fibers are used as reinforcement material and these short fibers are held in a handgun and resins are sprayed randomly into the mold. As compared to hand lay-up technique this process can be faster especially in complex-shaped parts.

To manufacture hollow cylindrical composite structures, filament winding manufacturing processes can be used. In the filament winding process, tensioned continuous fiber tows are passed through a resin bath before being wound onto a rotating mandrel in a variety of orientations, controlled by the fiber feeding mechanism, and rate of rotation of the mandrel <sup>30</sup>. Filament winding is a computer-controlled manufacturing technique and provides high strength to weight ratio and uniformity for composite parts. The filament winding process is demonstrated in Figure 2.5, schematically<sup>31</sup>.

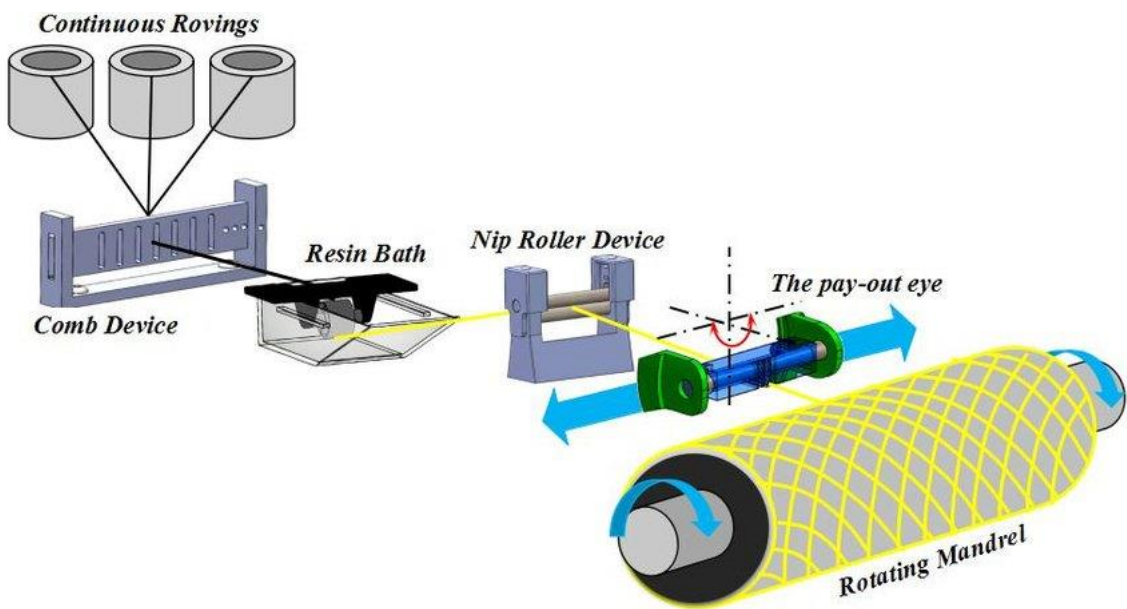


Figure 2.5. Filament winding technique for composite manufacturing

(Source: Quanjin et al., 2019)

Vacuum bag molding is a type of closed mold composite manufacturing technique. In vacuum bag molding, firstly, reinforcement fabrics are wetted with a resin system and placed to the mold. Then the wet fabrics are covered with flexible film and then the system is sealed. External vacuum pressure is applied to the system and excess resin is removed<sup>32</sup> (Figure 2.6).

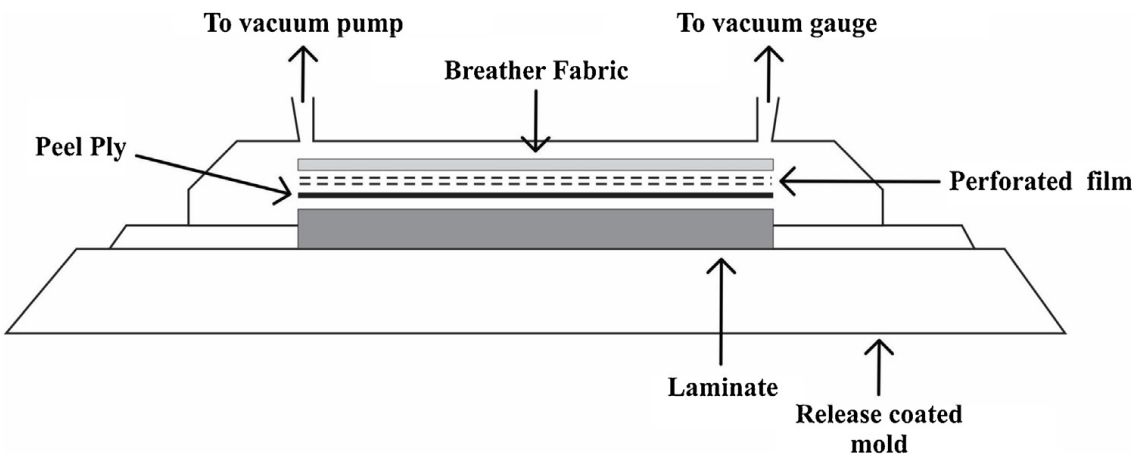


Figure 2.6. Vacuum bag molding technique for composite manufacturing

(Source: Rajak et al., 2019)

Vacuum infusion technique is very similar to the vacuum bag molding technique, however, in the vacuum infusion technique, vacuum pressure is applied before resin is applied. In this technique, dry reinforcement fabrics are placed on the mold, then the system is sealed and vacuum pressure is applied. Then resin is infused into the sealed system with the help of pressure differences. Vacuum infusion technique is a very common technique to manufacture some specific parts such as; wind turbine blades, automotive and aircraft parts. Sealing is very important in this technique since it can directly affect the quality of the composite parts. A sealed vacuum infusion set up can be seen in Figure 2.7<sup>33</sup>.



Figure 2.7. Vacuum infusion technique for composite manufacturing <sup>33</sup>  
(Source: Altropol)

In resin transfer molding (RTM), dry reinforcements are placed in the mold cavity and resin is injected with pressure using an injection machine. There is some advantage in the RTM process such as it provides good surfaces for both faces of the composite part and the process occurs at room temperature with fast cycle time <sup>34</sup>. RTM process is given in Figure 2.8 schematically <sup>35</sup>.

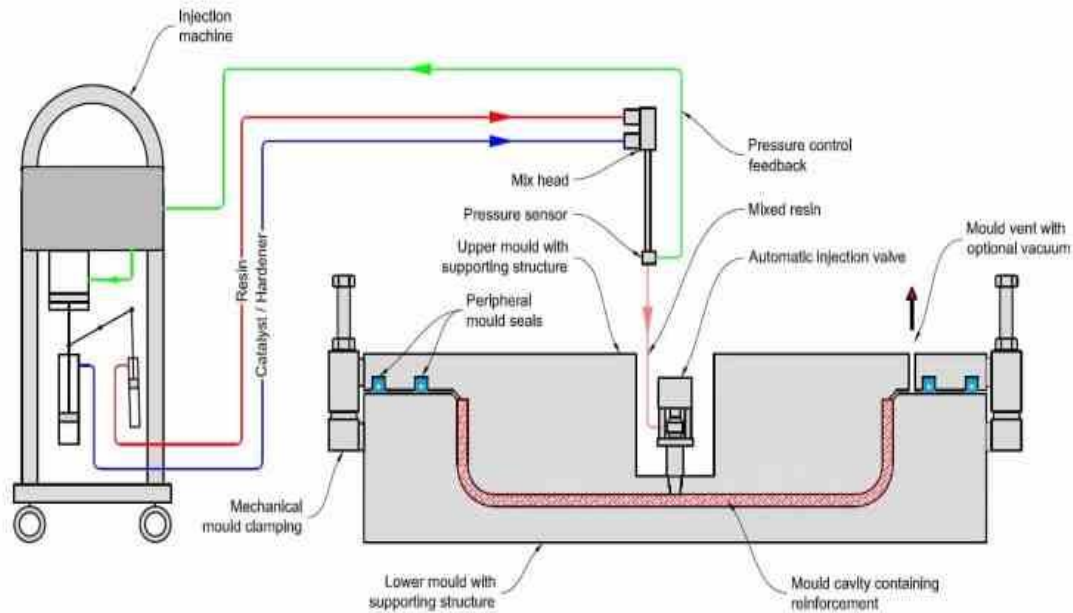


Figure 2.8. Resin transfer molding technique for composite manufacturing  
 (Source: Technicalmarvel)

In the compression molding technique, metal molds are preheated on large molding presses. This process is generally useful for complex-shaped fiberglass parts that need large volume and high pressure. The pultrusion process is used for manufacturing constant cross-section composite parts. It is a continuous manufacturing process and suitable for simple and complex shaped composite parts<sup>36</sup>. The pultrusion process can be seen in Figure 2.9<sup>37</sup>.

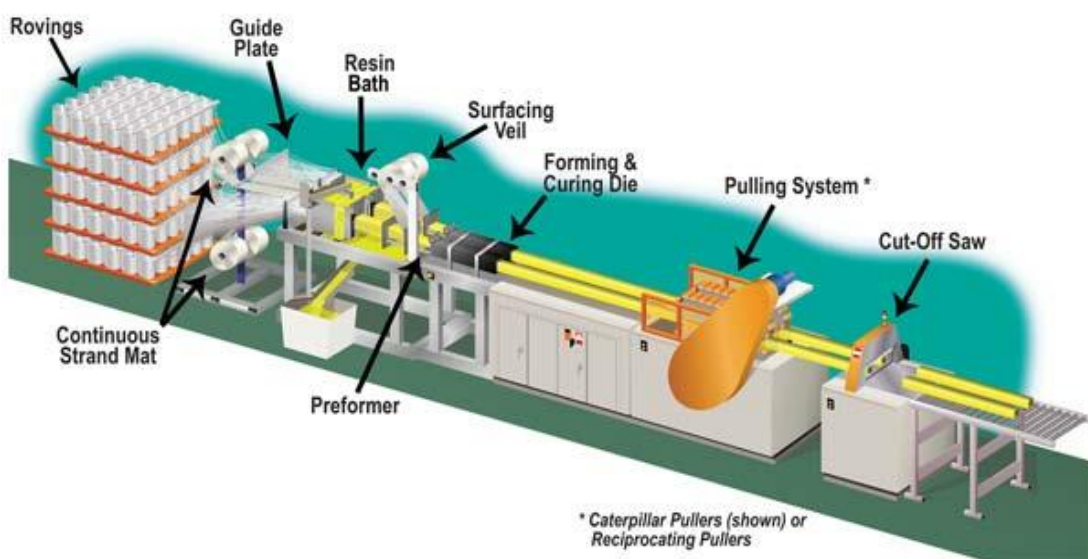


Figure 2.9. Pultrusion technique for composite manufacturing  
 (Source: Cyccomposites)

The reinforced reaction injection molding (RRIM) process contains two or more different resin systems and these resin systems are mixed in a chamber and produce a thermoset polymer system. Reinforcement materials are added to this mixture and this mixture is pumped into a mold by using a high-pressure injection pump <sup>38</sup>.

In the centrifugal casting process, resin and reinforcement materials are stored inside the surface of the cylindrical rotating mold. Centrifugal force is used to hold the mixture before it gets cured and solidified<sup>39</sup>. Continuous lamination manufacturing process helps to produce products having an opaque, translucent flat, panel-like structures<sup>40</sup>.

The additive manufacturing technique uses a different manufacturing process in which composites are manufactured layer by layer. Different types of matrix and reinforcement materials have been developed for this manufacturing technique. This manufacturing process provides flexibility over fiber volume and fiber orientations <sup>41</sup>.

#### **2.1.4. Applications of Composite Materials**

Composite materials have a very wide range of application areas such as; automotive, aerospace, mechanical parts, marine, bio-medical applications, and piping systems because of their lightweight, high strength and stiffness values, high corrosion and fatigue resistance. The advantages of composite materials are firstly used in automotive applications. For example, in automotive brake systems, the temperature reaches very high levels and the brake system should perform well. Carbon fiber reinforced silicon carbide (C-Si) brake materials are used for this aim<sup>42</sup>.

Carbon emission is very critical for the automotive industry and to decrease carbon emission value the fuel consumption should be decreased. Carbon fiber reinforced plastics (CFRP) are a solution to this problem because of their lightweight<sup>43</sup>. Since the transportation industry causes a serious carbon emission and increase the global warming, CRFP's are widely used in automotive industry to decrease to weight of the vehicles. Different vehicle body or interior parts can be produced by using composite materials. A carbon fiber hood, tub chassis and a door trim are given as examples of lightweight composite body parts in Figure 2.10 <sup>44</sup>.



(a)



(b)



(c)

Figure 2.10. Lightweight CFRP automotive body parts (a) hood (b) tub chassis (c) door trim

(Source: Livescience)

Aerospace is another important industry for the usage of composite materials. Nowadays aircraft brakes, aircraft structures, gas turbines and aircraft seats are made of composite materials. Aircraft structures should have resistance to temperature variation, also they should have high strength and stiffness values. Therefore, composite materials take place the conventional materials such as aluminum used in the aerospace industry<sup>45,46</sup>. As it can be seen in Figure 2.11, Boeing 787 Dreamliner airplane is made of %50 percent of composite material<sup>47</sup>.

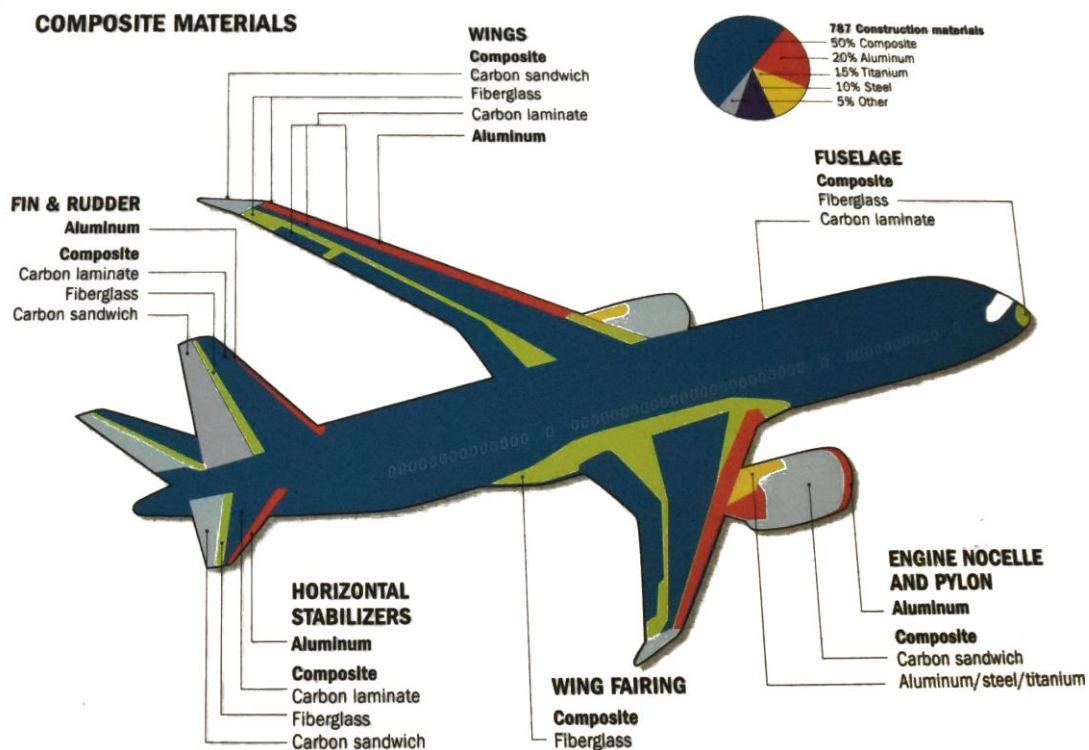


Figure 2.11. Composite material usage in Boeing 787 airplane<sup>47</sup>.

(Source: MSE)

In the marine industry, conventionally alloys of aluminum and stainless cast steel and aluminum bronze were used as a propeller material. However, these conventional materials are not resistant to corrosion, cavitation and formation of the galvanic cell. Furthermore, propellers are subjected to multi-axial loads during their operation. Therefore, CFRP composites are the best alternatives to these conventional materials because of their superior properties such as high strength to weight ratio, high fatigue resistance, non-corrosion and high thermal resistance<sup>48</sup>. Composite materials are also widely used in structural parts of marine crafts. A composite propeller is displayed in Figure 2.12<sup>49</sup>.



Figure 2.12. Composite propeller used in marine industry

(Source: Airborne)

Composite materials have been introduced to the piping systems due to their superior properties such as high specific strength and low weight which make them easier for transportation and high corrosion resistance which provides longer life compared to conventional engineering materials such as steel and aluminum. Composite piping systems can carry fluids such as water, oil, and gas with the lowest rate of loss since their inside surface quality is better as compared to conventional materials<sup>50</sup>.

Besides, composite materials are very popular in the sporting goods markets such as rackets, fishing rods, golf shafts, bicycles, etc. are made of composite materials. These products offer lightweight, high performance and functionality. In Figure 2.13, a bicycle made of composite material can be viewed<sup>51</sup>.



Figure 2.13. Lightweight bicycle made of composite material.

(Source: Composite Manufacturing Magazine)

## 2.2. Hydrogen

### 2.2.1. Hydrogen as an alternative energy carrier

Energy is an important part of our everyday life, and it is required to perform virtually all human activities. 80% of all the energy consumed in the world is supplied by fossil fuels such as petroleum, natural gas, and coal<sup>52</sup>. However, since fossils fuels are responsible for global warming, using an environmentally clean, economical and more sustainable energy other than fossil fuel systems could solve these global energy problems. Hydrogen is regarded as the new energy source for the next century due to zero greenhouse emission, high energy efficiency and unlimited in nature. Hydrogen can be a secure energy system for transportation, heating, industry and electricity sectors which are responsible for two-thirds of the global CO<sub>2</sub> emissions (Figure 2.14) <sup>53</sup>.

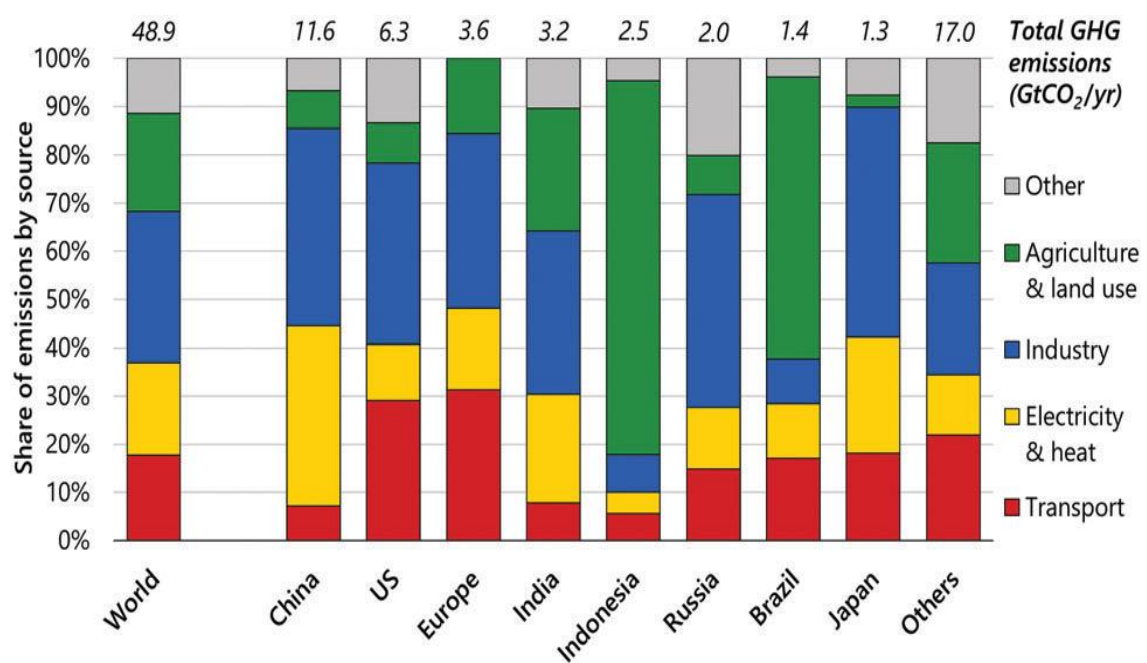


Figure 2.14. Global greenhouse emissions

(Source: Staffel et al., 2019)

Hydrogen can be obtained from both renewable energy sources such as, wind, wave, solar, biomass and geothermal energy sources, and also fossil fuels such as natural gas, coal, and nuclear energy sources. Hydrogen has become a great alternative energy

carrier for transportation by the development of fuel cells. Hydrogen powertrains for hydrogen vehicles (Figure 2.15) also known as fuel cell electric vehicles (FCEVs) can be compared to its rivals which are internal combustion engines (ICEs), battery electric vehicles (BEVs) and plug-in hybrid vehicles (PHEVs) such as;

- Cost: FCEVs have a higher cost than BEVs nowadays. However, the cost of FCEVs can be decreased when the manufacturing rate increase <sup>54</sup>.
- Range and Refilling time: FCEVs have a longer driving range and shorter refilling time as compared to conventional BEVs <sup>55</sup>.
- Safety: Hydrogen is very flammable but due to the nature of hydrogen, hydrogen fire can cause little damage <sup>55</sup>.

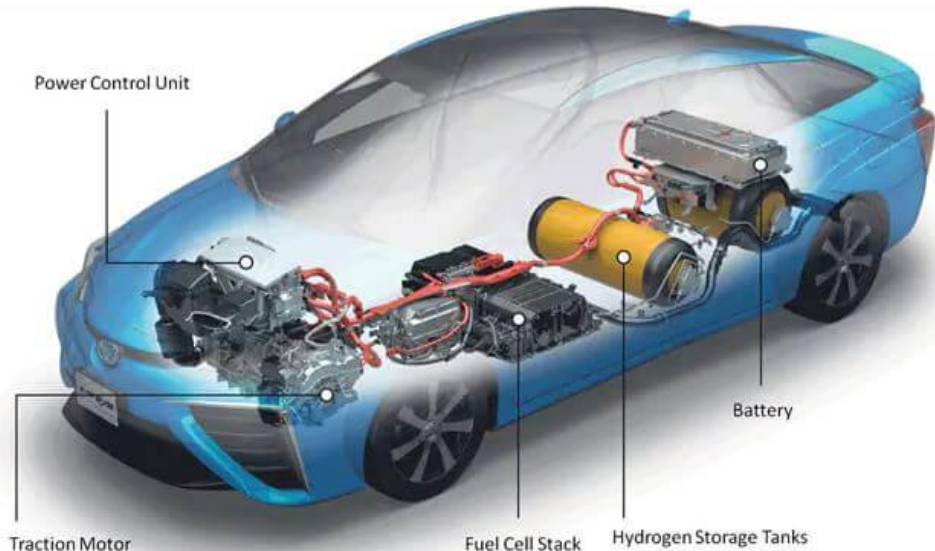


Figure 2.15. Powertrain of a FCEVs

(Source: Fuel cell store)

To decrease the greenhouse emissions caused by transportation, the transportation industry must focus on passenger cars since half of the transportation market consists of passenger cars. Therefore, many passenger car manufacturers have been developing FCEVs to manufacture environmentally friendly cars with zero greenhouse gases emissions. The summary of the FCEVs currently in production and available commercially in the market are tabulated in Table 2.1.

Table 2.1. Summary of the FCEVs currently in available<sup>56</sup>

Vehicle	Production (Year)	Combined Fuel Economy (miles per gallon gasoline equivalent)	Range (km)
<b>Toyota Mirai</b>	2015-present	66	502
<b>Honda Clarity</b>	2016-present	67	589
<b>Hyundai Tucson</b>	2014-present	49	426

Hydrogen is also taking attention to heavy-duty vehicles such as fuel cell buses are started to use in cities. Today there are 83 operating fuel cell buses in Europe and 44 in North America<sup>57</sup>. Trucks also have significant potential for fuel cell adoption since hydrogen can supply zero-emission and high energy. A fuel cell bus is given Figure 2.16.<sup>58</sup>



Figure 2.16. A fuel cell bus used in public transportation.

(Source: Fuel cell store)

## 2.2.2. Hydrogen Storage Techniques

For on-board hydrogen storage, there are some different storage techniques such as compressed gas storage, cryogenic hydrogen storage, metal and chemical hydrides.

These techniques can be classified as either ‘reversible on-board’ or ‘regenerable off-board’. Also, there is a difference between system and material-based storage. The hydrogen storage system consists of all related components such as **tank, valves, piping, insulation**, while material-based means for only reactants or materials possessing hydrogen<sup>59</sup>. There are some advantageous and disadvantageous of all techniques and none of them can meet all the requirements at the moment. The classification of hydrogen storage techniques is classified in Figure 2.17.

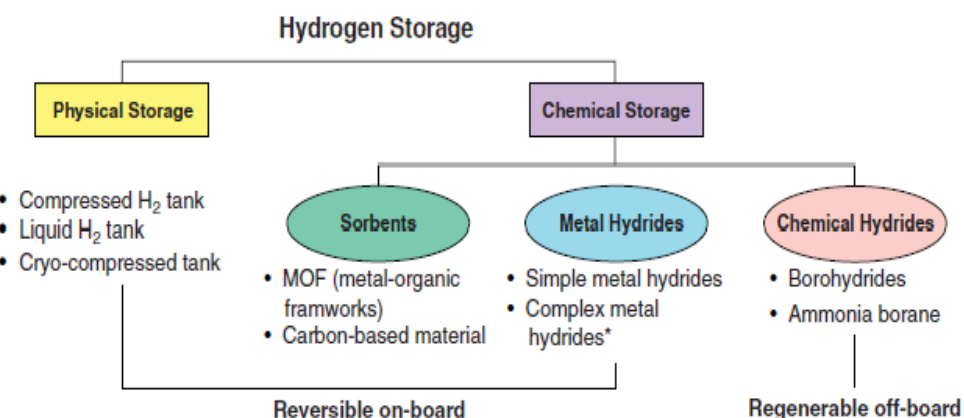


Figure 2.17. Classification of hydrogen storage techniques.

(Source: He-wang and Varma, 2014)

Compressed gas storage is the most widely used technique for hydrogen storage. Compressed hydrogen tanks are used for FCEVs. Detailed information about compressed hydrogen tanks will be given in the forward sections. Another technique for hydrogen storage is cryogenic storage. Hydrogen can be liquefied and by this way the volumetric capacity of hydrogen increases. However, when **hydrogen is stored as a liquid form it must be stored below its boiling point**. Therefore, in this technique a serious thermal insulation is needed. **The liquid hydrogen tanks have double-walled, and there is vacuum pressure between these walls to provide thermal insulation.** Although thermal insulation is applied to liquid hydrogen tanks, the liquid hydrogen can evaporate, which causes **hydrogen loss**. Because of this reason liquid hydrogen tanks are not frequently used<sup>60</sup>. As mentioned above, liquid hydrogen tanks are not very efficient, compression and liquid storage are combined and cryo-compressed hydrogen storage is obtained<sup>61</sup>.

Metal hybrids have great potential about on-board hydrogen storage applications for fuel cells. However, their gravimetric capacity is too low and they have a very high

cost therefore they are not suitable for vehicular applications<sup>62</sup>. Chemical hybrids supply higher energy densities as compared to metal hybrids because of containing lighter elements. Moreover, they can release hydrogen at lower operating conditions. However, the dehydrogenation reactions are irreversible, so they are not appropriate for on-board applications<sup>63</sup>.

## 2.3. Composite High-Pressure Tanks

### 2.3.1. Applications of Composite Tanks

Composite storage tanks also known as composite overwrapped pressure vessels (COPVs) have taken significant attention because of their excellent properties, such as high strength, excellent fatigue, and corrosion resistance. Also, they have a higher strength-to-weight ratio than metallic pressure vessels for similar tasks. Therefore, composite tanks have been used in some applications such as onboard fuel tanks for vehicles and aerospace power systems. Especially for high-pressure hydrogen storage, COPVs plays a very critical role<sup>64,65</sup>. In Figure 2.18, Hyundai Tucson FCEV uses a composite hydrogen storage tank can be seen<sup>66</sup>.

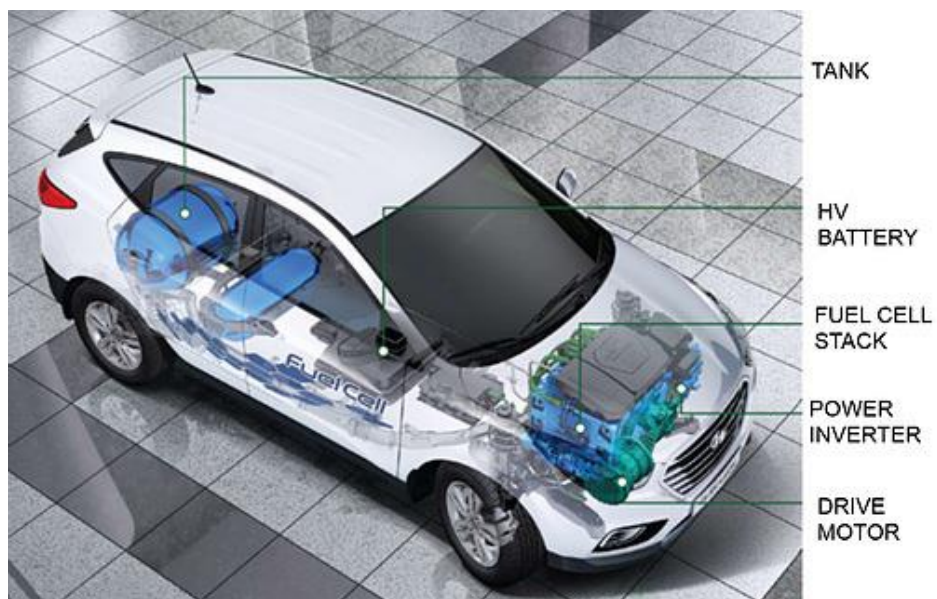


Figure 2.18. Classification of hydrogen storage techniques.

(Source: Energy)

### 2.3.2. Classification of Composite Tanks

The high-pressure hydrogen storage tanks can be divided into five different categories according to their performance and cost<sup>67</sup>.

**Type-I:** These types of tanks have **all-metal construction**, generally steel. They are cheap but heavy and not suitable for mobile applications.

**Type-II:** These tanks have a **metallic liner** but **only the hoop section is overwrapped** with the composite section. They are lighter than Type I tanks but more expensive.

**Type-III:** They have also **metallic liner** similar to Type-II tanks but **all of the liner overwrapped with composite section**. Only 10% percent of the load is carried by the metallic liner.

**Type-IV:** There are **polymeric liners** in these types of tanks. They are lighter than Type-III tanks but more expensive.

**Type-V:** These types of tanks **contains no liner**. Only consist of **composite shell**. The five different types of high-pressure tanks are given in Figure 2.19<sup>68</sup>.

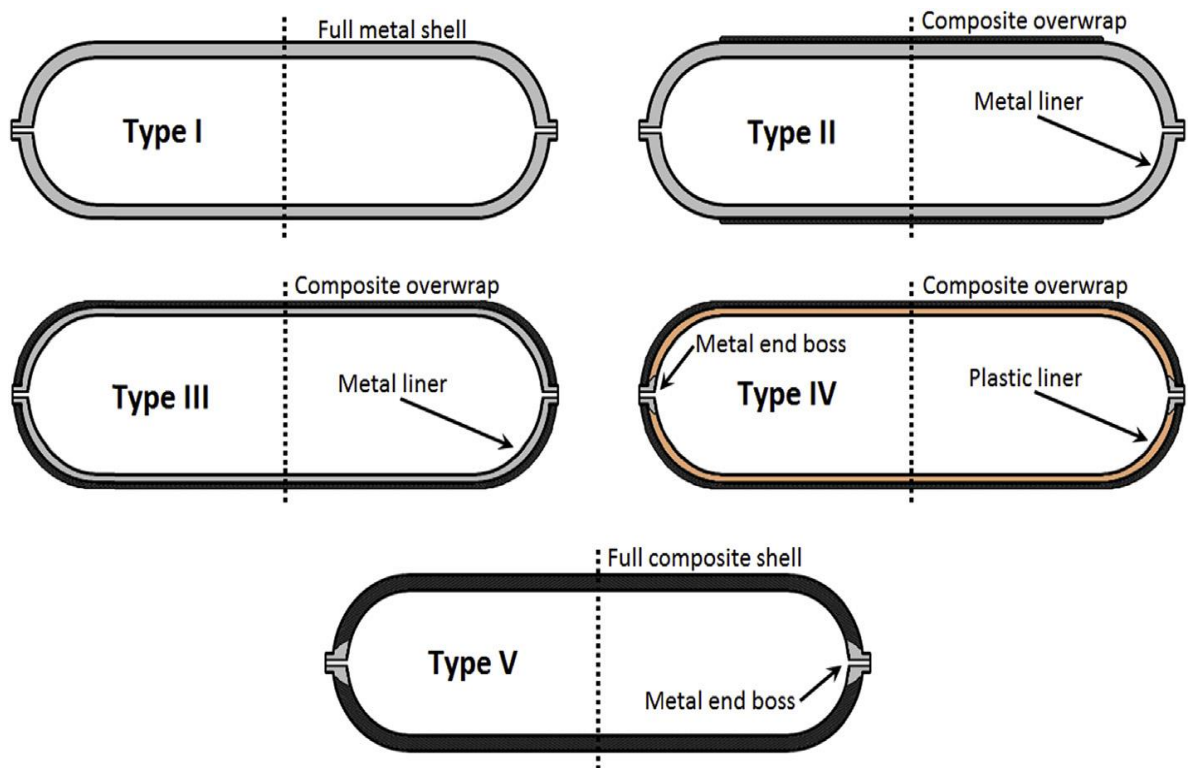


Figure 2.19. Classification of composite storage tanks.

(Source: Fowler et al., 2016)

For on-board applications, Type-III and Type-IV composite tanks give the most promising solutions. The working pressures of composite tanks are generally 350 bar for automotive applications. However, new generation hydrogen vehicles require approximately 4 kg of hydrogen gas for 400 km continuous operation range, which needs about 22.5 L internal volume. This internal volume is considerably high for the new generation of hydrogen vehicles and can be reduced by storing hydrogen at higher pressures (700 bar)<sup>69</sup>.

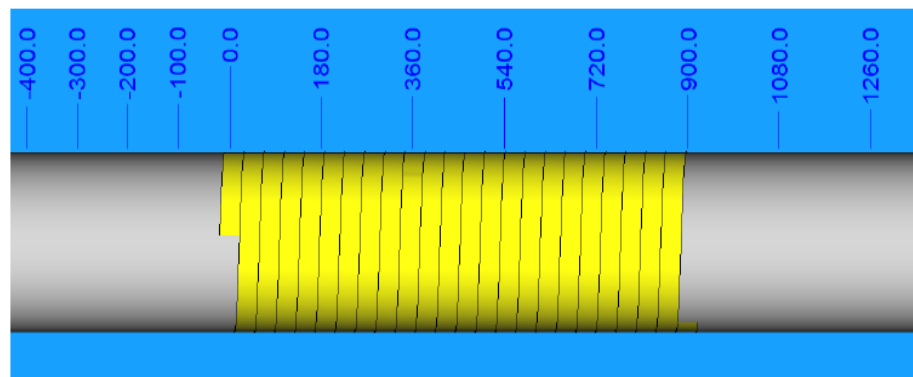
### 2.3.3. Manufacturing of Composite Tanks by Filament Winding Technique

The main manufacturing technique to produce composite tanks is the filament winding method. The filament winding technique was found in the 1950s as a composite manufacturing technology and it has been developed considerably over time<sup>70</sup>. This process consists of continuous filaments, tensioner mechanism for this continuous filament, a resin bath for wet winding. The filament winding process was summarized in section 2.1.3.

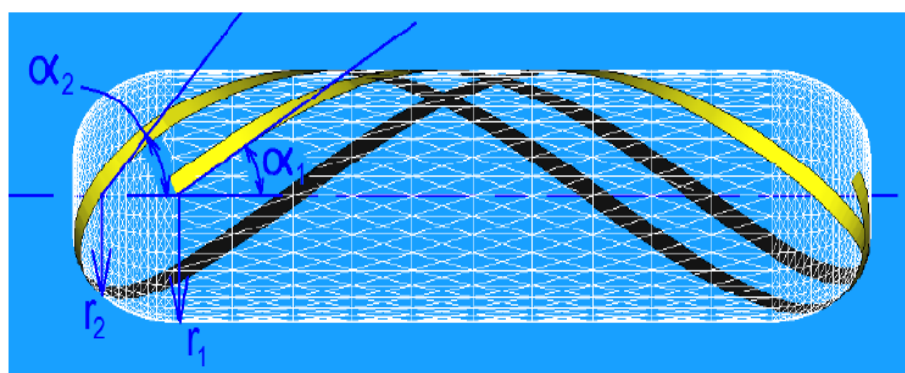
Filament winding machines that used to produce composite tanks are 4 axis and computer numeric controlled machines (CNC). These CNC controlled filament winding machines need G-Codes and these G-Codes can be produced by using commercial CAM software suitable for the filament winding process. To produce these G-codes, liner shape, fiber type, degree of coverage value, friction factor, etc. should be defined to the software properly.

For the filament winding process, there four different types of winding processes which are hoop winding, helical winding, polar winding and non-geodesic winding. Hoop winding also known as circumferential winding is the basic type of filament winding process and the winding angle is nearly 90°. Hoop winding is suitable for giving hoop and crush strength for pressure vessels but does not provide tension/compression and bending strength. Helical layers can be used for lower winding angles as compared to hoop winding onto axisymmetric pressure vessels but helical winding is suitable for vessels that have equal pole openings. Polar winding is only suitable for pressure vessels which length is shorter than its twice diameter. Also, polar winding is used for covering vessels completely up to the poles. Non-geodesic winding is the most useful and

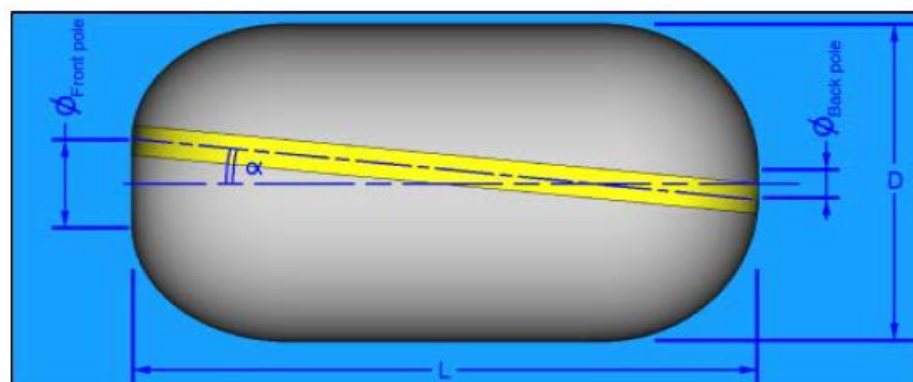
multifunctional winding type to produce composite tanks. Geodesic winding path is the shortest path across the surface of a mandrel between two points. However, non-geodesic winding path uses friction between the fiber and the mandrel to move away from the geodesic path. Friction factor between the surfaces directly affects the winding angle and winding path in non-geodesic winding. Non-geodesic winding is the most effective winding type to produce cylindrical composite parts. The different winding types are displayed in Figure 2.20.



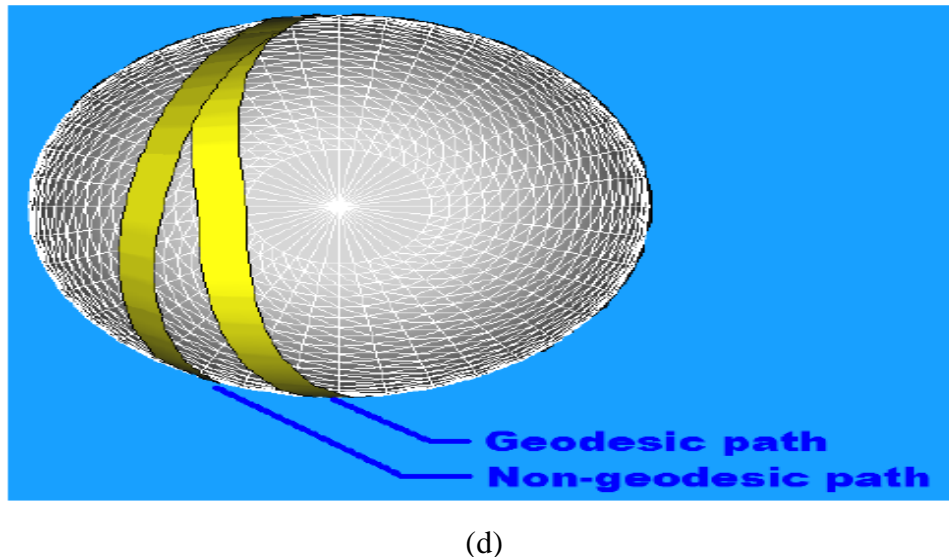
(a)



(b)



(c)



(d)

Figure 2.20. Winding types for filament winding (a) Hoop winding, (b) Helical winding  
 (c) Polar winding and (d) Non-geodesic winding.

#### 2.3.4. Performance of Composite Tanks

As mentioned above, composite tanks are the most critical mediums for hydrogen storage, it is essential to understand the performance and failure mechanisms of these systems. Some researchers studied the mechanical properties and burst pressure of composite vessels in the literature. ISO/TS 15869:2009 delivers requirements and safety factors for each type of composite tanks to be used in onboard applications<sup>71</sup>.

Shao et al. manufactured aluminum lined composite tanks with epoxy and vinlyester matrices and carbon fiber reinforcements. The winding angle of the helical layer was selected  $\pm 15^{\circ}$  to the longitudinal axis of the vessel and 1 mm helical layer was wound and a total of 1.5 mm hoop layer was wound. Besides, a preliminary experimental investigation was carried to determine the effect of matrix type on the tensile behavior of the composites. For this aim unidirectional composite plates were manufactured with filament winding machine. Tensile test specimens obtained from these plates and subjected to tensile testing.

Composite tanks were subjected to hydrostatic tests up to burst pressure increasing internal pressure with a rate of 20 MPa/min to obtain the failure modes and burst pressure performance of composite tanks.. During the burst pressure test, for full strain measurement, the digital image correlation technique (DIC) was used. In addition,

to measure the local radial deformations, five strain gauges were used at the center, front and back portions of the cylindrical sections. To compare with strain values obtained from strain gauges measurements, the DIC evaluations of the average strain components were performed on three sections, front, center and back<sup>72</sup>. A specimen prepared for DIC and strain gauge measurements is given in Figure 2.21 .

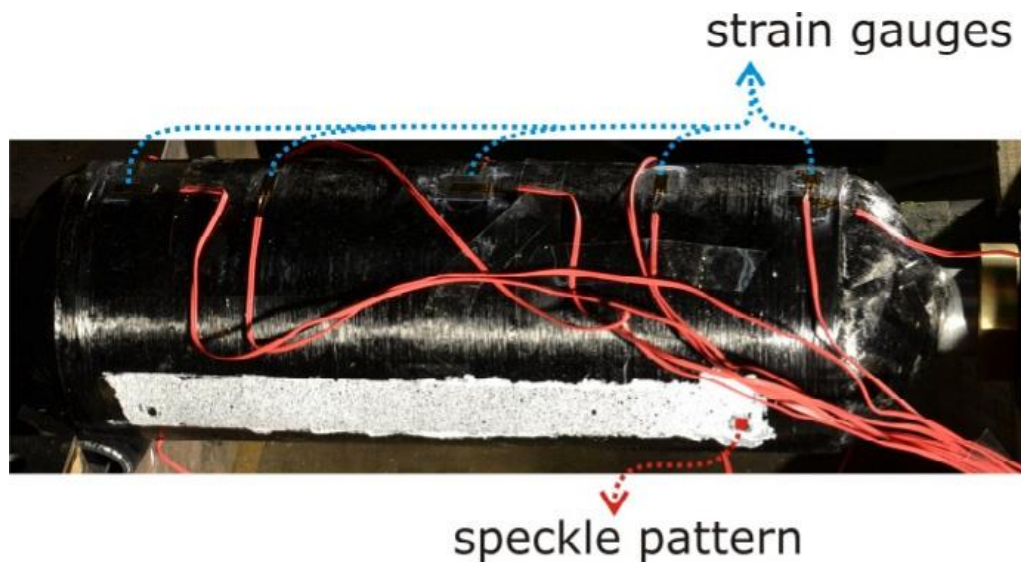


Figure 2.21. A specimen prepared for burst pressure testing.

(Source: Shao et al., 2016)

The preliminary tensile test results showed that, carbon/epoxy UD plates have higher tensile properties as compared to carbon/vinlyester UD plates. However, the burst pressure test results showed that carbon/vinlyester composites tanks have higher burst pressure results than carbon/epoxy composite tanks. Carbon/vinlyester composites tanks have an average burst pressure of 76.5 MPa however carbon/epoxy composite tanks 73 MPa. The failure modes of composite tanks showed that, all the specimens were failed from the front dome sections. Moreover, it was observed that hoop layers failed first, then helical layers and finally liner. It also observed that strain values obtained from strain gauges and DIC technique showed similar results. The strain results obtained from DIC technique and strain gauge measurements were given in Figure 2.22.

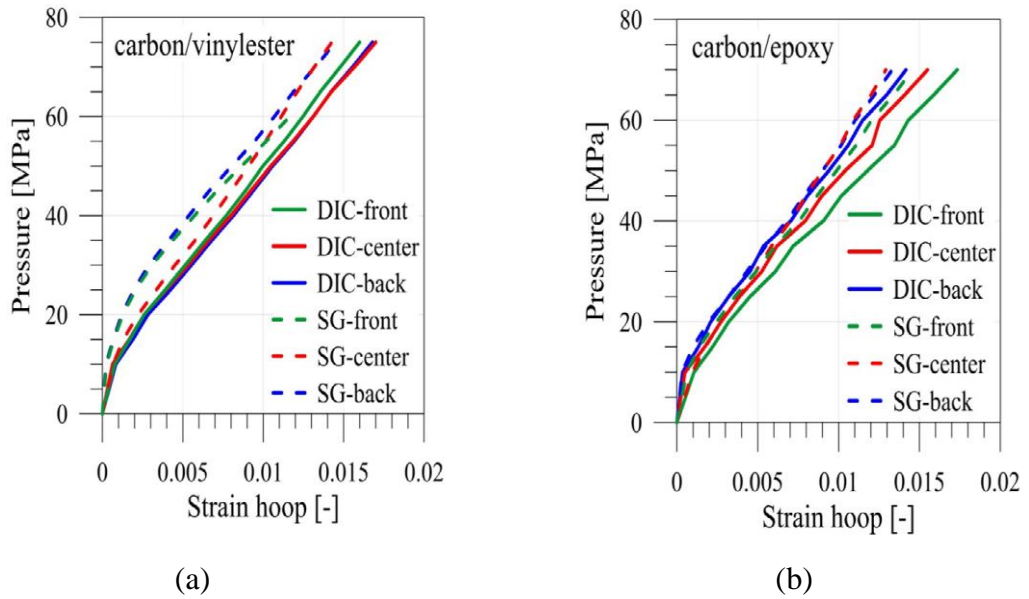


Figure 2.22. Pressure vs. hoop strain curves of DIC and strain gauges measurements: (a) carbon/vinylester specimen; (b) carbon/epoxy specimen.

(Source: Shao et al., 2016)

For another study, Shivamurthy et al. fabricated and tested aluminum lined epoxy-glass composite tanks for high-pressure gas storage. They used aluminum 6063 as a liner material. 1200 tex S-glass were used as a reinforcement material and the epoxy resin system was used as matrix material.  $9.8^0$  helical winding angle was used and a total of 10 pressure vessels were manufactured. 4 of them were subjected to burst pressure tests and the rest of them were used for the cyclic test. For the cyclic test, composite tanks were hydrostatically pressurized up to service pressure of 35 bar for 13000 cycles and no leakage was observed. For burst tests, composite tanks were pressurized up to 1.25 times the service pressure for 5000 cycles no failure was observed <sup>73</sup>.

Harada et al. studied to predict the burst pressure of Type- III composite tanks by considering the inhomogeneity of carbon fiber packing through experimental work. The proposed method for predicting the burst pressure enables to estimate the change in the burst pressure due to the difference in fiber volume fraction. Aluminum 6061-T6 was used as a liner material, carbon and glass fiber was used as a reinforcement. Composite tanks were manufactured with the filament winding method by using different filament winding tension (from 1 N to 42.7 N) and different laminate orientation.  $14.3^0$  helical winding angle for carbon fiber and  $12.7^0$  for glass fiber was used and hoop layers were winded over the helical layers. The local deformations at the surfaces of the composite

tank were measured by using strain gauges. The burst pressure results showed that composite tanks having additional glass fiber layers have higher burst pressure as compared to only carbon fiber layered composite tanks nearly 150 bar. Also, it was observed that filament winding tension has no significant effect on the burst pressure of composite tanks. In addition to experimental work, the proposed method to predict the burst pressure rely on the constant stress model helps consideration of the progressing of local fiber failure before to fracture and to quantitatively estimate the change in the burst pressure because of the variation in fiber volume fraction <sup>74</sup>. The experimental burst pressure result of manufactured composite tanks was given in Figure 2.23.

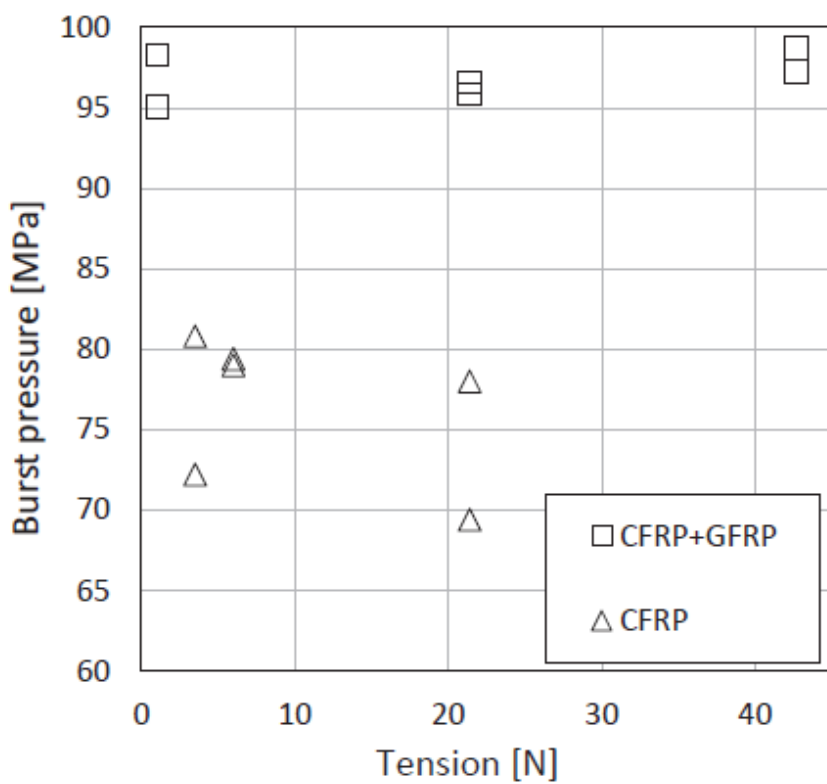


Figure 2.23. Experimentally measured burst pressure of composite tanks.

(Source: Harada et al., 2018)

Zu et al. proposed a design approach to determine the optimal winding parameters of composite tanks based on non-geodesic trajectories. The optimal roving bandwidth and the number of the tangent points on the fiber trajectory design were determined, and the burst pressures of composite tanks were determined experimentally and numerically. The model showed optimum roving bandwidth is 8.2 mm and the number of tangent points is 13. To verify the accuracy and feasibility of the model a specimen was manufactured for

the burst test. The helical winding angle and the friction factor are approximately  $11.5^\circ$  and 0.008, respectively. During the burst pressure test, a hydrostatic load is applied firstly up to autofrettage and then the load is released. After the autofrettage process, the composite tank was subjected to the hydrostatic load up to burst pressure. The burst pressure results showed that the composite pressure tank has a burst pressure of 850 bar, the developed model gives the burst pressure of 891 bar which means there is only a difference of 4.82%. Furthermore, the results showed that increasing of the roving bandwidth causes to fibers seriously overlapping. When the roving bandwidth decreases, the layer thickness of the dome section increases. It is also shown that a suitable increase in the number of tangent points reduces the fiber overlap, and the thickness of composite layers is distributed more uniformly along dome sections<sup>75</sup>. The number of tangents points are presented in Figure 2.24.

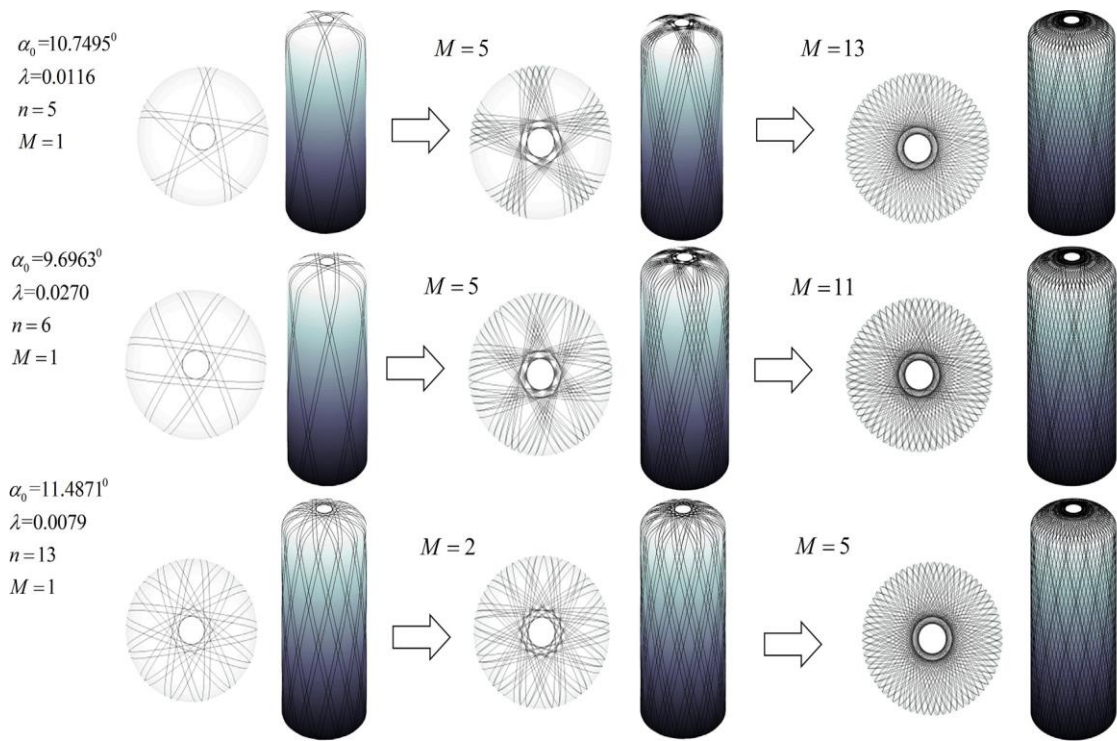


Figure 2.24. The number of tangent points used for optimization.

(Source: Zu et al., 2019)

Hocine et al. developed an analytical model that provides an exact solution for stresses and strains on the cylindrical section of the hydrogen storage tanks. The theoretical model was validated by manufacturing and experimental testing of some

prototypes. Aluminum 6061-T6 was used as a liner material. Toray T-700 12K carbon fibers were overwrapped the aluminum liner with an M10 epoxy resin system by filament winding technique. The pressure test as carried out at three stages. First of all, a sealing test was applied by using oil up to 40 bar. Then the sizing procedure of the three test-tubes at a 200-bars pressure was applied. After the sizing operation, the test-tubes are subjected to a progressive loading pressure. Burst test results showed that 718 bar burst pressure has been obtained which is 16% higher compared with the calculation prediction of 600 bar<sup>76</sup>.

The influence of filament winding parameters and the fiber volume fraction on the strength of composite tanks were studied by Cohen (1997), and Cohen et al. (2001) respectively. These studies indicated that manufacturing parameters such as laminate stacking sequence, winding tension and winding time significantly affect the final burst pressure of the composite tanks<sup>77,78</sup>.

Nimdum et al. carried out a study to determine the axial behavior of composite storage tanks manufactured with filament technique at the beginning of the pressurization process. The liner material used in this study is polyamide 6 thermoplastic material and two stainless steel metallic bosses were integrated this liner. The pre-impregnated carbon fibers (towpregs) overwrapped plastic liner surface by filament winding process and Type-IV composite tank was manufactured. 7 mm carbon fiber roving width and 40 N filament winding tension were used during the filament winding process. The deformations occurred during burst pressure test was determined by using three different measurement technique. First, a linear variable differential transformer (LVDT) sensor attached at the top of a pressure vessel to determine the total axial displacement. Secondly, three strain gauges attached to the dome and cylindrical zones to measure the local deformations. Lastly, the DIC technique was performed to obtain high accurate both of displacement and strain field during burst testing<sup>79</sup>.

In another study, Hwang et al. carried out experimental tests and developed an analytical method to determine the size effect on the strength of a composite pressure tank. To verify the of the analytical method, experimental tests were performed using fiber strand specimens, unidirectional laminate specimens and composite tank. The composite tanks were manufactured by 4-axis filament winding by using T800 carbon fiber/ Epon826 epoxy resin. 3 helical and 7 hoop layers were winded over the liner with 15 N winding tension and 10 mm roving bandwidth. After the filament winding process the composite tanks were subjected to the curing process at 80<sup>0</sup> C for 1 hour and 120<sup>0</sup> C

for 3 hours. The composite tanks were subjected to burst tests and during burst test local deformations were measured by using strain gauges. In the analytical method, the Weibull weakest link model and the sequential multi-step failure model are studied and compared. The results showed that, there is a good agreement between experimental and analytical results for the unidirectional laminates and hoop layers in composite tanks<sup>80</sup>. Hwang et al. has another study about the determination of fiber material properties used for composite tanks. Fiber material properties have the dominant effect on the burst pressure and performance of composite tanks so their properties should be measured accurately. For this aim, they developed the hoop ring test which ring specimens are obtained from full-scale composite tanks. The results showed that hoop ring test results gives the similar values with burst test results<sup>81</sup>.

Wang et al. investigated the residual performance of five type IV composite tanks used for hydrogen storage. The composite tanks have a capacity of 39 L and a working pressure of 700 bar. The composite tanks have a plastic liner which made of polyamide 6 material. Carbon fibers were overwrapped this plastic liner with epoxy resin and for outermost layer glass fiber was used to provide good impact resistance. To investigate the residual performance of composite tanks, some tests were carried out after 46500 km driving distance. Firstly, external and internal visual inspections were carried out. After than crystallinity test, hardness test, and tensile test for plastic liners were performed for one tank. The remaining four tanks were subjected to hydraulic burst and fatigue test. For fatigue test, two composite tanks were subjected to hydraulic pressure ed between 20 and 875 bar for 5500, 11,000 cycles, respectively with a cycle rate of 8 cycles per minute. For the burst test, two tanks after fatigue test and two tanks before fatigue test were used. The fatigue test results showed that there is no leakage between both two vessels even after 46500 km driving experience. However, during the refueling—the emptying process shrinkage phenomenon of composite tanks was observed. It is also determined that, composite tanks after fatigue test have burst pressure 65 bar lower than composites tanks which subjected to direct burst test<sup>82</sup>. It was also observed that composite tanks were divided a few separate parts after failure. The front and back dome sections of the composite tanks are divided from the cylindrical section. The failure modes of the two different composite tanks after the burst test are given in Figure 2.25.

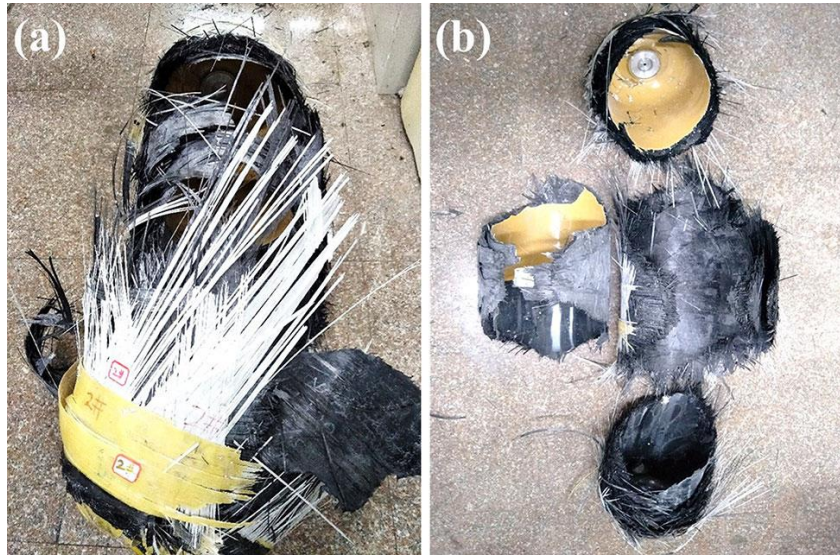


Figure 2.25. Composite tanks after burst test<sup>82</sup>.

(Source: Wang et al., 2012)

Frias et al. developed methodologies for structural health monitoring (SHM) of the composite tank. The main objective of the study is to reduce safety risks during operation by determining critical aspects. Fiber Bragg grating optical sensors and polymeric piezoelectric were used. The sensors were attached to the liner composite interface during composite tank manufacturing. Steel liner is with a 0.7 mm thickness with a 24 L volume capacity was used. The different types of sensors were placed over the steel liner in specific locations. After then the composite layer was overwrapped over the liner and sensors. Glass fiber and polypropylene thermoplastic was used with a 25 mm bandwidth by using ten rovings. 22° helical winding angle was applied and the polypropylene matrix was melted at 250°C. The values obtained from the sensors were compared with the analysis of test data<sup>83</sup>.

Perillo et al. studied impact events on composite tanks. The composite tanks were subjected to low-velocity impact loads experimentally and a finite element model was developed to compare experimental and numerical results. The composite tanks were composed of a polyethylene liner, glass fiber as a reinforcement material and vinylester resin. The inlet and outlet boss sections also attached to the polymeric liner. The experimental impact results were accurately predicted by the finite element model with the various impact locations and energies<sup>84</sup>.

Zu et al. investigate the stress/strain distributions and the ultimate strength analysis for composite spherical tanks manufactured by filament winding technique based on non-geodesic winding trajectories in another study. To identify the suitable tangent points, the non-geodesic patterns were simulated. Aluminum 6061-T6 was used as a liner material and T800 carbon fiber and EW-60D epoxy resin were used as a reinforcement and matrix material, respectively. The number of tangents points were selected as 6 since when the number of tangent point increases, fiber builds up increases. Strain gauges were placed in the composite tank to measure the hoop and longitudinal strains. The results showed that burst pressure according to the maximum strain criterion is found as 910 bar, and the experimental burst pressure is found as 1050 bar<sup>85</sup>. The manufactured composite spherical tank is given in Figure 2.26.

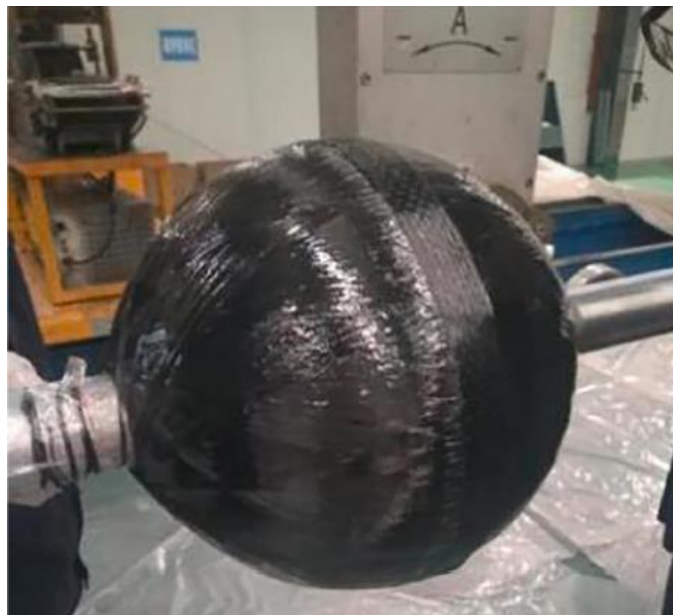


Figure 2.26. The manufactured composite spherical tank.

(Source: Zu et al., 2019)

The same research group Zu et al. was carried out another study to determine the mandrel profiles after each wounded composite layer and then generate new winding paths. To understand the effects of winding paths obtained from updated mandrel profiles, different winding angles, dome thickness distribution and friction factor were investigated. The burst pressure was also predicted by finite element analysis including progressive failure method. To obtain mandrel profiles which, change after each wounded composite layer, the laser scanner was used. First of all, the neat liner is scanned by the

laser scanner to determine the of mandrel profiles coordinates and generate the original winding path. Then the mandrel is updated after the wounded composite layer according to the former mandrel. Also, numerical simulations are carried out according to winding paths obtained until the end of experiments. Aluminum 6061- T6 was used as liner material and Toray T700 carbon fiber is used with a reinforcement material with epoxy resin. The aluminum liner with unequal dome parts is shown in Figure 2.27.

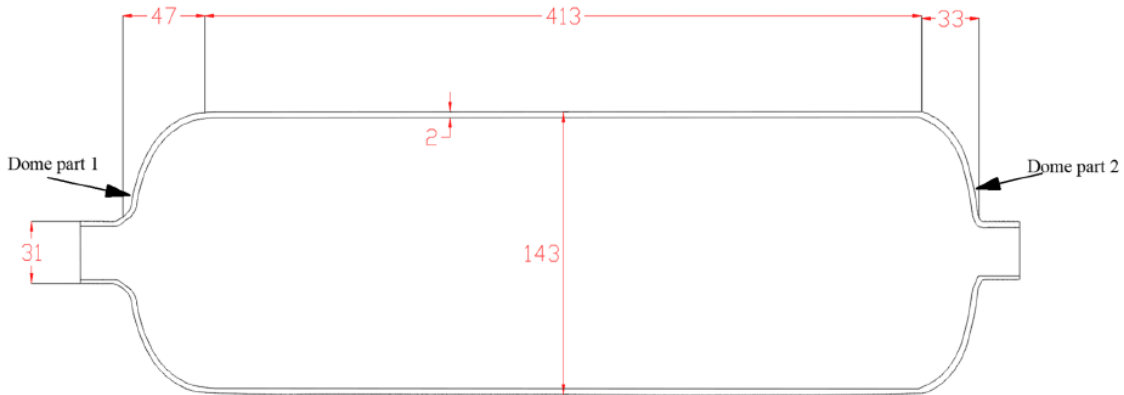


Figure 2.27. The geometry of aluminum liner with unequal dome section.

(Source: Zu et al., 2020)

The results showed that, as the layer thickness increase with a range of 0-30 mm, winding angles do not have a significant change. However, the winding angles which are closed to polar openings change significantly. As compared to the original mandrel, the winding angle increases as the mandrel profiles update. It is also shown that, when the mandrel profiles updated, the slippage coefficient decreases, which directly affects the winding path. The thickness obtained by applying the not-updated method, the thickness distribution around polar openings is reduced by updating the mandrel profile. The load-carrying capability of the composite section in the circumferential direction is increased by this method so the burst pressure performance of the composite tanks was also increased. The burst pressure value of a composite tank designed with a non-updated profile was found as 84 MPa. However, by applying an updated profile design to the composite tank, the burst pressure is found as 88 MPa<sup>86</sup>.

The strength and fatigue performance of the composite tanks significantly decrease at high temperature and there is an important temperature increase for composite tanks during the fast filling process. Zheng et al. studied the fatigue life of a composite tank for hydrogen storage under a real hydrogen environment. The fatigue test system

was designed for 700 bar pressure since 700 bar working pressure is critical for hydrogen vehicles to reach the required driving range. Five specimens were tested at the same time and the hydrogen filing and un-filling time is 10 min. Composite pressure tanks consist of an aluminum liner, carbon fiber reinforcements and epoxy matrix with a 70 MPa working pressure was used for fatigue test. Temperatures variations during filling and un-filling processes determined by using temperature sensors placed on the different positions of the composite tank. It is observed from the temperature test that the temperature in the composite tank did not exceed 100 °C throughout the test which means the composite tank can be used safely for onboard applications. Fatigue test results showed that after 500 cycle fatigue tests, the burst pressure of the composite tank was 119 MPa which is 15% percent lower than it's designed burst pressure of 140 MPa. Moreover, an additional sample was subjected to a fatigue test until the failure with a pressure of 70 MPa under a hydrogen environment. The failure mode was observed as a hydrogen leakage on the outer surface of the composite vessel. The fatigue life of the composite tank was found as 5122 cycles which is less than 12000 cycle hydraulic fatigue test life. It is understood from this study, high-pressure cyclic loading and elevated temperatures are directly affecting the mechanical properties of the epoxy resin and carbon fiber/epoxy composites, thus the performance of the composite tank<sup>87</sup>. The composite tank after fatigue test can be seen in Figure 2.28



(a)



(b)

Figure 2.28. (a) Composite tank and (b) fragments after failure.

(Source: Zheng et al., 2013)

Bai et al. investigate the strain response of glass fiber reinforced epoxy matrix composite tanks subjected to pressure tests. Three different filament wound composite tanks were fabricated and subjected to pressure. During the pressure test, the strain values at the outer and inner surface of the vessels were measured. To compare the measured values obtained from the experiment, a 3D finite element method featuring a progressive damage model based on Hashin Criterion was developed. Material characterization tests such as tensile, double cantilever beam and flexural test were carried out to obtain material data required for the numeric model. The results showed that radial strain values are higher than axial strain values and there was a 12% difference between the experimental numerical results<sup>88</sup>.

The characterization of the mechanical properties of the composite section of the composite tanks is also very important since these mechanical properties directly affect the performance of the composite tanks. Therefore, some researchers studied the mechanical properties of filament wound composites. Reddy et al. investigated the effect of different reinforcement materials on the mechanical properties of filament wound composites. Toray T-300 12K, T-700 12K and E-glass prepreg filament were used as a reinforcement material and LY 556 epoxy resin system was used as a matrix material. A steel rectangular plate was manufactured and attached to the filament winding machine. These different reinforcement materials were wounded over the steel mandrel and composite unidirectional plates were manufactured by filament winding technique. The test specimens were prepared from these plates according to relevant standards. Tensile, compression, flexural and interlaminar shear strength (ILSS) behavior of composite for each different reinforcement materials were determined. The tensile test results showed that, composite specimens obtained from T-300 and T-700 carbon fibers have similar tensile strength and tensile modulus. The compression strength was found 721.79 MPa for glass fiber reinforcement, 674 MPa for T-700 reinforcement and 551 MPa for T-300 reinforcement. For flexural strength and ILSS, the maximum value was obtained from T-300 reinforcement. However, ILSS test results showed that, E-glass reinforcement has higher ILSS results as compared to T-700 reinforcement. Actually, T-700 carbon fiber has higher mechanical properties as compared to T-300 carbon fiber, so the authors claimed that the wet resin system could not be suitable for T-700 carbon fiber<sup>89</sup>.

In another study, mechanical properties of composite plates manufactured by filament winding technique was determined. Carbon/epoxy towpregs from were used as a reinforcement material. Carbon fiber is Toray T-700 and the epoxy resin system is

UF3369. The towpreg filaments were wounded over a steel plate by dry winding (Figure 2.29).



Figure 2.29. Manufacturing of composite plate by filament winding technique.

(Source: Almedia et al., 2014)

After the winding process, the plates were cured by hot compression for 150 min at 125<sup>0</sup> C. Tensile, compressive and shear properties of composite laminates were determined. For the tensile test, modulus of elasticity in the fiber direction was found as 129.8 GPa and 9.1 GPa in the transverse direction. Also, Poisson's ratio was measured by using longitudinal and transverse extensometers and found as 0.31. Compression strengths were found as 520 MPa and 103.3 GPa for axial and transverse directions, respectively. However, the V-notched shear test results did not give acceptable results, since most of the specimens failed on the top and bottom sections<sup>90</sup>.

Hamed et al. characterize the mechanical properties of carbon/epoxy and glass/epoxy composite plates manufactured with filament winding machine. First of all, a neat epoxy matrix was tested. Tensile test specimens were prepared from the epoxy matrix according to relevant standards. The ultimate tensile strength of the epoxy matrix was found as was 51 MPa. To determine the tensile and shear properties of the composite sections, carbon/epoxy and glass/epoxy composite plates were manufactured by filament winding technique using a wood mandrel. The tensile test specimens were cut from these composite plates for angles of 0°, 90° and 45°. Tensile modulus as found 101.2 MPa for carbon/epoxy composite and 36.6 MPa for glass/epoxy composite. The shear stress

properties of the composite were also investigated by prepared specimens from 45° direction. The in-plane shear modulus is found 4.34 MPa for carbon/epoxy composites and 4.08 for glass epoxy composites<sup>91</sup>. The tensile stress-strain behavior of carbon/epoxy and glass/epoxy composites for 0° is given in Figure 2.30.

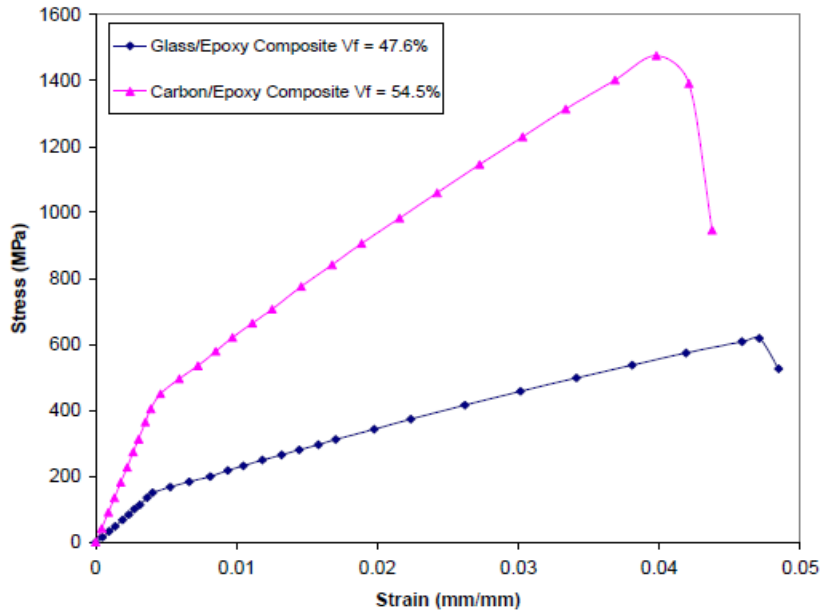


Figure 2.30. Stress-strain behavior of carbon/epoxy and glass/epoxy composites.

(Source: Hamed., 2008)

Chen et al. investigated the interfacial behavior of T800 carbon fiber/epoxy composites by ring test, short beam shear test and fracture surface observation. Also, scanning electron microscopy (SEM), X-ray photoelectron spectroscopy (XPS) and atomic force microscopy (AFM) were used. Toray T800 carbon fibers were used with three different epoxy resin system. The composite specimens were manufactured by filament winding technique with a winding tension of 25 N. The ILSS and tensile strength obtained from the ring test of T800 CFs reinforced composites were found 123 MPa and 2570 MPa respectively which is quite higher than commercial T300 or T700 composites. After ILSS tests, SEM observations of the interphase regions were carried out. SEM observations showed that, composites had strong interfacial adhesion, carbon fibers covered well by epoxy resins<sup>92</sup>.

In addition to the helical and hoop layers overwrapped by the filament winding process, doily layers can be utilized to reinforce the front and the end dome sections of the composite tanks to reduce the total usage of carbon fiber and to improve the burst pressure performance of composite tanks. The front and end dome sections of the

composite tanks are known to the weakest portions of the tanks. Since it is not possible to wind hoop layers on the end domes directly by filament winding technique, an additional layer, either a unidirectional or woven fabric, can be placed on the end domes. In literature there are very limited studies about the utilization of doily layers and none of them are experimental study. Roh et al. studied finite element analysis of composite tanks for hydrogen storage and their study includes an examination of the usage of doily layers to reinforce the dome and the boss sections of the composite tanks. For model, Toray T-700 was selected as reinforcement material with 60% fiber by volume. The composite tanks were designed for a minimum burst pressure of 158 MPa. High-density polyethylene (HDPE) was modeled as a liner material. 3-D FE analysis was developed using ABAQUS with the Wound Composite Modeler. To decrease the carbon fiber usage and need for several helical layers, doily layers were placed at the dome section for reinforcement as shown in Figure 2.31.

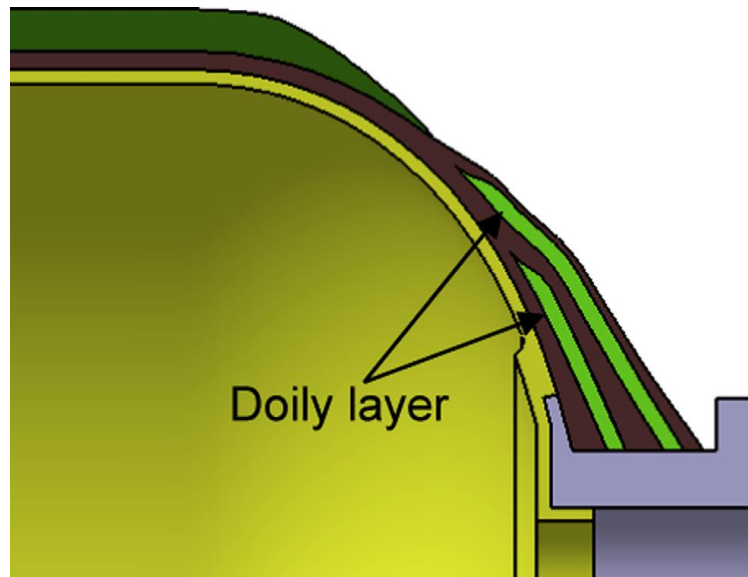


Figure 2.31. Integrated doily layers the numeric model.

(Source: Roh et al., 2013)

Effect of winding angle, dome shape, helical and hoop layer thickness on the performance of composite tank investigated by numeric modeling. The results obtained from the numeric model indicated that changing the hoop layer winding angle can be helpful to reduce carbon fiber usage up to 5% percent. Using doily layers reduced the stresses near the dome sections. However, the transition section from the cylindrical part to the dome section did not affected since this section does not reinforced by doily layers.

In another study, Musthak et al. developed a mathematical model to predict the inter-laminar stresses and strains of the composite tank. They placed additional doily layers at the end dome section. The design pressure of the composite tanks was 50 bar and low-density polyethylene was used as a liner material. E-Glass reinforcements with epoxy layers were wound over the liner with filament winding technique. Netting analysis was used to calculate the helical, hoop, and doily layers thicknesses. The composite tanks were designed with a 0.6 to 0.8 stress ratio to prevent the dome or boss section failure. The number of helical hoop layers was calculated according to netting analysis. The designed layer orientations on the composite tank were shown in Figure 2.32. The developed mathematical model for the composite tank was validated experimentally. The composite tank burst pressure was as 55.3 bar which shows the developed model was safe. Furthermore, it was understood that the transverse shear force was responsible for failures at pole openings and hoop-doily junctions<sup>94</sup>.

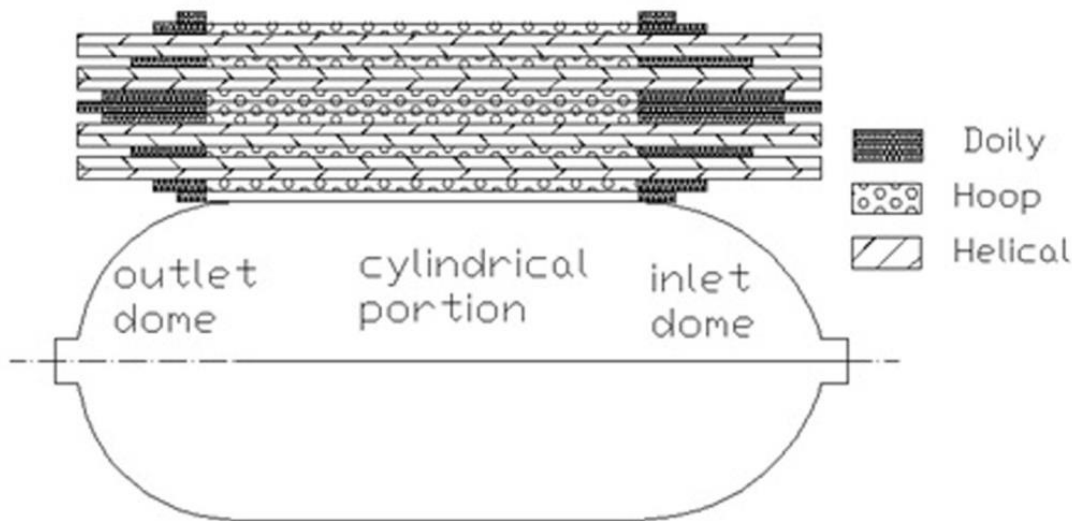


Figure 2.32. Layer orientations of composite tank.

(Source: Musthak et al., 2016)

Hua et al. modeled a composite hydrogen storage tank by using ABAQUS. T700 carbon fiber with epoxy composite was considered in which the epoxy was replaced with a low-cost vinylester resin and low-cost resin with an alternate sizing. The model also consists of doily layers for dome section reinforcements. However, in the model, it is assumed that doily layers were manufactured by braiding technique and they were placed in the dome section at 45° fiber direction. Therefore, the strength of doily layers was decreased by 30% in the model since braided material has lower strength as compared to

filament wound fiber. The results showed that replacing epoxy with a low-cost vinyl ester resin and alternate sizing reduces the tank weight. The alternate tank design showed a potential 4-7% saving in composite usage<sup>95</sup>.

Kumar et al. studied the failure analysis of the geodesic dome section of the composite tanks. The classical laminate theory of composites was used to predict the failure conditions of the geodesic dome portion. Also, Finite element model was developed to the analysis of geodesic dome end and a cylindrical portion. Carbon fiber and epoxy resin were used for the model. Helical, hoop and doily layers were placed to the model. It is considered that doily layers were placed at 0° and 90° fiber orientations. Thickness of hoop, helical, doilies were calculated by using netting analysis and taken as 0.2mm, 0.45mm, 0.5mm, respectively. The failure was predicted by Classical laminate theory, Maximum stress, Tsai-Wu theories. The results showed that the operating pressure of the dome portion is 20MPa and the complete failure of the dome portion occurs at 25 MPa. At this portion 10 helical and 6 doily layers were used and 10.5mm total thickness was obtained<sup>96</sup>. The stress distribution of the geodesic dome section at failure pressure is given in Figure 2.33.

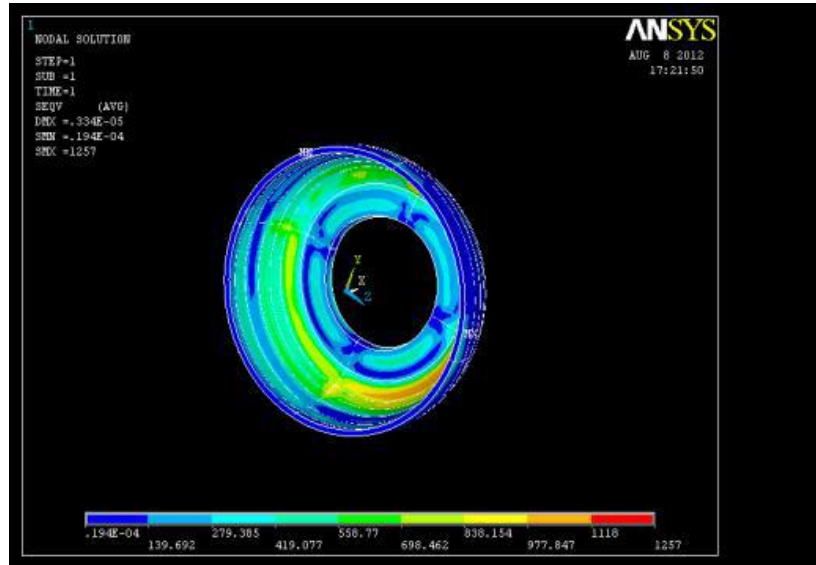


Figure 2.33. Stress distribution of geodesic dome section at failure pressure.

(Source: Kumar et al., 2012)

Madhavi et al., developed a methodology to determine the structural characteristics of composite tanks with integrated end domes. To predict the deformations and stresses in the composite tank three-dimensional finite element method was

developed. CarbonT300/ epoxy with a volume fraction of 0.51 was selected in the model. Doily layers were adapted to the model as an additional reinforcement layer. Four helical layers were used in the model but the number of hoop layers varies along the cylindrical section s and a constant hoop thickness of 0.3 mm was utilized. The thickness of the composite layer varies from cylinder to end dome junction. At the end dome section, the thickness is increased up to 25.6 mm. The helical thicknesses at the dome section junction were insufficient to provide cover to the hoop stresses therefore doily layers were utilized at the dome sections. Rubber liner was modeled with a thickness of 3 mm inside the composite section. A burst pressure value of 12.4 MPa was calculated in the cylindrical section and it increased towards the pole openings<sup>97</sup>. Burst pressure at different locations of the composite tank is shown in Figure 2.34.

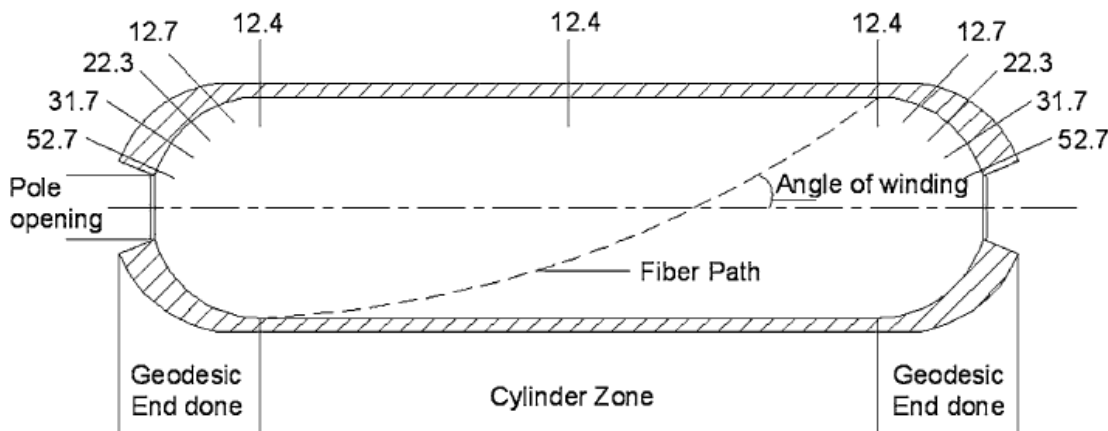


Figure 2.34. Burst pressure at different locations of the composite tank, MPa.

(Source: Madhavi et al., 2014)

The composite tank was subjected to hydraulic pressure to determine the burst pressure performance experimentally. The composite tank has a burst pressure of 11.2 MPa and the failure occurred at the cylindrical section. It is observed that the hoop fiber on the top layer of the composite tank had begun the fiber breakage failure from this location. When the pressure increases, the breakage of composite hoop layers propagated on the cylindrical section towards the end dome. The numerical results also showed that the metallic polar boss has minimum deformations as compared to rubber liner and the composite layers. Moreover, the analysis results indicated that rubber liner transferred the entire load to the composite section and the composite section became the major load-

bearing part<sup>97</sup>. A comparison of the stresses of all the components in the composite tank can be seen in Figure 2.35.

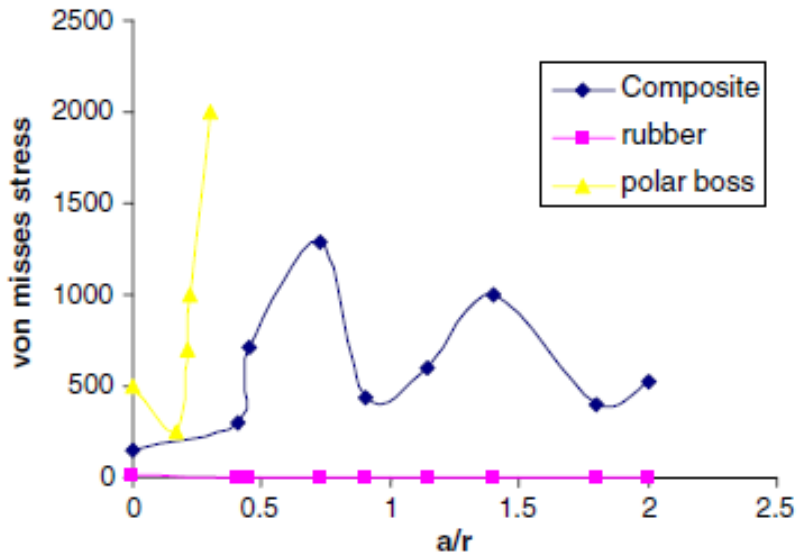


Figure 2.35. Stresses of all the components in the composite tank, MPa.

(Source: Madhavi, 2014)

# CHAPTER 3

## EXPERIMENTAL

### 3.1. Materials

In this thesis, glass fibers and carbon fibers were used as reinforcement materials. E-Glass fibers were obtained from Şişe Cam Inc. (Turkey), with a model name of FWR6 1200 tex. This type of glass fiber is developed for filament winding operations and suitable with epoxy resins.

Two different type of carbon fiber reinforcements were used. 800 tex A-49 carbon fiber filaments provided from DowAksa Inc. (Turkey), and 800 tex T700SC-12K carbon fiber filaments purchased from Toray Industries, Inc. (Japan). Both of them are suitable for filament winding applications, especially Toray T-700 carbon fibers are the most widely used carbon fiber reinforcement for composite pressure tanks all around the world. It is widely used in aerospace, sporting goods, and general industrial applications. These fibers were obtained with a form of standard dimensions and weight which are suitable for filament winding tensioner system.

A three-component, high-temperature cure epoxy system from Huntsman Inc. was selected as matrix material in this study. This epoxy system includes Araldite MY740 epoxy resin, Aradur MY918 curing agent, and DY062 accelerator. Viscosity of this epoxy resin type is suitable for filament winding applications and it is not cured in the room temperature which is critical for filament winding. The mechanical properties of all reinforcement types and resin system is given in Table 3.1.

Table 3.1. Mechanical properties of the fibers and the matrix

Property	Glass Fiber	T-700 Carbon Fiber	A-49 Carbon Fiber	Epoxy Resin
Elastic Modulus (GPa)	73	230	250	3.6
Tensile Strength (MPa)	2400	4900	4900	61
Strain at Failure (%)	1.2	2.1	2	2

Steel tubes were obtained and used as a liner component. The steel liners were originally manufactured for commercially used oxygen, nitrogen etc. tanks but it is modified as a liner for this study. Steel liners were manufactured with a 34CrMo4 type of steel with an average wall thickness of 4 mm. The drawing of the steel liner is given in Figure 3.1.

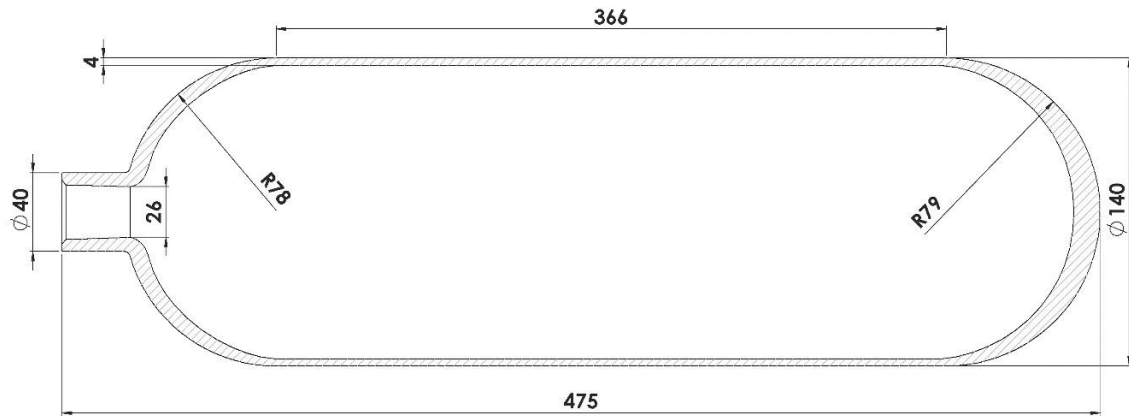


Figure 3.1. The geometry of the steel liner (dimensions are in mm)

The aluminum liners were manufactured by a local manufacturer. These liners were made of Al-6061-T6 with an internal volume capacity is about 5 L. The liners were manufactured by using the deep-drawing and spinning technique. The liners which can be used for filament winding applications must have ellipsoid and parabolic shape dome sections, however, the local manufacturer did not have a manufacturing capacity for ellipsoid or parabolic back dome sections. Therefore, the back dome section was manufactured as a flat shape, then the machining operation was applied to obtain an ellipsoid shape. The geometry of the aluminum liner can be seen in Figure 3.2.

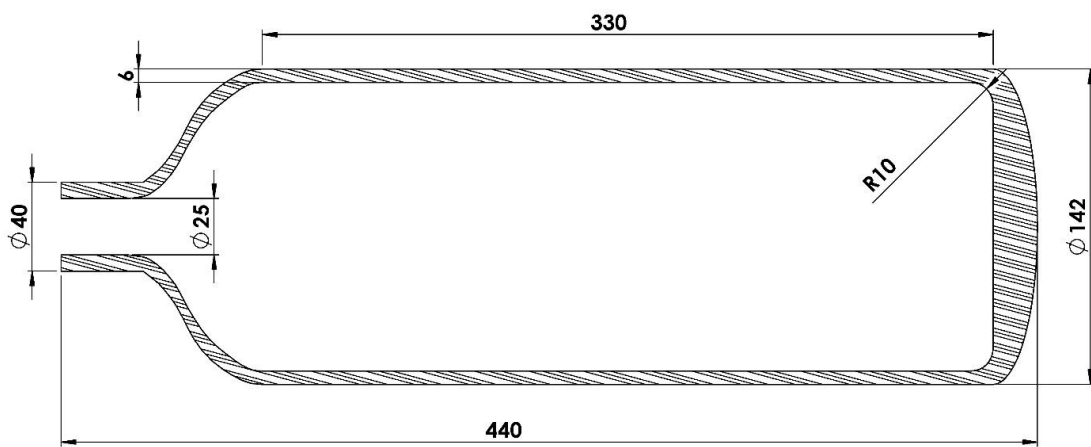


Figure 3.2. The geometry of the aluminum liner (dimensions are in mm)

### 3.2. Determining the Mechanical Properties of Composite Section and Liner

A preliminary experimental investigation was conducted to determine the mechanical properties of the aluminum liners and the composite section. To characterize the tensile properties of the aluminum liner, tensile test specimens were cut from the aluminum liner by using a water jet, and the tensile tests were performed using at least five specimens according to ASTM E8 – 16a standard<sup>98</sup>. The prepared specimen and the tensile test set up are given in Figure 3.3.

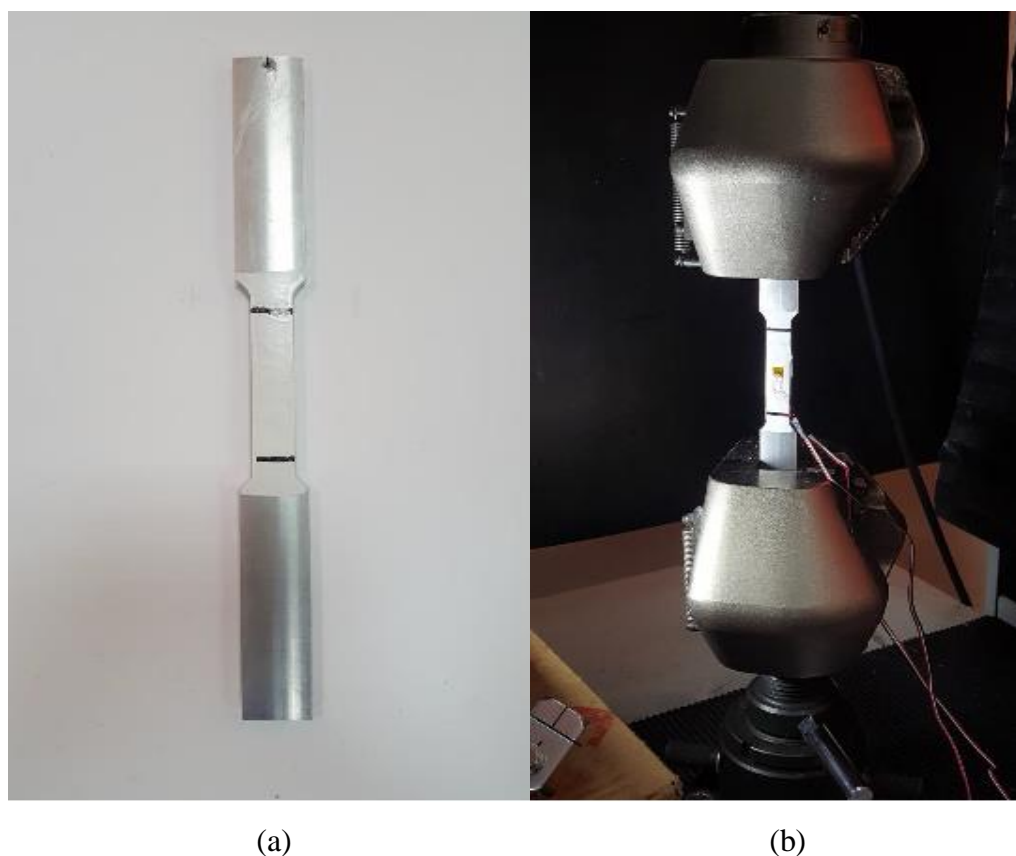


Figure 3.3. (a) Tensile test specimen sectioned from liner (b) Tensile test set up.

The mechanical properties of the composite section were also determined. For this aim, unidirectional (UD) carbon/epoxy and glass/epoxy plates were manufactured by filament winding technique. A square shape aluminum plate was manufactured with dimensions of 25 mm thickness and 350 mm length. This aluminum plate was attached to the filament winding machine and then a teflon film was coated over the aluminum

mandrel to separate the composite section from aluminum liner after the curing process. The composite plate manufacturing is illustrated in Figure 3.4.

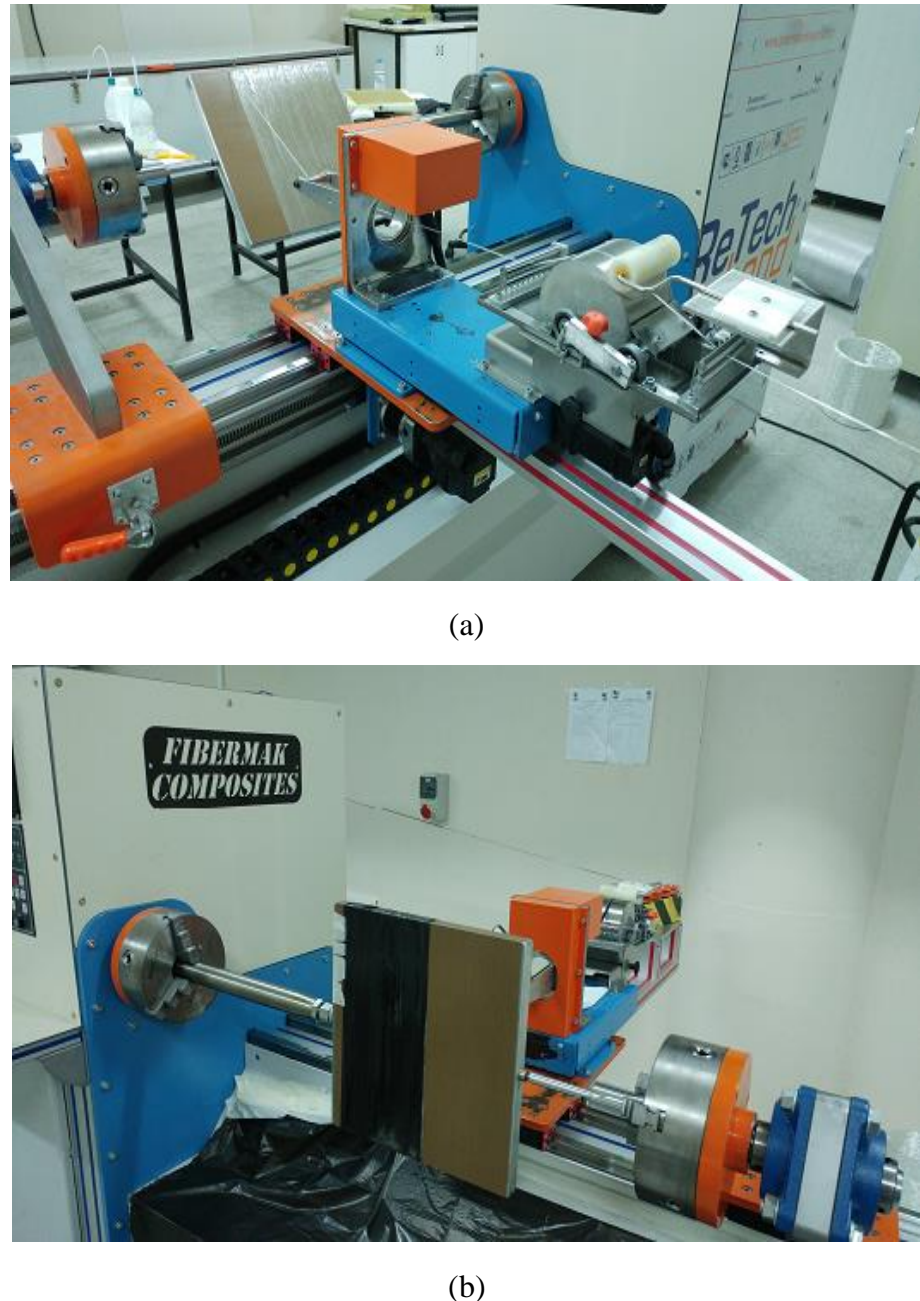


Figure 3.4. (a) Glass fiber/epoxy (b) Carbon fiber/epoxy plates manufacturing by filament winding

The composite test specimens were obtained from these composite plates by cutting using a diamond saw. Tensile tests were carried out for both fiber direction and transverse direction according to ASTM D3039-17 test standard with a dimension of 15x150 mm. At least five test specimens were used for each glass fiber and carbon fiber specimens. Shimadzu AG-IC 100KN universal test machine was used for tensile testing

and all tests were conducted at room temperature with a constant crosshead speed of 2 mm/min. The carbon fiber/epoxy composite test specimen during tensile testing is given in Figure 3.5.



Figure 3.5. Carbon/epoxy tensile test specimen during tensile testing.

### 3.3. Determining the Fiber Mass Fractions of Composite Sections

Matrix digestion test was carried out to calculate the mass fractions of composite plates according to ASTM D3171-Procedure B standard. In this procedure, sulfuric acid ( $H_2SO_4$ ), and hydrogen peroxide ( $H_2O_2$ ) were needed. First of all, nearly 1 g test specimens were prepared and weighted to the nearest 0.0001 g. Then each specimen was placed in a 100 mL glass beakers. Minimum 20 mL sulfuric acid was added to a glass beaker and the beaker was placed on a hot plate and heated until the mixture starts to fume.

After the solution was dark (with no appreciable change in color for 5 min), 50 or 30 % hydrogen peroxide was added down the side of the beaker to oxidize the matrix. The fibers floated to the top of the solution, and the solution appeared clear. In Figure 3.6. the floated fibers and clear appeared solution can be seen. After the solution appeared clear, the beaker was removed from the hot plate and allowed the solution to cool. The

fibers washed three times with distilled water and a final acetone wash was utilized after sulfuric acid and hydrogen peroxide was removed from the specimen. After washing, the specimens were dried in an oven for 1 hour and 100 °C. Finally, the dried specimens were weighted and new values were recorded.



Figure 3.6. Carbon/epoxy specimen in an acid solution during the matrix digestion test.

After dissolving the matrix and obtain only the weight of fibers, the mass fraction of composites can be calculated by using the formula in Eqn. 3.1.

$$W_r = (M_f / M_i) \times 100 \quad (3.1)$$

In this formula  $W_r$  represents the weight percent of fibers,  $M_f$  represents the initial mass of the specimen, and  $M_i$  represents the final mass of the specimen.

### 3.4. Determining the Thermomechanical Properties of Composite Sections

The thermomechanical properties of composites were carried out by dynamic mechanical analysis (DMA) using TA<sup>TM</sup> Q800 equipment. A dynamic force was applied at a frequency of 1 Hz in a three-point bending mode. The temperature range was 20 to 150°C with a ramp of 3°C/ min. The dimensions of the specimens were 3x13x60 mm. Dual cantilever mode which specimen is clamped at two ends and bent in the mid-point of the specimen were utilized for DMA tests. The glass transition temperature of both carbon/epoxy and glass/epoxy specimens was obtained by using a tangent delta ( $\tan\delta$ ) peak. The DMA test machine is given in Figure 3.7.



Figure 3.7. TA<sup>TM</sup> Q800 DMA test equipment.

### 3.5. Filament Winding Simulations

Before the filament winding process, winding simulations were conducted with CADWIND CAM<sup>99</sup> software. Filament winding parameters such as mandrel shape, fiber type, friction factor, number of rovings, winding patterns, etc. were given to the software as input values. Then winding simulations were carried out and G-codes were produced.

These G-codes were adopted to the filament winding machine winding started. Details of these simulations is given in the following sections.

### 3.5.1. Mandrel Definitions

To start filament winding simulations in CADWIND CAM software, first of all mandrel shape must be defined. For this purpose, the steel and aluminum liners were modeled in a CAD software. Then 60 points were selected on the outer section of modeled geometry and the coordinates of these points were adopted to the CADWIND software. Although it is possible to create mandrel in CADWIND software by using CADWIND's automatic mandrel creation tools, the above-mentioned method was selected because of its accuracy.

For steel liners, the diameter is defined as 140 mm, the length of the front and back dome is 40 mm. The boss section outer diameter is 35 mm. The steel liner defined as a mandrel to the software can be seen in Figure 3.8. In this mandrel, the apparatus is also defined which attach the mandrel to the filament winding machine.

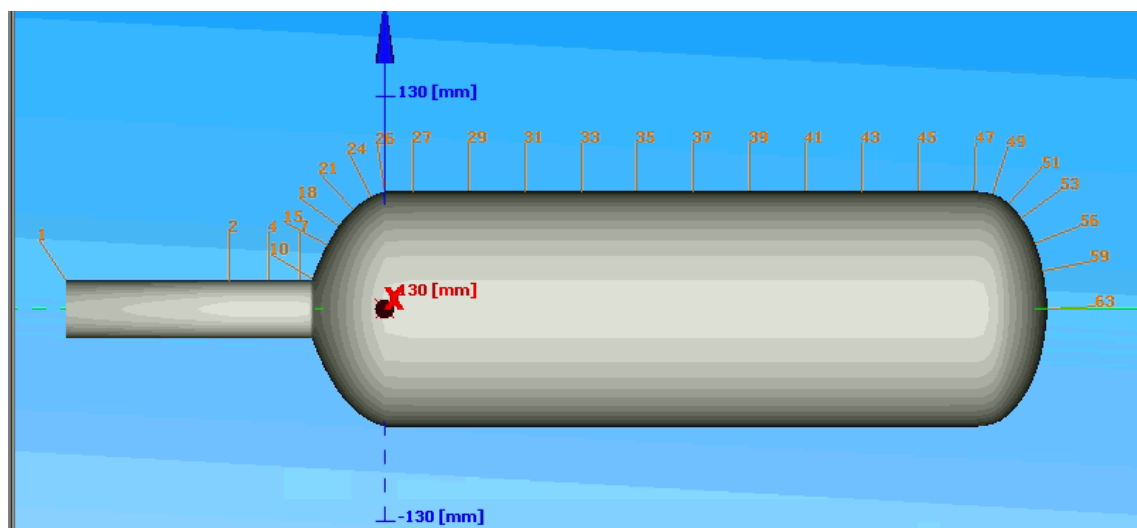


Figure 3.8. Steel liner defined as a mandrel in the CADWIND software

The aluminum liner has an outer diameter of 142 mm, front dome length is 35 mm and back dome length is 20 mm. The boss section has an outer diameter of 40 mm. Since the back dome length of the aluminum liner is too short as compared to commercial

aluminum liners, it is very critical to define mandrel correctly. The aluminum liner model is created CADWIND's automatic mandrel creation tools, critical dimensions of the liner were defined to the software. Aluminum liner defined as a mandrel is shown in Figure 3.9.

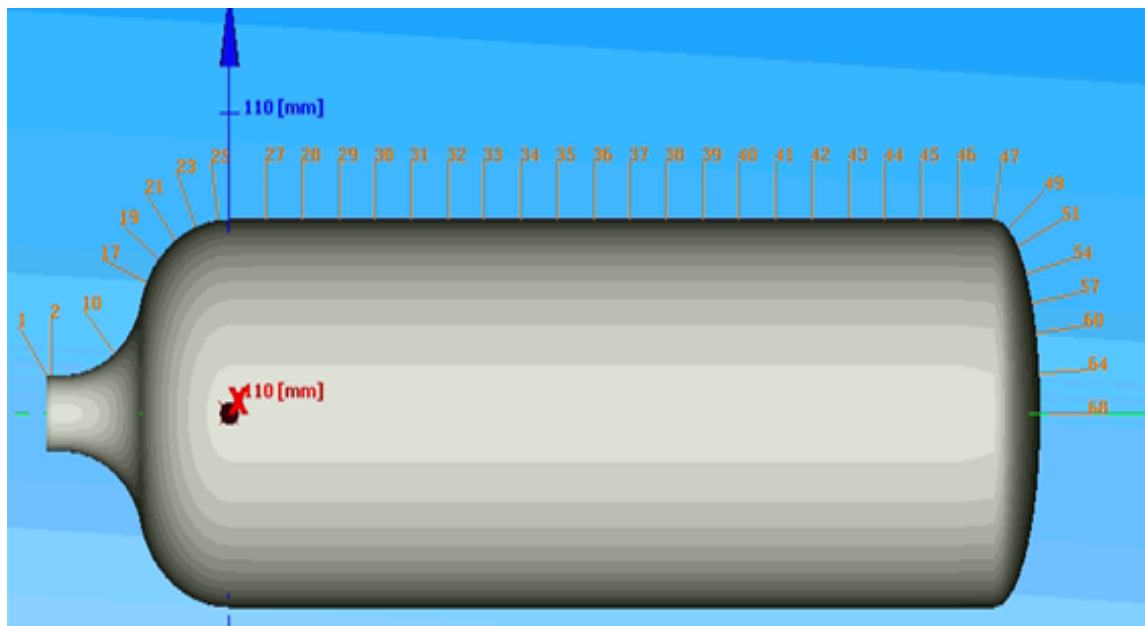


Figure 3.9. Aluminum liner defined as a mandrel in the CADWIND software

### 3.5.2. Winding Parameters Definitions

Winding parameters directly affect the winding angle, winding type, and winding time even winding can be possible or not. Therefore, winding parameters must be correctly defined to the software as input parameters. Material type, roving with, resin density, winding angle, friction factor, degree of covering, and dwell values should be defined.

#### 3.5.2.1. Winding Parameters Definitions for Steel Composite Tanks

Steel based composite tanks consisted of **two different reinforcements which are glass fibers and Aksa A-49 carbon fibers**. The material properties of these fibers and resin systems were defined to the software. During the steel-based composite tank

manufacturing, only one roving was used because of the manufacturing conditions. The defined material properties are given in Figure 3.10.

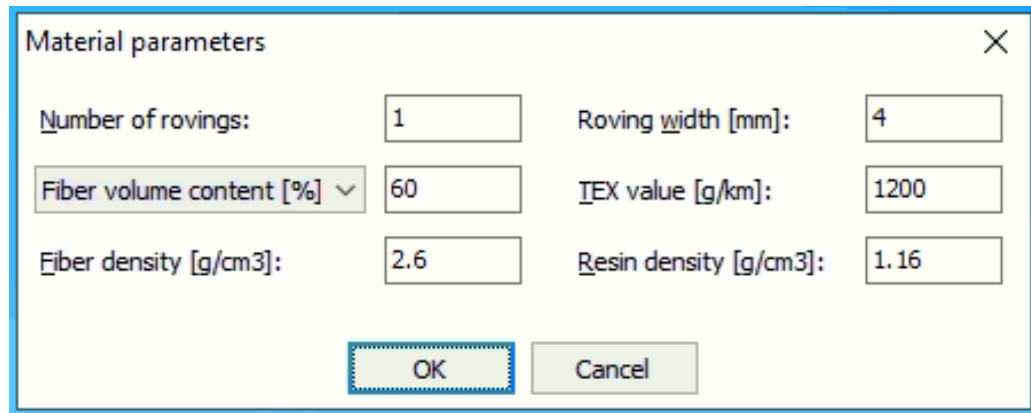


Figure 3.10. Glass fiber and epoxy material properties defined to the software

The winding types were mentioned above sections. Helical layers are critical for composite hydrogen storage tanks to carry longitudinal loads. Helical winding or non-geodesic winding is used to helical layer simulations. Helical layer winding simulation needs the same polar opening for both dome sections. However, the liners used in this study have only one pole opening at the front dome section which is the boss section for this reason, non-geodesic winding filament simulations were carried out.

The most important point of the non-geodesic winding is that, the back-dome sections and front dome sections must be covered with fibers. For steel liners, to cover the front and back dome section completely, angle variation options were utilized which means different angles were used in the same layer. The front dome section was winded with 16° and back dome and cylindrical parts were winded with 11°. If only one angle used bigger than 11°, there are pole opening in the back-dome section, however, if only 11° used it is possible to close back the dome section, but there are openings in the front dome section at this time. Therefore, different angles at the same layer were used. Also, 0.1 friction factor was used with a 105% degree of coverage. The aim of using 105% degree of coverage is to be sure about the complete composite coverage. The pattern number was suggested by software so -25/7 pattern was selected. The winding parameters defined for non-geodesic winding can be found in Figure 3.11.

Non-geodesic parameters

<u>Winding angle [°]:</u>	18...19	19...20	20...21	21...22	22...23	<input type="button" value="Set range"/>
<input type="button" value="Var/Const"/>	16.4	16.4	16.4	11	11	<input type="button" value="Const thick"/>
	<		>			

Friction factor:

Pattern number:  Number of layers:

Deg. of covering [%]

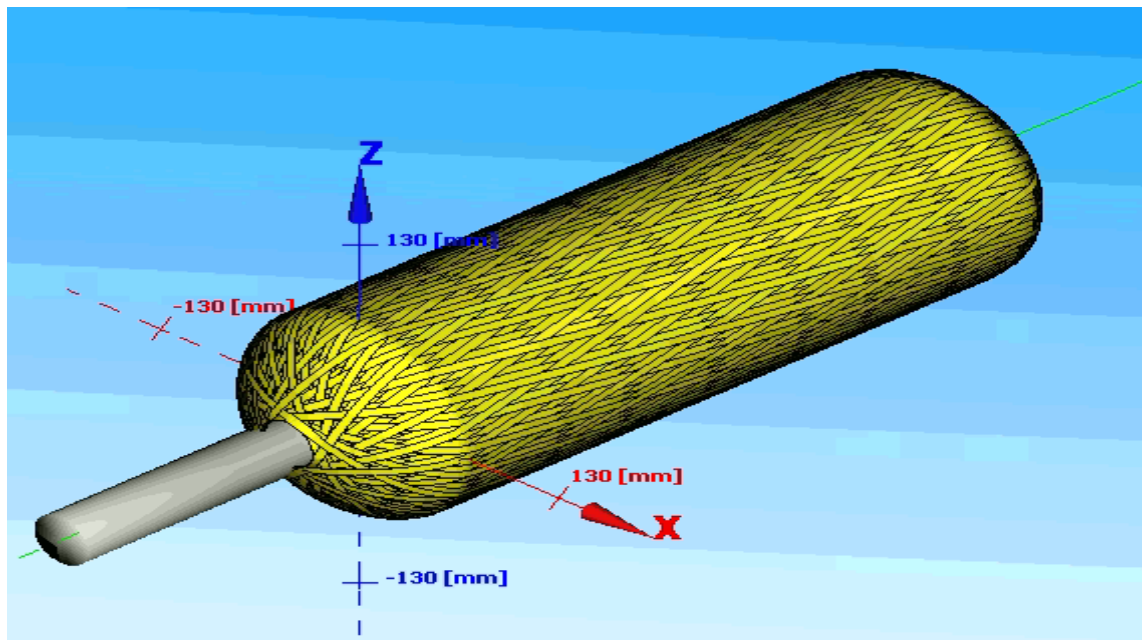
Turning zone front to:  Turning zone back from:

Starting frame:  Starting position [°]:

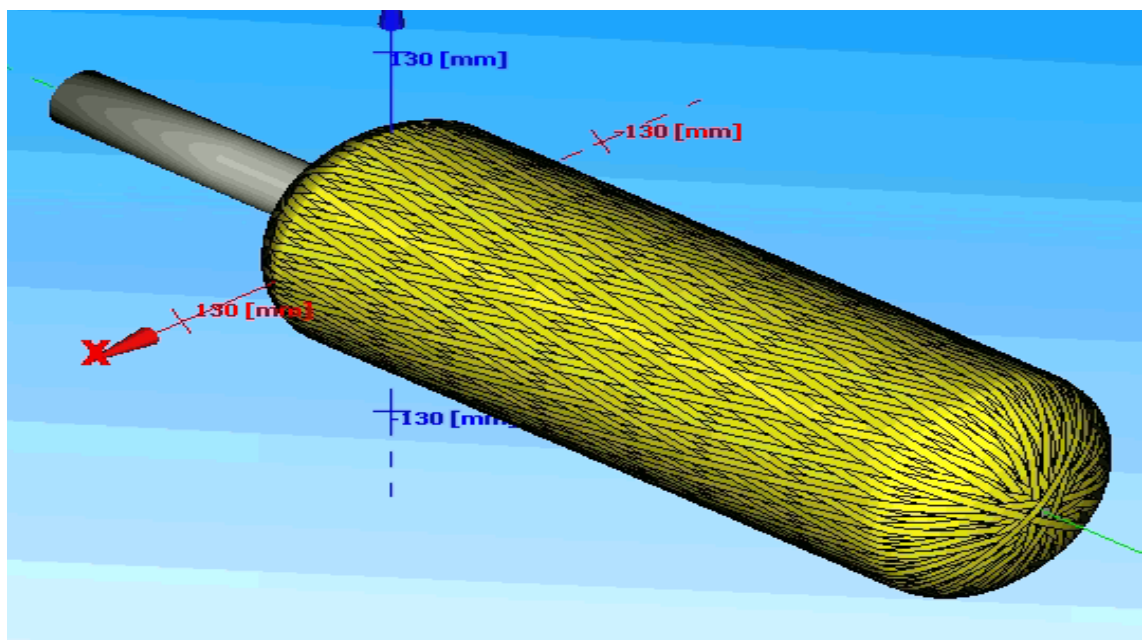
Dwell front [°]:  Dwell back [°]:

Figure 3.11. Defined winding parameters to the software and angle variations.

Winding simulations were carried out according to the parameters above and the full coverage of liner can be obtained. The slippage of fibers during the filament winding process is a serious problem so friction factor value should be given to the system carefully. 0.1 friction factor was selected according to the software manufacturer's suggestion. When friction factor increases, the number of different helical winding angle was an increase but the risk of fiber slippage during the manufacturing process can be increased. Due to the fiber slippage risk an optimum value of 0.1 was used. 105% degree of coverage was selected to be sure that steel liner was fully covered by the composite section and unnecessary fiber consumption was prevented. Therefore, after winding simulations, G-codes were obtained and provided to the filament winding machine. Also, dry winding was utilized to be sure about the compatibility between the software and filament winding machine. The full coverage of the liner front and back dome sections are simulated in Figure 3.12.



(a)



(b)

Figure 3.12. Fully covered (a) front dome section (b) back dome section with angle variations.

### 3.5.2.2. Winding Parameters Definitions for Al Based Composite Tanks

Aksa™ A-49 carbon fiber and Toray™ T-700 carbon fiber reinforcements together with aluminum liner were used in this work. The material properties of carbon fibers and epoxy matrix were also defined to the software similarly. However, three rovings were used as compared to steel-based composite tank simulation. Utilizing three rovings at the same time, decrease the winding time significantly.

The winding simulations revealed that; to cover the back and front dome of the liner completely, we have to use 14° winding angle. Angle variation in the same layer was not necessary since 14° winding angle is adequate for full coverage. 0.1 friction factor value was given to the software to prevent fiber slippage. The winding parameters defined for non-geodesic winding simulation of Al-based composite tanks are given in Figure 3.13.

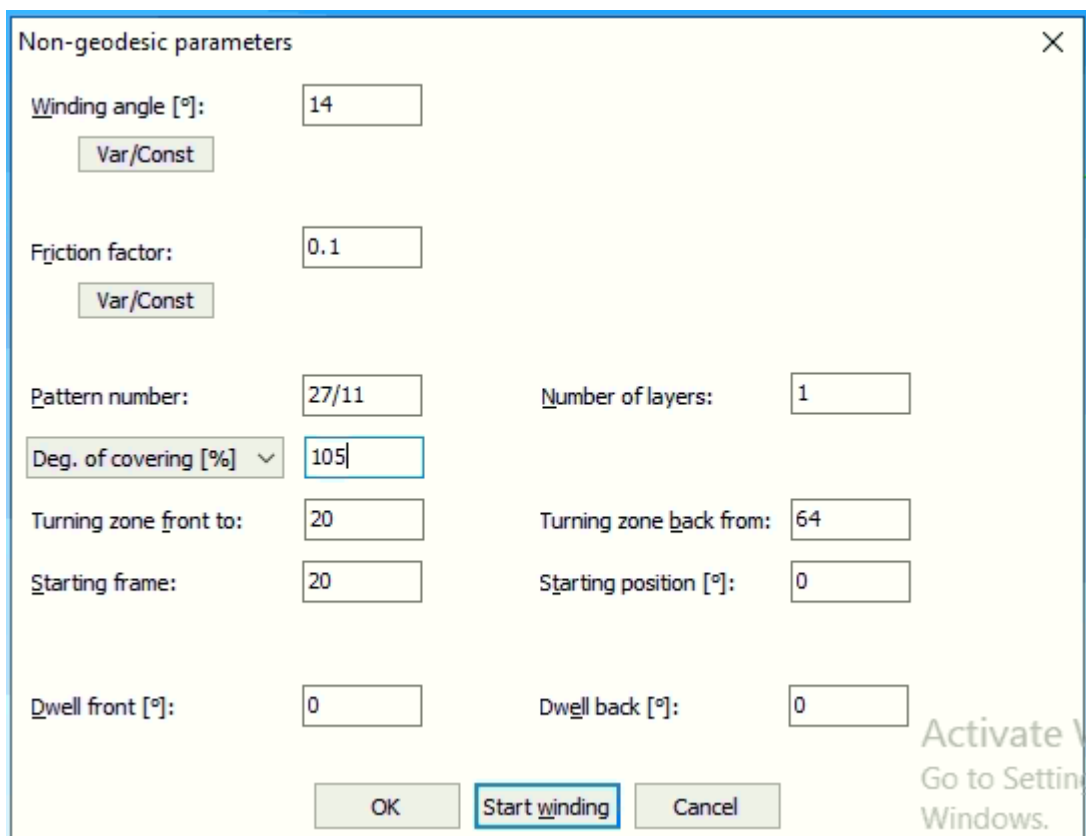


Figure 3.13. Defined winding parameters to the software for Al-based composite tank

It is possible to obtain winding simulation results such as fiber consumption, laminate weight etc. from software. Therefore, required fiber quantity can be calculated from these inputs and fiber extinction can be prevented during filament winding. The calculation result for a one-layer helical composite winding obtained from the software is shown in Figure 3.14.

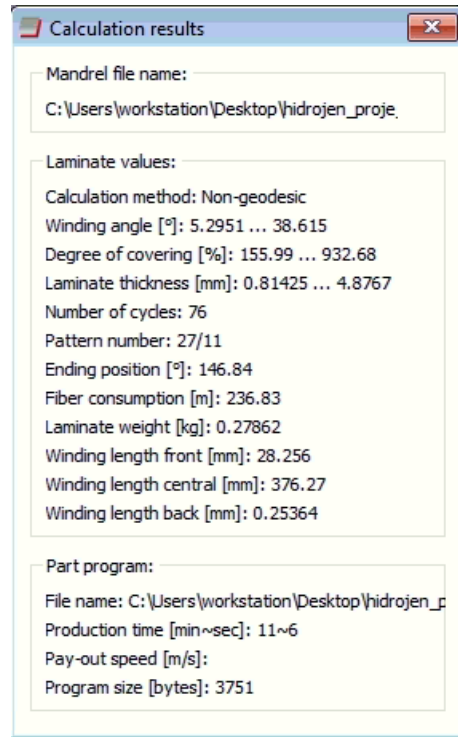
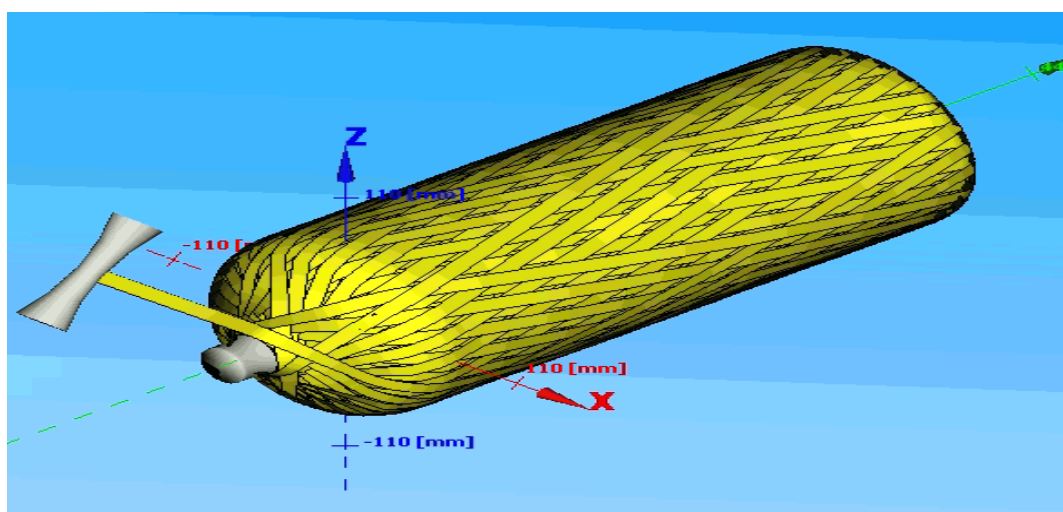
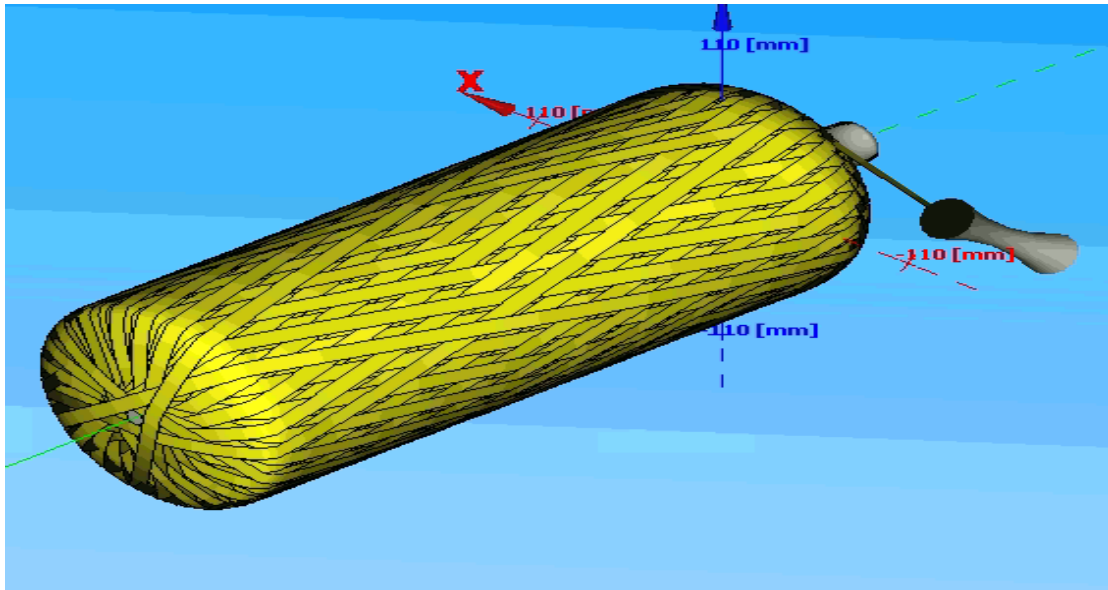


Figure 3.14. Calculation results of helical layer winding for one composite layer

Helical layer simulations for 14° winding angle can be seen in Figure 3.15.



(a)



(b)

Figure 3.15. Fully covered (a) front dome section (b) back dome section of Al based composite tanks.

### 3.6. Manufacturing of Composite Tanks

The composite pressure tanks were manufactured by filament winding technique, which is the fabrication technique of high-pressure composite storage tanks. The filament winding machine was manufactured by Fibermak Composites Inc. The CNC-controlled filament winding machine has a 4-axis operating capacity. The machine has a winding dimensions capacity of **2000 mm in length and 300 mm in diameter**. It is possible to produce composite pressure vessels, composite tubular structures, and composite plates by using this filament winding machine.

The produced G-codes from CADWIND software mentioned above sections, are loaded the filament winding machine by using the control unit of the filament winding machine . The compatibility of the filament winding machine and software was checked before filament winding operations. The 4-axis operating capacity, CNC controlled filament winding machine is pictured in Figure 3.16.

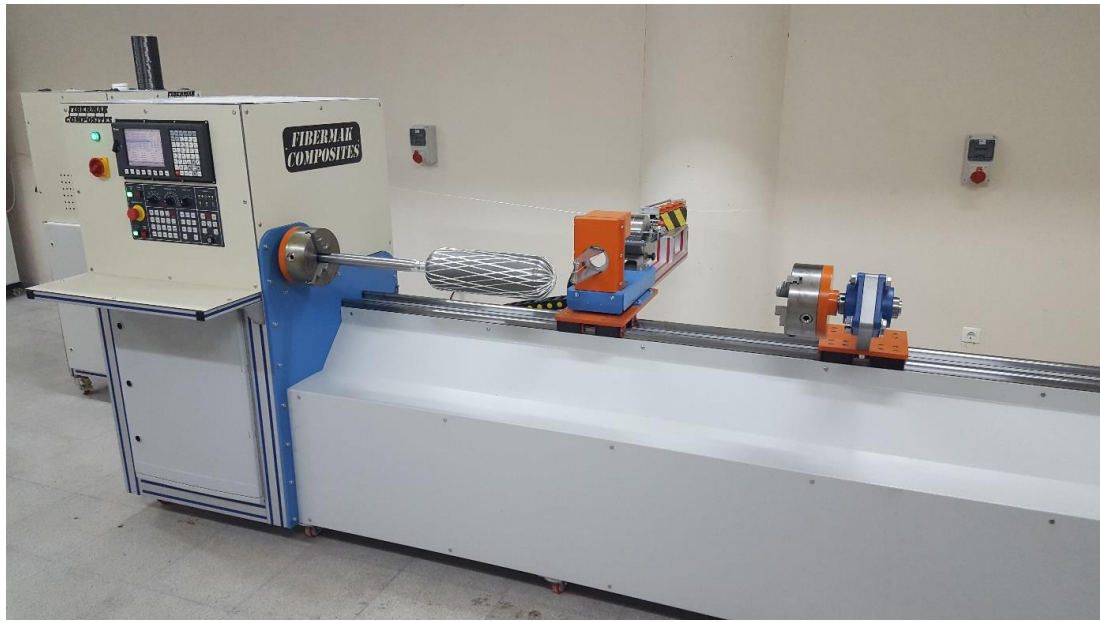


Figure 3.16. Filament winding machine used for composite tank manufacturing.

The fiber tension during the filament winding process is a very critical parameter for composite pressure tank performance. Due to the importance of fiber tension, the filament winding machine has a servo-controlled fiber tensioner system. The fiber tensioner system has a capacity of 4 rovings feeding at the same time. The fiber tensioner system are illustrated in Figure 3.17.



Figure 3.17. Fiber tensioner system for filament winding manufacturing.

Another important filament winding equipment component is a resin bath. Fibers pass through the resin bath and wetting with epoxy resin. The epoxy resin quantity can be arranged by using the resin bath which is critical for fiber mass fraction for composites. The resin bath used for the filament winding application can be seen in 3.18.



Figure 3.18. Resin bath for filament winding manufacturing.

The last step for filament winding process is curing the composite part within a oven. After the winding process, composite pressure tanks were cured at 80°C for 2 hours using a rotating shaft in a curing oven and additionally post-cured at 120°C for 2 hours. The rotation during curing proses provides homogeneity for all parts of the composite. The rotating shaft curing oven is shown in Figure 3.19.



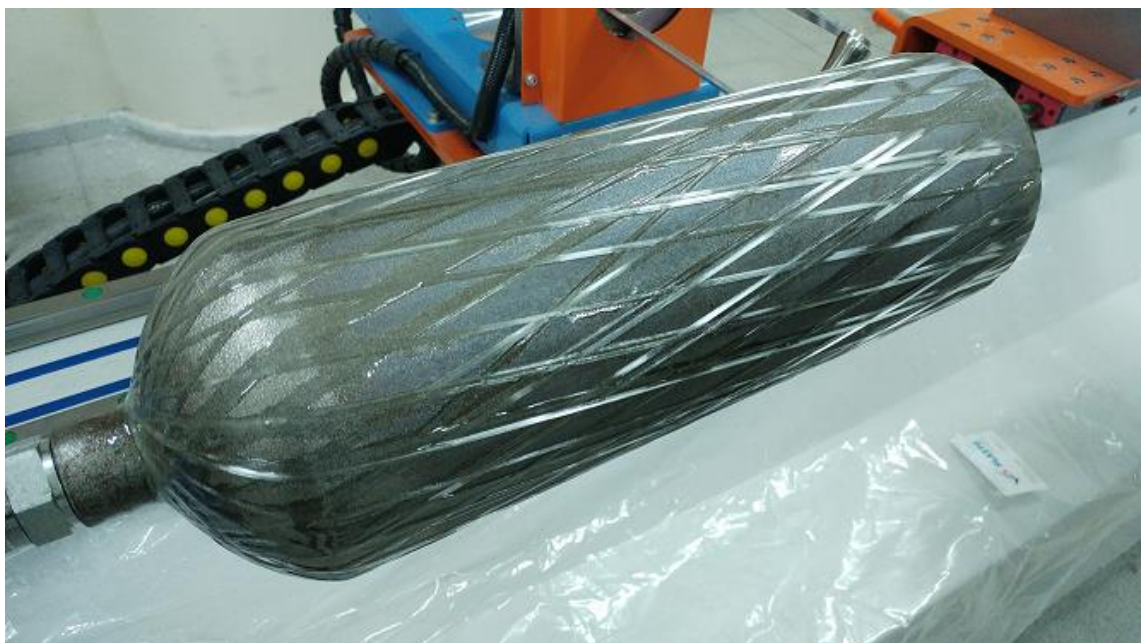
Figure 3.19. Curing oven with rotating shaft.

### 3.6.1. Manufacturing of Steel-based Composite Tanks

The composite tanks consist of steel liners were produced in this thesis as a preliminary filament winding study. To get experience for the filament winding process and testing process, steel tubes were purchased and modified as a liner. In this preliminary study, the effect of the number of the composite layers and hybrid layers on the burst pressure performance of composite tanks were investigated.

Helical and hoop layers were wound over the steel liner by filament winding machine. Only one roving was used to overwrap the steel liner with a roving bandwidth of 4 mm for glass fiber and 5 mm for carbon fiber. The steel liner was attached to the filament winding machine with an apparatus. A steel rod was manufactured with a 40 mm diameter and the end of the rod was threaded according to the boss section of liners.

During the filament winding process, the epoxy resin quantity was controlled. Since the liner has a specific geometry such as the front dome has an open end and the back dome has closed end, the fiber slippage problem occurred during the manufacturing process. Especially, the fibers were tending to slip from the back dome section because there was no apparatus to hold the fibers. For this reason, the winding process requires careful observations. Helical and hoop winding process can be seen in Figure 3.20.



(a)



(b)

Figure 3.20. The filament winding of (a) a helical layer and (b) a hoop layer over the steel liner

Different types of composite tanks were manufactured by using steel liner. In the first type only glass fiber was used as a reinforcement material with epoxy matrix. The effect of number of helical and hoop layer on the burst pressure performance of composite pressure vessels were investigated. For this purpose, composite tanks consist of 3 helical and 3 hoop layers were manufactured with the glass fiber reinforcement, then 6 helical and 6 hoop layers were produced with the glass fiber reinforcement again. The required winding parameters were mentioned above sections.

For the hybrid composite tanks, in addition to glass fiber, carbon fibers were also used as a reinforcement material. The effect of the utilization of hybrid fibers on the performance of composite pressure tanks were investigated. The hybrid composite tanks have 3 helical and 3 hoop layers. The glass fiber reinforcement was used in helical layers, however for hoop layers, 2 layers were wined with carbon fiber, and the outermost layer was wined with a glass layer. The hybrid layers were used in the hoop section since the failure was expected in the cylindrical section. The configurations and the properties and properties of the manufactured steel liner based composite tanks are tabulated in Table 3.2.

Table 3.2. The configurations and the properties of the manufactured steel liner based composite tanks.

Tank Code	Matrix	Fiber Reinforcement	Layer Orientation	Total # of Plies
1	Epoxy	Glass Fiber	$[\pm 11^\circ/\pm 90^\circ]_3$	6
2	Epoxy	Glass Fiber	$[\pm 11^\circ/\pm 90^\circ]_3$	6
3	Epoxy	Glass Fiber	$[\pm 11^\circ/\pm 90^\circ]_3$	6
4	Epoxy	Glass Fiber	$[\pm 11^\circ/\pm 90^\circ]_3$	6
5	Epoxy	Glass Fiber	$[\pm 11^\circ/\pm 90^\circ]_6$	12
6	Epoxy	Glass Fiber	$[\pm 11^\circ/\pm 90^\circ]_6$	12
7	Epoxy	Glass Fiber / Carbon Fiber (Hybrid)	$[\pm 11^\circ/\pm 90^\circ]_3$	6
8	Epoxy	Glass Fiber / Carbon Fiber (Hybrid)	$[\pm 11^\circ/\pm 90^\circ]_3$	6

In Table 3.2,  $\pm 11^\circ$  represents the helical winding and  $90^\circ$  represents the hoop winding. After the winding process, composite tanks were cured at 80 °C for 2 hours using a rotating shaft in a curing oven and post-cured at 120 °C for 2 hours. The manufactured and cured hybrid tank is shown in Figure 3.21.



Figure 3.21. A steel liner-based carbon/glass fiber hybrid composite tank after curing.

### 3.6.2. Manufacturing of Al-based Composite Tank

Aluminum liners were used for manufacturing high-pressure resistant lightweight composite pressure tanks due to its lower density as compared to steel. Aluminum liners were overwrapped with carbon fiber and epoxy resin. 3 rovings were used at the same time to decrease the winding time. The aluminum liners were attached to the filament winding machine with an aluminum rod which has a diameter of 30 mm. Moreover, to minimize the fiber slippage from the back dome section, a special apparatus was designed and manufactured and adapted to the system. This specific study aims to reach 1400 bar burst pressure which is critical for automotive applications as mentioned above. To reach 1400 bar burst pressure, various number of composite layers were used, different techniques were adopted to the filament winding manufacturing. The filament winding manufacturing for aluminum liner based composite tank is shown in Figure 3.22.



Figure 3.22. A helical layer winding of carbon/epoxy over the aluminum liner.

As a first type, aluminum liner based composite tanks were manufactured with AKSA<sup>TM</sup> A-49 carbon fibers. However, preliminary results showed that, some composite tanks have leaking problems even at low pressures. For investigations, one liner was sectioned using water jet. It was observed that there are some quality problems for the aluminum liners manufactured as a first try, demonstrated in Figure 3.23. It can be seen

that the thickness along the cylindrical section is not uniform. Also, the thickness at the base section shown as  $X_0$  in Figure 3.23 is very thin (about as 1.5 mm). Moreover, the liner is not symmetrical, as can be seen in Figure 3.23,  $X_1$  and  $X_2$  have different thickness values. Furthermore, some macro cracks were visible and those liners were not able to pressurized. Due to these reasons, the manufacturer produces new aluminum liners and all the liners were subjected to sealing tests at 100 bar.



Figure 3.23. Cross section of aluminum liners manufactured as first try.

The new manufactured liners were sectioned and sectioned parts were investigated. It was observed that the thicknesses along the cylindrical section have the uniformity. The asymmetry problem of the liner was also solved. Dome section thicknesses were also increased and thickness distribution during the dome section was appropriate. However, for this group the cylindrical section was thicker than the dome section (Figure 3.24). The dome section thickness is expected to be higher than those for the cylindrical section. However, no more manufacturing try was affordable and those liners were used within the study.



Figure 3. 24. Cross section of the manufactured liners used within the study.

Since the front dome section is thinner than the cylindrical section, doily layers were adopted and utilized together with the filament winding manufacturing technique for some manufactured composite tanks. Doily layers are woven carbon fiber fabrics and these carbon fiber fabrics were cut appropriately for the dome shapes. The doily layers were wetted with epoxy resin by hand lay-up technique and placed between the helical layers (Figure 3.25).

Doily layers provide extra strength at the dome sections and decrease the need for number helical layers which decreases the winding time and carbon fiber usage. Other advantages of doily layers are, they provide extra friction during the helical winding and decrease the risk of fiber slippage during the manufacturing. Especially, as the number of the helical layer increases, the thicknesses in the dome section increases significantly, so doily layers can be useful for this problem.

The failure location is also an important parameter for composite pressure tanks. The failure must occur at the cylindrical section and doily layers can be also useful for this issue. The weak portion of the composite pressure tanks can be reinforced locally by utilizing the doily layer.



Figure 3.25. Doily layers placed over the boss region during the filament winding process.

A total of 35 different composite tanks were manufactured and tested to reach the 1400 bar burst pressure. The first 15 composite tank was manufactured with aluminum liners which have leakage and thickness problems as mentioned above. AKSA™ A-49 carbon fibers were used with these liners. For the rest, Toray™ T-700 carbon fibers with second type of aluminum liners were used. Doily layers were started to adopt after tank # 21 and the final design was obtained with composite tank # 31-35. The results and details of these configurations is given in Chapter 4. All of the manufactured composite tanks were tabulated in Table 3.3.

Table 3.3. Configurations of the manufactured Aluminum liner based composite tanks.

Tank Code	Carbon Fiber Reinforcement Type	Layer Orientations	Number of Front Doily Layer	Number of Back Doily Layer
1	A-49	$[\pm 14^\circ]_3 / [\pm 90^\circ]_3$	-	-
2	A-49	$[\pm 14^\circ]_3 / [\pm 90^\circ]_3$	-	-
3	A-49	$[\pm 14^\circ]_3 / [\pm 90^\circ]_6$	-	-
4	A-49	$[\pm 14^\circ]_3 / [\pm 90^\circ]_9$	-	-
5	A-49	$[\pm 14^\circ]_6 / [\pm 90^\circ]_6$	-	-

(cont. on next page)

(cont.) Table 3.3.

6	A-49	$[\pm 14^\circ]_6 / [\pm 90^\circ]_6$	-	-
7	A-49	$[\pm 14^\circ]_5 / [\pm 90^\circ]_3$	-	-
8	A-49	$[\pm 14^\circ]_{10} / [\pm 90^\circ]_{10}$	-	-
9	A-49	$[\pm 14^\circ]_{11} / [\pm 90^\circ]_{11}$	-	-
10	A-49	$[\pm 14^\circ]_9 / [\pm 90^\circ]_9$	-	-
11	A-49	$[\pm 14^\circ]_{13} / [\pm 90^\circ]_{10}$	-	-
12	A-49	$[\pm 14^\circ]_9 / [\pm 90^\circ]_6$	-	-
13	A-49	$[\pm 14^\circ]_3 / [\pm 90^\circ]_3$	-	-
14	T-700	$[\pm 14^\circ]_9 / [\pm 90^\circ]_9$	-	-
15	T-700	$[\pm 14^\circ]_9 / [\pm 90^\circ]_8$	-	-
16	T-700	$[\pm 14^\circ]_{12} / [\pm 90^\circ]_{11}$	-	-
17	T-700	$[\pm 14^\circ]_{13} / [\pm 90^\circ]_{11}$	-	-
18	T-700	$[\pm 14^\circ]_{15} / [\pm 90^\circ]_{11}$	-	-
19	T-700	$[\pm 14^\circ]_9 / [\pm 90^\circ]_8$	-	-
20	T-700	$[\pm 14^\circ]_9 / [\pm 90^\circ]_7$	-	-
21	T-700	$[\pm 14^\circ]_9 / [\pm 90^\circ]_7$	7	
22	T-700	$[\pm 14^\circ]_9 / [\pm 90^\circ]_7$	11	
23	T-700	$[\pm 14^\circ]_9 / [\pm 90^\circ]_7$	15	
24	T-700	$[\pm 14^\circ]_9 / [\pm 90^\circ]_7$	17	
25	T-700	$[\pm 14^\circ]_9 / [\pm 90^\circ]_7$	17	
26	T-700	$[\pm 14^\circ]_9 / [\pm 90^\circ]_7$	17	
27	T-700	$[\pm 14^\circ]_9 / [\pm 90^\circ]_7$	17	5
28	T-700	$[\pm 14^\circ]_9 / [\pm 90^\circ]_7$	17	5
29	T-700	$[\pm 14^\circ]_9 / [\pm 90^\circ]_7$	17	-
30	T-700	$[\pm 14^\circ]_9 / [\pm 90^\circ]_6$	17	-
31	T-700	$[\pm 14^\circ]_9 / [\pm 90^\circ]_7$	17	9
32	T-700	$[\pm 14^\circ]_9 / [\pm 90^\circ]_7$	17	9
33	T-700	$[\pm 14^\circ]_9 / [\pm 90^\circ]_8$	17	9
34	T-700	$[\pm 14^\circ]_9 / [\pm 90^\circ]_{7.5}$	17	9
35	T-700	$[\pm 14^\circ]_9 / [\pm 90^\circ]_{7.5}$	17	9

It was observed that some composite tanks have leakage problems at elevated temperatures especially above 900 bar. The composite sections of the tank did not show failure modes, however microcracks have occurred in the aluminum liner. To solve

to this problem an innovative solution was developed. The inside walls of the aluminum liners were coated with a polyurethane based resin system. Duratek KLB 75 polyurethane resin system was obtained and covered the inside surface of the composite tank. The tank was rotated until the resin system is cured inside the tank. Finally, the inside of the composite pressure tank was observed using snake cam to control the uniformity of the resin system, as it can be seen in Figure 3.26.



Figure 3.26. Inside wall control of a composite tank by snake cam.

### 3.7. Burst Pressure Testing

#### 3.7.1. Burst Pressure Testing of Steel based Composite Tanks

The composite tanks manufactured with steel liners were subjected to the burst pressure test. For this aim composite tanks and steel liners were loaded hydrostatically until the burst point. During the burst pressure test, three rosette-type strain gages were used to measure the local axial and radial deformations. A special adapter was designed and manufactured to connect the steel liner based composite tank to the hydrostatic test system. This adapter was made of steel and sealed with O-rings. The technical drawing and the photograph of this adapter were presented in Figure 3.27.

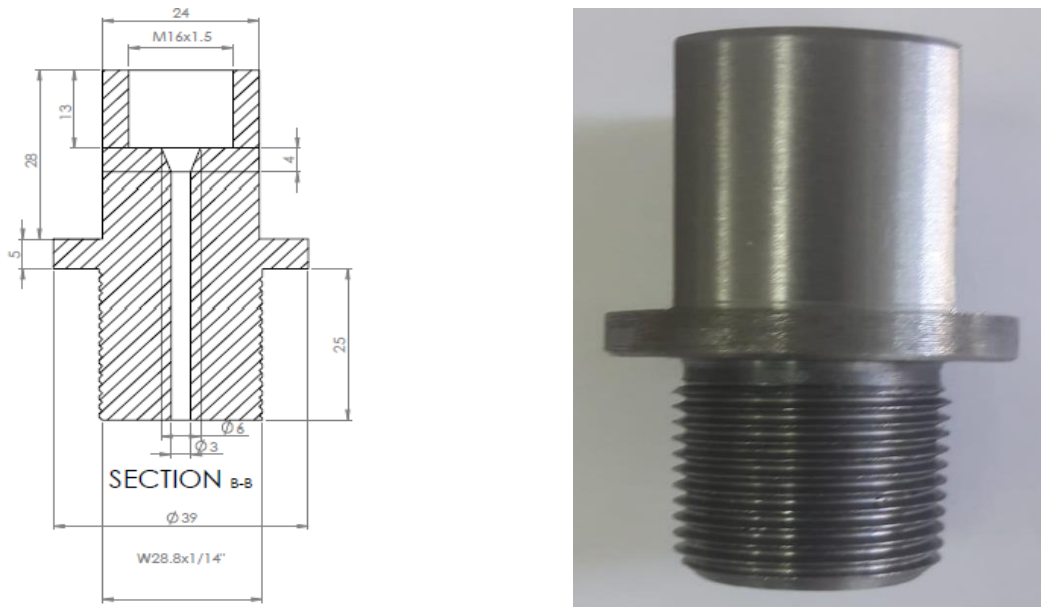
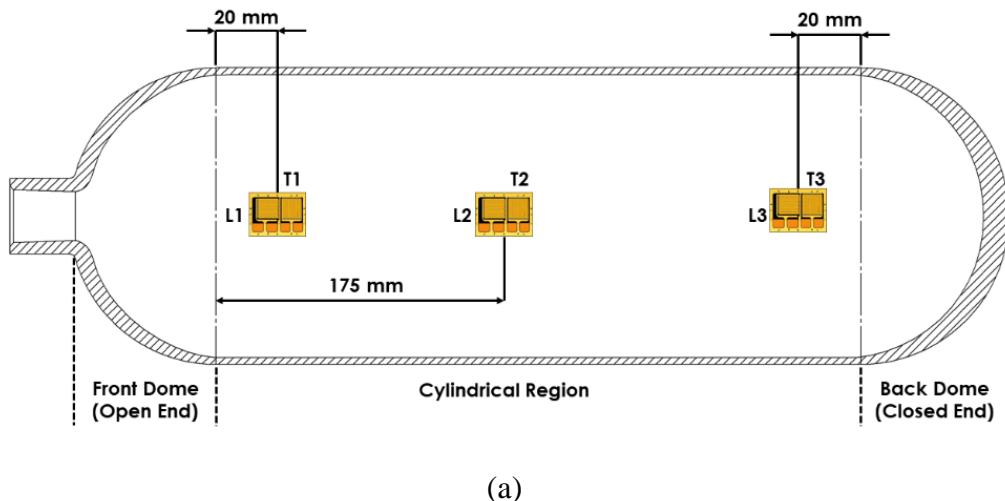
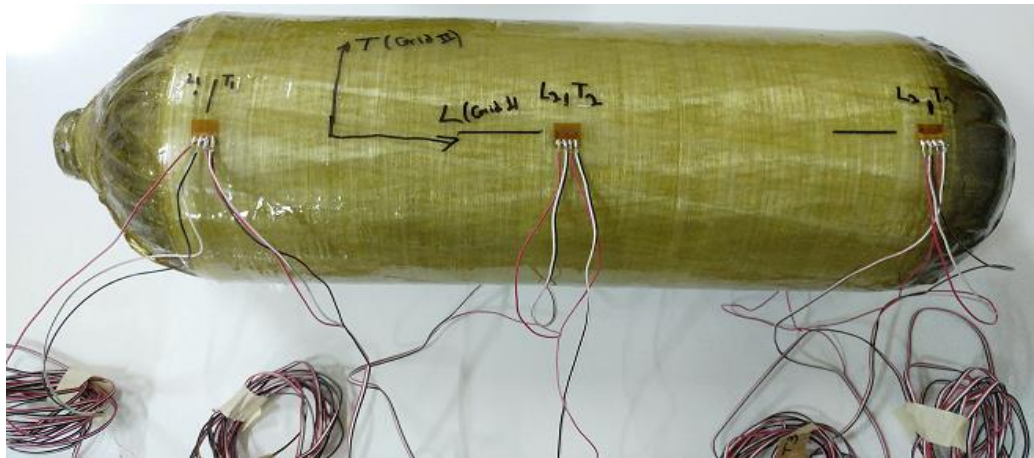


Figure 3.27. (a) Technical drawing and (b) photograph of adapter for steel-based tank.

The strain gages were placed at 20 mm away from both ends of the cylindrical section and a strain gage at the center of the cylindrical section of the tanks. The schematic of strain gages positions, a test ready composite tank, and a composite tank at the test set up are illustrated in Figure 3.28. The burst pressure test set-up has a capacity of 2000 bar and the internal pressure can be increased with an average rate of 5 bar/sec.





(b)



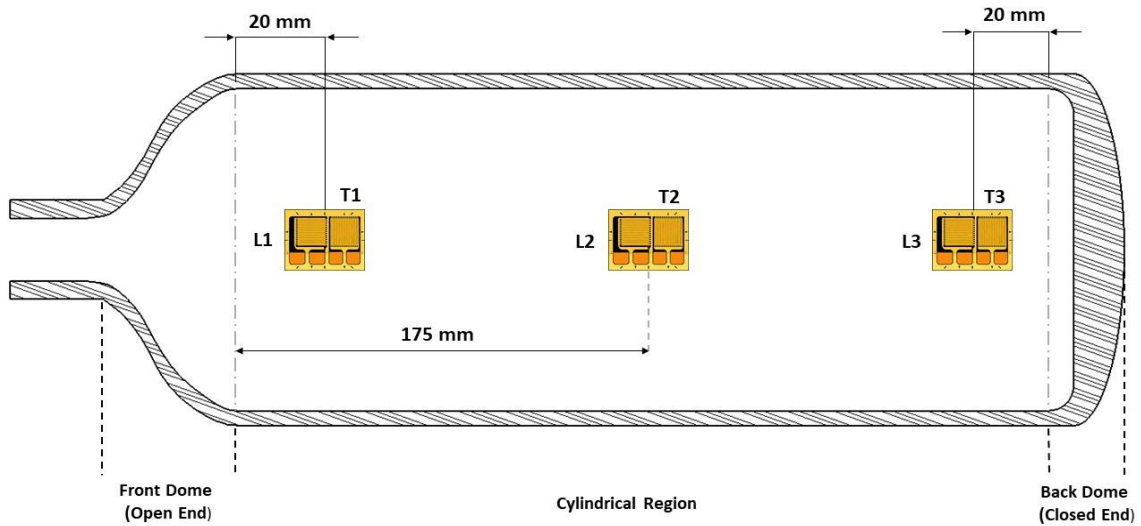
©

Figure 3.28. (a) Schematic of strain gages positions (b) a test ready composite tank (c) test set-up for steel-based composite tank.

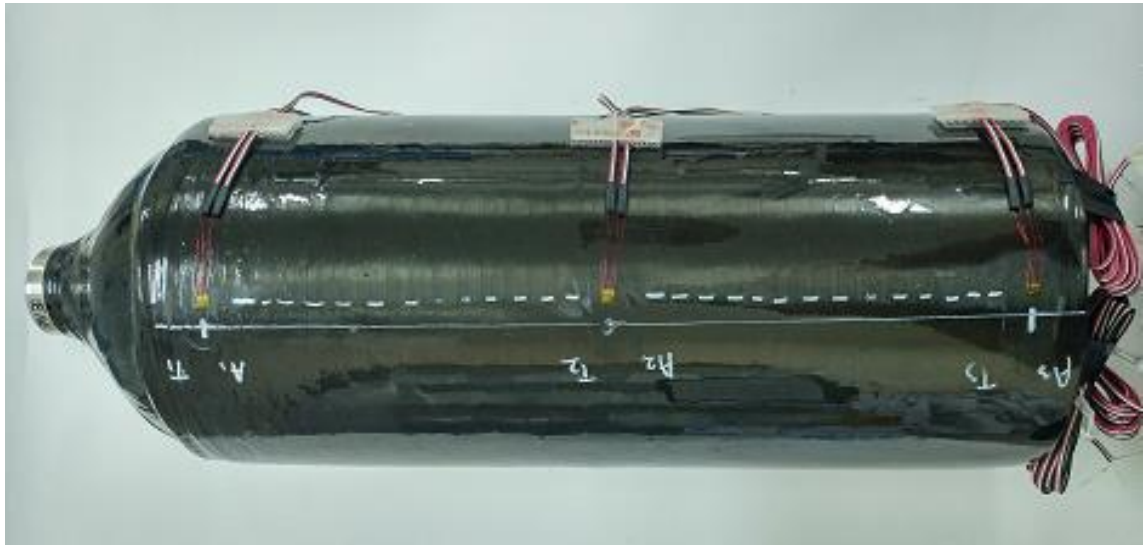
### 3.7.2. Burst Pressure Testing of Al-based Composite Tanks

The similar process mentioned above was utilized with aluminum liner based composite tanks for burst pressure testing. Internal hydrostatic pressure was utilized to aluminum liners up to burst failure. Before burst test a steel adapter was designed and manufactured which is suitable for the boss section of aluminum liner based composite tank. The adapter has an O-ring to provide sealing. The local strain values of the composite tanks were measured during the hydrostatic pressure test by using strain gages. The burst pressure tests were carried out at different places from steel-based composite tanks. The burst pressure test set up has a maximum capacity of 1500 bar and the internal pressure

can be increased with an average rate of 5 bar/sec, manually. Strain gage positions on the aluminum-based composite tanks, an actual specimen ready for burst pressure testing, and a specimen in the test chamber is displayed in Figure 3.29.



(a)



(b)



©

Figure 3.29. (a) Strain gage positions, (b) burst pressure testing ready specimen, (c)  
specimen in the burst testing chamber

## CHAPTER 4

### RESULTS AND DISCUSSION

#### 4.1. Tensile Test Results of Liner and Composite Sections

Tensile test specimens were cut from the aluminum liner by using water jet and the tensile tests were performed using at least five specimens. Tensile strength, modulus of elasticity, Poisson's Ratio, and yield strength values of the aluminum liner were given in Table 4.1 and the stress-strain curve is given in Figure 4.1.

Table 4.1. Experimentally found mechanical properties of the Al Liner

<i>Symbol</i>	<i>Description</i>	<i>Unit</i>	<i>Value</i>
$E_{al}$	Young's Modulus	Gpa	57.5
$\nu_{12,al}$	Poisson's Ratio		0.33
$\sigma_{y,al}$	Yield Strength	Mpa	240.3
$\sigma_{ult}$	Ultimate tensile strength	Mpa	317.0

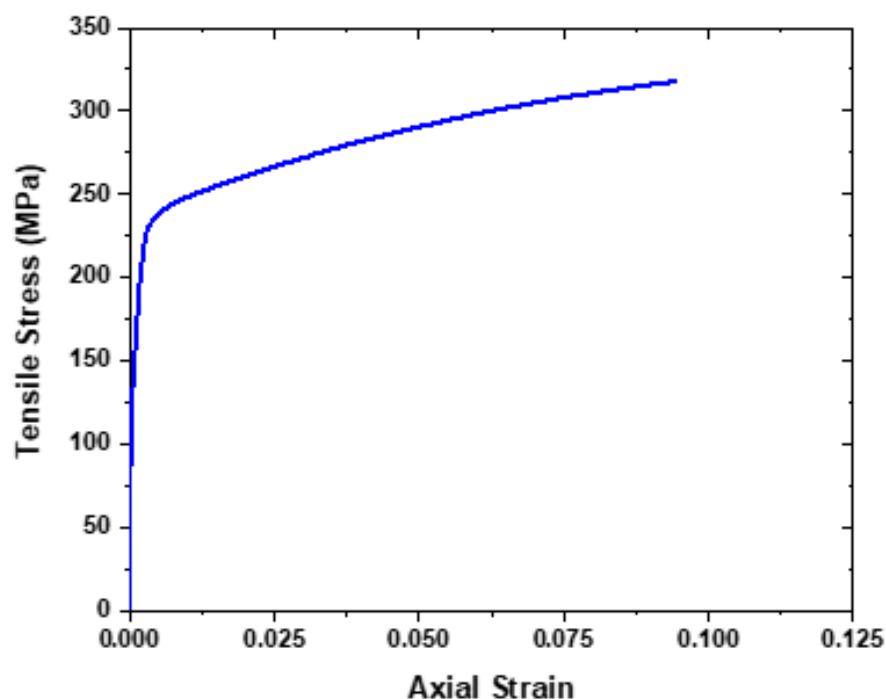


Figure 4.1. Experimental average tensile stress-strain curve of the aluminum liner.

Composites tensile test specimens obtained from filament wound composite UD plates were tested to determine the tensile properties of the composite. Composite plates manufactured from **Şişecam FWR-6 glass fiber, Aksa A-49, and Toray T700 carbon fiber** **were tested**. Tensile strength from  $0^\circ$  and  $90^\circ$  directions of composites were calculated. Experimental findings are tabulated in Table 4.2. Failure modes of tensile test specimens, aluminum, and carbon fiber/epoxy composite after the tensile test are given in Figure 4.2.

Table 4.2. Tensile test results of glass fiber/epoxy and carbon fiber/epoxy plates.

<i>Specimen</i>	<i>Longitudinal Tensile Str. (Mpa)</i>	<i>Transverse Tensile Str. (Mpa)</i>	<i>E<sub>1</sub> (Gpa)</i>	<i>E<sub>2</sub> (Gpa)</i>
<i>Şişe Cam FWR6 GF / Epoxy</i>	609.8	14.9	27.93	13.23
<i>DowAksa A-49 CF /Epoxy</i>	1082	15.2	108.3	8.82
<i>Toray T700SC-12K CF / Epoxy</i>	1100	-	95.6	-



(a)



(b)

Figure 4.2. Failure modes of (a) aluminum liner and (b) carbon/epoxy specimen

## 4.2. Fiber Mass Fractions of Composites

Fiber mass contents of the manufactured composites were determined since the fiber content of composites affect the performance of composite materials significantly. The fiber mass content of the composites is shown in Table 4.3

Table 4.3. Fiber mass fractions of glass fiber/epoxy and carbon fiber/epoxy plates.

<i>Specimen</i>	<i>Average Fiber Content (wt.%)</i>
<i>Şişe Cam FWR6 GF / Epoxy</i>	58.14
<i>DowAksa A-49 CF /Epoxy</i>	61.41
<i>Toray T700SC-12K CF / Epoxy</i>	60.06

The fiber content results showed that, the fiber contents are very similar for carbon fiber reinforced composites. Moreover, the average fiber content of glass fiber reinforced composites was slightly lower than carbon fiber reinforced composite. This may be occurred because of epoxy wettability of glass fiber is lower than carbon fiber, slightly.

## 4.3. Dynamic Mechanic Analysis (DMA) of Composites

Thermo-mechanical properties of composite materials can be important especially at high working temperatures. The glass transition temperature of composites is tabulated in Table 4.4. It was observed that, there is no significant difference between different composites since they have the same epoxy matrix.

Table 4.4. DMA results of manufactured composite specimens.

<i>Specimen</i>	<i>Glass Transition Temperature (°C)</i>
<i>Şişe Cam FWR6 GF / Epoxy</i>	154.8
<i>DowAksa A-49 CF /Epoxy</i>	153.43
<i>Toray T700SC-12K CF / Epoxy</i>	151.41

#### 4.4. Burst Pressure Performance of Steel Based Composite Tanks

Burst pressure test was applied to both steel liners, glass fiber composite tanks and glass/carbon fiber hybrid composite tanks. The average burst pressure of steel liners was found as a 657 bar. The glass fiber composite tanks had an average burst pressure of 880 bar, which was nearly the same as hybrid composite tanks and had an average burst pressure of 904 bar. Glass fiber composite tanks which have 6 helical and 6 hoop layers had an average burst pressure 1113 bar. Burst pressure results of all pressure vessels are summarized in Table 4.5.

Table 4.5. Burst pressure results of manufactured steel-based composite tanks.

Tank Code	Fiber Reinforcement	Layer Orientation	Total # of Plies	Burst Pressure (bar)
Steel Liner 1	---	---	---	622
Steel Liner 2	---	---	---	692
1	Glass Fiber	$[\pm 11^\circ/\pm 90^\circ]_3$	6	965
2	Glass Fiber	$[\pm 11^\circ/\pm 90^\circ]_3$	6	848
3	Glass Fiber	$[\pm 11^\circ/\pm 90^\circ]_3$	6	831
4	Glass Fiber	$[\pm 11^\circ/\pm 90^\circ]_3$	6	879
5	Glass Fiber	$[\pm 11^\circ/\pm 90^\circ]_6$	12	1129
6	Glass Fiber	$[\pm 11^\circ/\pm 90^\circ]_6$	12	1096
7	Glass Fiber / Carbon Fiber (Hybrid)	$[\pm 11^\circ/\pm 90^\circ]_3$	6	922
8	Glass Fiber / Carbon Fiber (Hybrid)	$[\pm 11^\circ/\pm 90^\circ]_3$	6	887

The burst pressure test results showed 3 helical and 3 hoop layer reinforcement increased the burst pressure performance of steel liner up to 25% percent. However, it is observed that hybridization did not increase the burst pressure performance of composite tanks. This can be explained by the stiffness difference between the carbon and glass filaments. 6 helical 6 hoop layer glass fiber reinforcement increased the burst pressure performance of steel liner up to 70% percent. The burst failure modes of all composite

tanks are shown in Figure 4.3. The final rupture occurred on the cylindrical section thus identified as safe burst mode.

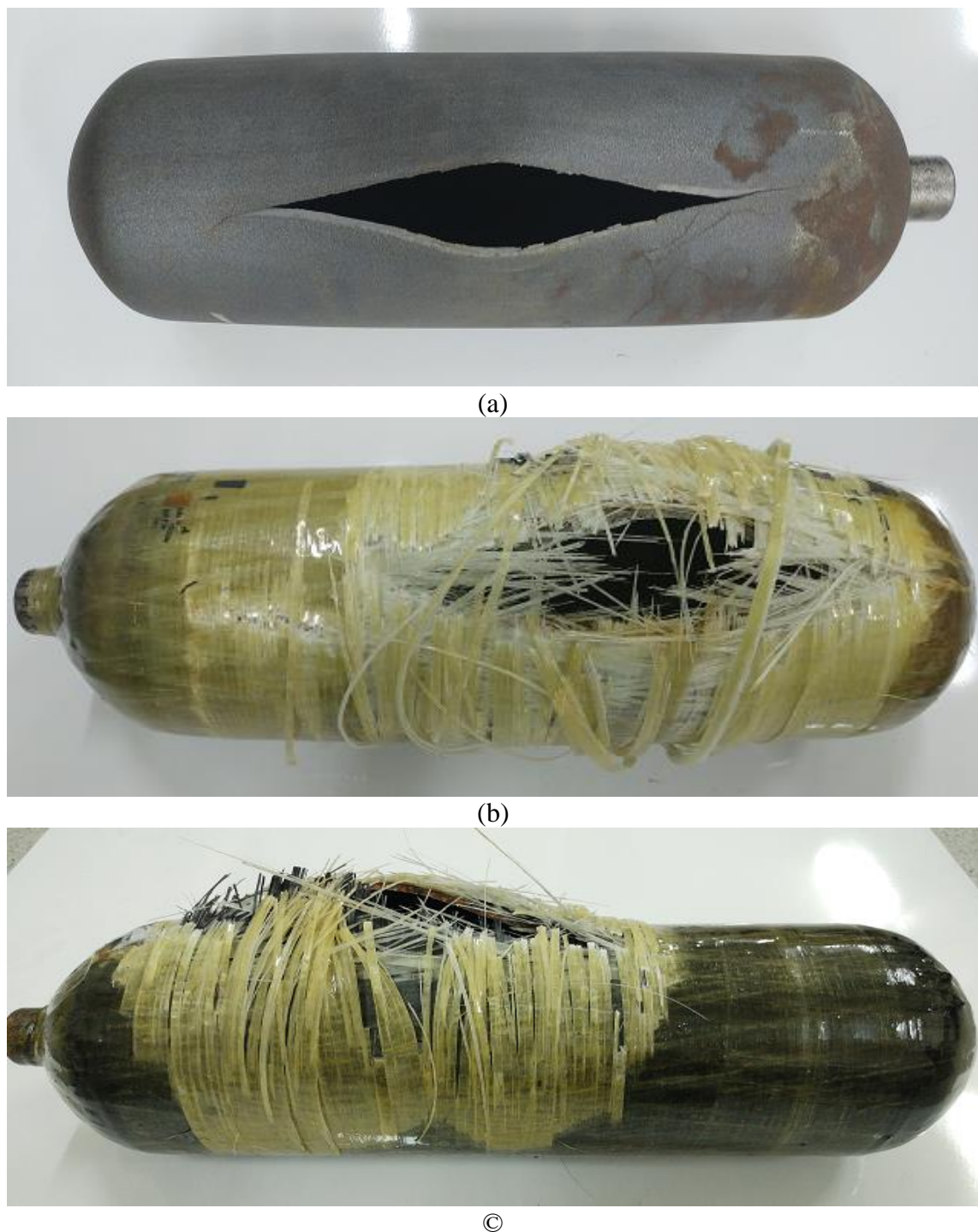


Figure 4.3. (a) steel liner, (b) glass fiber, (c) hybrid fiber tanks after hydrostatic burst pressure testing.

The local axial and radial deformations of the steel-based composite tank during burst pressure tests were obtained by using strain gages. The comparison of the hoop and axial strain values of the different manufactured type composite tanks obtained from the strain gages located at the front, central and back cylindrical section of the vessels, and were shown in Figure 4.4 to Figure 4.9, respectively.

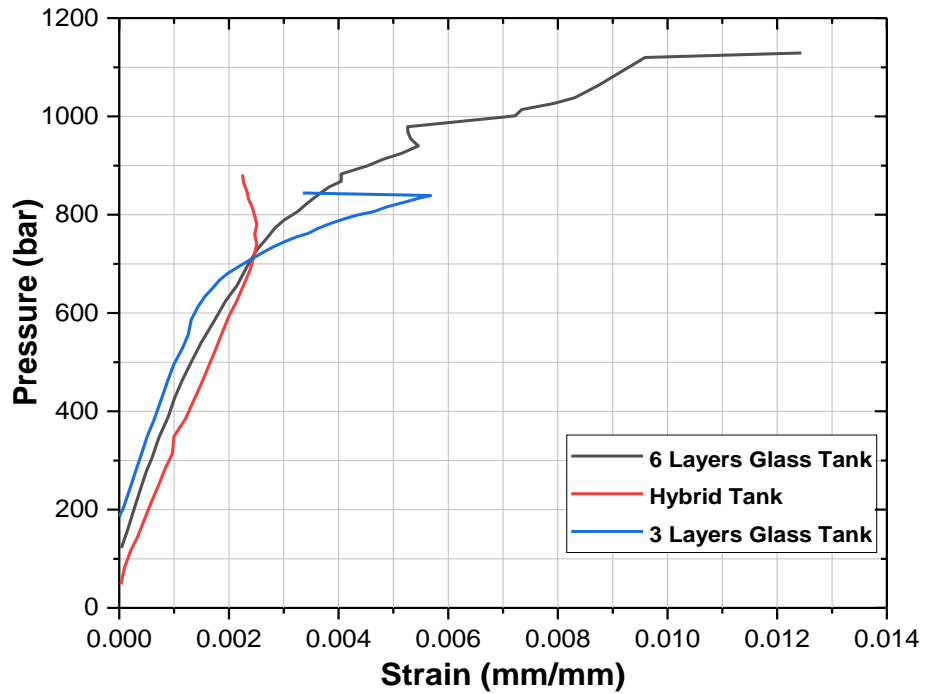


Figure 4.4. Comparison of axial strain values of composite tanks at the front (L1) cylindrical section.

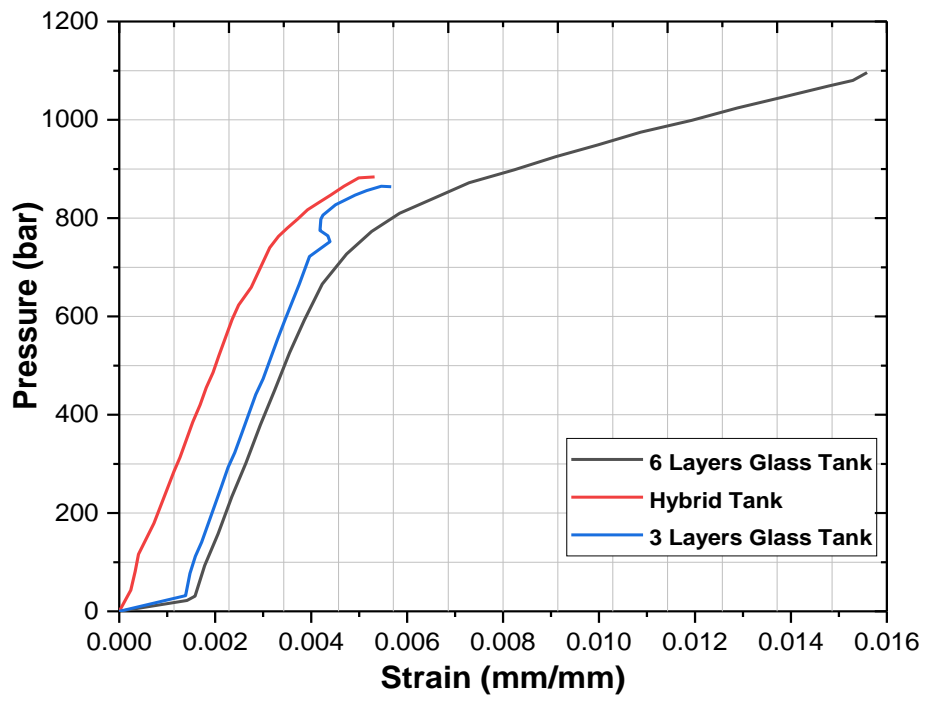


Figure 4.5. Comparison of radial strain values of composite tanks at the front (T1) cylindrical section.

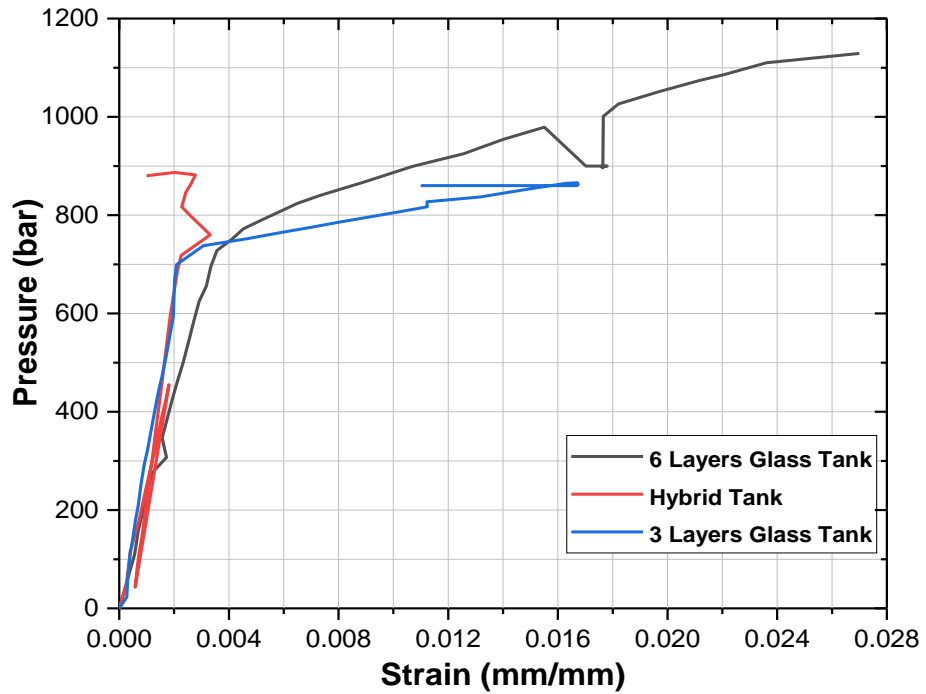


Figure 4.6. Comparison of axial strain values of composite tanks at the central (L2) cylindrical section.

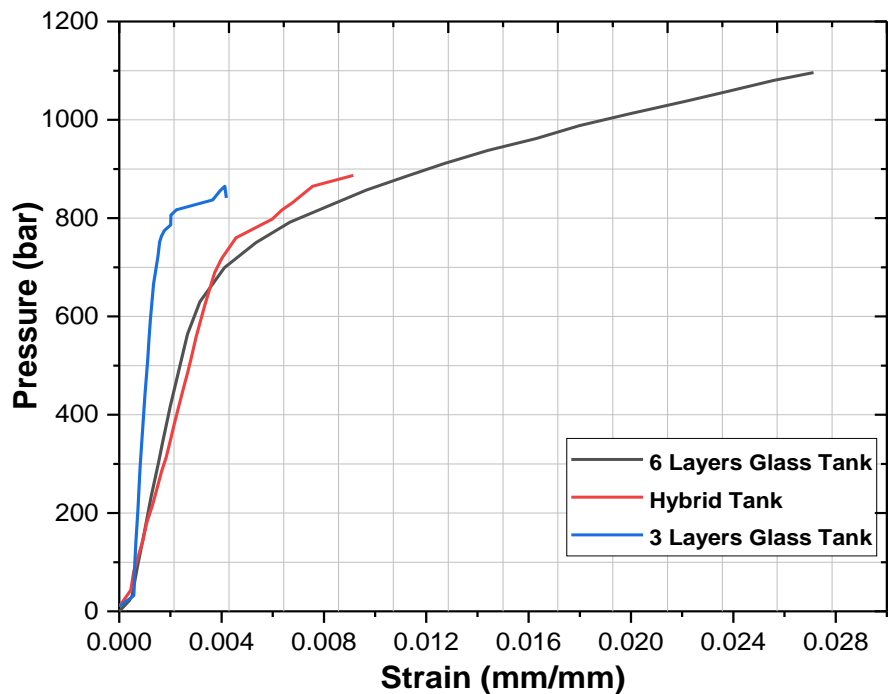


Figure 4.7. Comparison of radial strain values of composite tanks at the central (T2) cylindrical section.

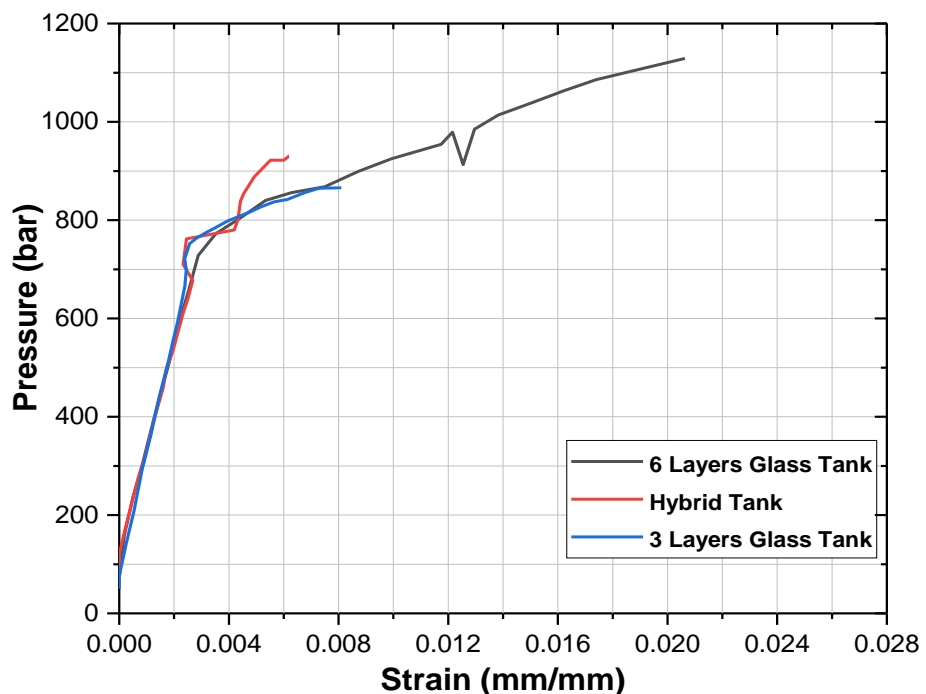


Figure 4.8. Comparison of axial strain values of composite tanks at the central (L3) cylindrical section.

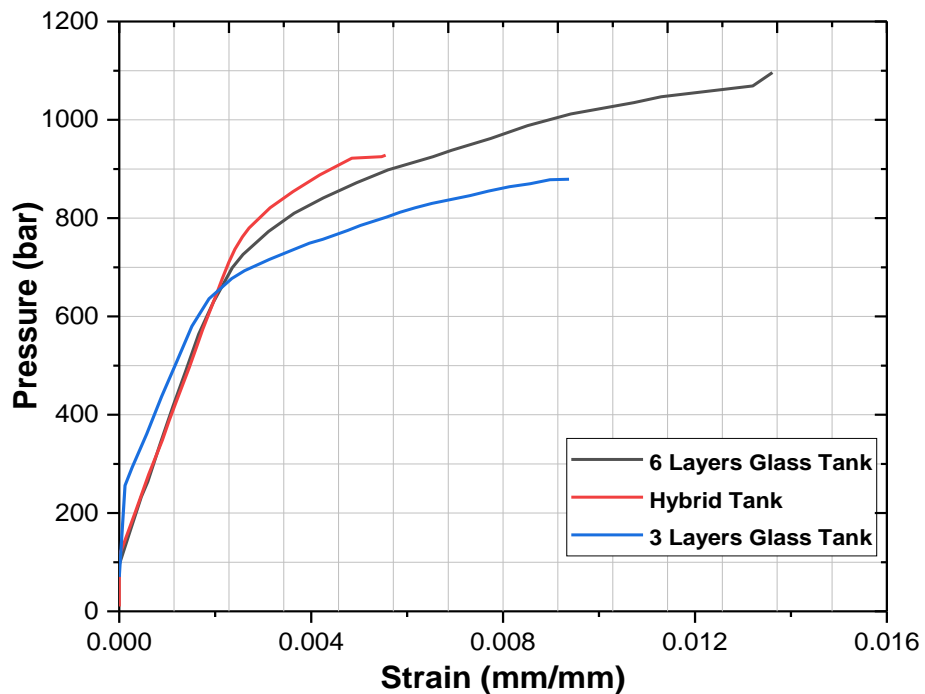


Figure 4.9. Comparison of radial strain values of composite tanks at the back central (T3) cylindrical section.

The strain gage measurements showed that, for axial directions, it was observed that there is no significant difference between 3 Layer glass fiber composite tanks and hybrid composites tanks since the helical layers were wound by using glass fibers for both tanks. 6 layers composite tanks have higher strain values as compared the other tanks since these tanks have thicker composite section and resistant to higher pressure.

For radial direction, deformation behavior hybrid composite was generally smaller than 3 layers glass composite tanks at the same pressure, which is an indication of a positive hybridization effect. However, this positive effect did not affect the burst pressure performance of composite tanks significantly. 6 layers of composite tanks again have higher strain values as compared to the other tanks.

Acoustic observations done during hydrostatic testing displayed that matrix cracking develops first. Followed by matrix failure, fiber breakage occurs especially on hoop layers (as larger strains measured on hoop direction) and after an inevitable degradation of reinforcing composite layer mechanical properties, final rupture occurs on the liner.

## **4.5. Burst Pressure Performance of Aluminum Based Composite Tanks**

The burst pressure tests were carried out for the aluminum liners and composite tanks and the results were given in Table 4.6. The average burst pressure of aluminum liners was measured as 275 bar.

Composite tanks 1 and 2 consist of 3 helical and 3 hoop layers. For tank 3 and 4, the number of helical layers were kept constant and hoop layers were increased to reinforce the cylindrical section since the previous study showed that all of the steel-based composite tanks failed from the cylindrical section. However, it was understood from the burst pressure test results, composite tanks 1 to 3 was failed from the back-dome section, also Tank 4 leaked. The burst pressure values for these tanks were not consistent and an increasing number of hoop layers did not work since the failure occurred at the back-dome section.

The number of helical and hoop layers were increased in Tank 5 and 6, such as 6 helical and 6 hoop layers were used. The burst pressure value was increased for Tank 5 but the failure again occurred in the back-dome section. Unfortunately, Tank 6 was leaked and burst pressure could not be determined. Tank 7 has 5 helical and 3 hoop layers to obtain failure in the cylindrical region and burst pressure was obtained as 500 bar.

After then, the number of helical and hoop layers was increased significantly to reach higher burst pressure. Nevertheless, Tank 8 and 9 were leaked and the burst pressure did not change significantly for Tank 10 and 11.

It was mentioned in the above that the first 14 Tank was manufactured with first batch manufactured liners which have some manufacturing problems. Therefore, accurate results could not be obtained in the first 14 Tank. For example, in Tank 11, 13 helical and 10 hoop layers were used but the burst pressure occurred in the back-dome section and only 705 bar burst pressure value was reached. Furthermore, a lot of composite Tank was leaked at the beginning of the test. It observed that some liners have micro-cracks and could not be pressurized.

After Tank 15, new produced liners were used and all the liners were subjected to sealing test before composite tank manufacturing. 9 helical and 8 hoop layers were used in Tank 15 and 1050 burst pressure value was obtained. Furthermore, the burst pressure has occurred at the front dome section. To reach 1400 bar burst pressure, the number of helical and hoop layer were increased significantly from Tank 16 to 18. However, the

burst pressure value did not improve and the failure continued to occur at the front dome sections.

Front dome doily layers were started to utilized after tank 21 such as 7 doily layers were used in the front dome section. The failure occurred at the front dome section again but the burst pressure was increased nearly 100 bar. The number of front doily layers was increased up to 17 for Tank 26 and it was observed that the burst pressure was reached to 1280 bar and failure occurred at the back-dome section. Back dome doily layers were also added to the composite tank to reinforce the back-dome section locally. From Tank 31 the final design was obtained and composite tanks have a burst pressure value of nearly 1400 bar and the failure occurred at the cylindrical section. Besides, leaking observed at the elevated pressure for tanks 27-30, to solve this problem the polyurethane resin system was utilized as mentioned above.

Table 4.6. Burst pressure results of manufactured aluminum-based composite tanks.

Tank Code	Layer Orientations	Number of Front Doily Layer	Number of Front Doily Layer	Burst Pressure (bar)	Failure Zone
Al Liner 1				277	Cylindrical (safe)
Al Liner 2				273	Cylindrical (safe)
1	$[\pm 14^\circ]_3 / [\pm 90^\circ]_3$	-	-	519	Back Dome (unsafe)
2	$[\pm 14^\circ]_3 / [\pm 90^\circ]_3$	-	-	383	Back Dome (unsafe)
3	$[\pm 14^\circ]_3 / [\pm 90^\circ]_6$	-	-	438	Back Dome (unsafe)
4	$[\pm 14^\circ]_3 / [\pm 90^\circ]_9$	-	-	Leaking	
5	$[\pm 14^\circ]_6 / [\pm 90^\circ]_6$	-	-	700	Back Dome (unsafe)
6	$[\pm 14^\circ]_6 / [\pm 90^\circ]_6$	-	-	Leaking	
7	$[\pm 14^\circ]_5 / [\pm 90^\circ]_3$	-	-	500	Cylindrical (safe)
8	$[\pm 14^\circ]_{10} / [\pm 90^\circ]_{10}$	-	-	Leaking	

(cont. on next page)

**(cont.) Table 4.6.**

9	$[\pm 14^\circ]_{11}/ [\pm 90^\circ]_{11}$	-	-	Leaking	
10	$[\pm 14^\circ]_9/ [\pm 90^\circ]_9$	-	-	735	Back Dome (unsafe)
11	$[\pm 14^\circ]_{13}/ [\pm 90^\circ]_{10}$	-	-	705	Back Dome (unsafe)
12	$[\pm 14^\circ]_9/ [\pm 90^\circ]_6$	-	-	530	Cylindrical (safe)
13	$[\pm 14^\circ]_3/ [\pm 90^\circ]_3$	-	-	520	Cylindrical (safe)
14	$[\pm 14^\circ]_9/ [\pm 90^\circ]_9$	-	-	Leaking at 640 bar	
15	$[\pm 14^\circ]_9/ [\pm 90^\circ]_8$	-	-	1050	Front Dome (unsafe)
16	$[\pm 14^\circ]_{12}/ [\pm 90^\circ]_{11}$	-	-	1050	Front Dome (unsafe)
17	$[\pm 14^\circ]_{13}/ [\pm 90^\circ]_{11}$	-	-	1050	Front Dome (unsafe)
18	$[\pm 14^\circ]_{15}/ [\pm 90^\circ]_{11}$	-	-	Leaking at 867 bar	
19	$[\pm 14^\circ]_9/ [\pm 90^\circ]_8$	-	-	1014	Front Dome (unsafe)
20	$[\pm 14^\circ]_9/ [\pm 90^\circ]_7$	-	-	1018	Front Dome (unsafe)
21	$[\pm 14^\circ]_9/ [\pm 90^\circ]_7$	7		1146	Front Dome (unsafe)
22	$[\pm 14^\circ]_9/ [\pm 90^\circ]_7$	11		1170	Front Dome (unsafe)
23	$[\pm 14^\circ]_9/ [\pm 90^\circ]_7$	15		1260	Front Dome (unsafe)
24	$[\pm 14^\circ]_9/ [\pm 90^\circ]_7$	17		1211	Front Dome (unsafe)
25	$[\pm 14^\circ]_9/ [\pm 90^\circ]_7$	17		Leaking at 1120 bar	
26	$[\pm 14^\circ]_9/ [\pm 90^\circ]_7$	17		1280 bar	Back Dome (unsafe)
27	$[\pm 14^\circ]_9/ [\pm 90^\circ]_7$	17	5	Leaked at 800 bar no burst	
28	$[\pm 14^\circ]_9/ [\pm 90^\circ]_7$	17	5	Leaked at 960 bar no burst	
29	$[\pm 14^\circ]_9/ [\pm 90^\circ]_7$	17	-	Leaked at 1000 bar no burst	

**(cont. on next page)**

**(cont.) Table 4.6.**

30	$[\pm 14^\circ]_9 / [\pm 90^\circ]_6$	17	-	Leaked at 800 bar no burst	
31	$[\pm 14^\circ]_9 / [\pm 90^\circ]_7$	17	9	1355	Cylindrical (safe)
32	$[\pm 14^\circ]_9 / [\pm 90^\circ]_7$	17	9	1397	Cylindrical (safe)
33	$[\pm 14^\circ]_9 / [\pm 90^\circ]_8$	17	9	1481 (no burst)	
34	$[\pm 14^\circ]_9 / [\pm 90^\circ]_{7.5}$	17	9	1388	Cylindrical (safe)
35	$[\pm 14^\circ]_9 / [\pm 90^\circ]_{7.5}$	17	9	1480 (no burst)	

The burst failure modes of all the liners and composite tanks tested are shown in Figure 4.10.



(a)



(b)



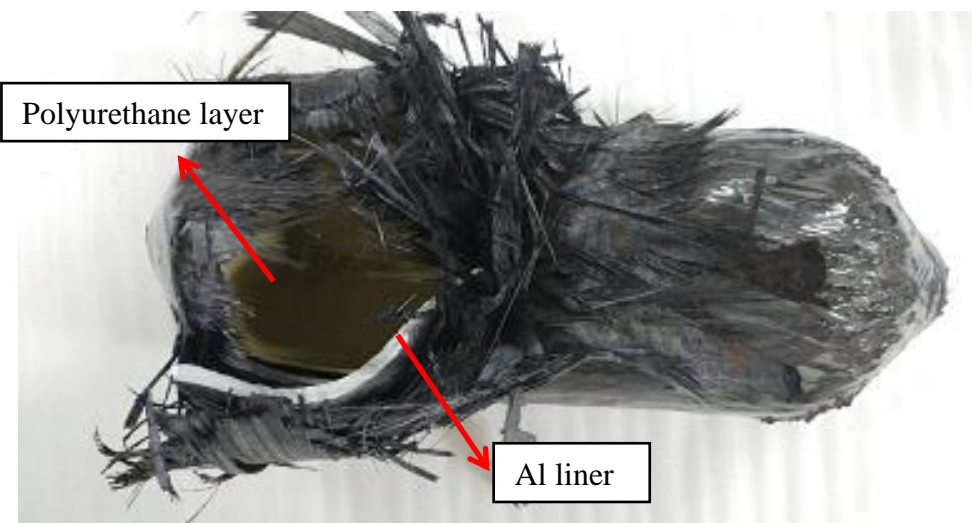
(c)



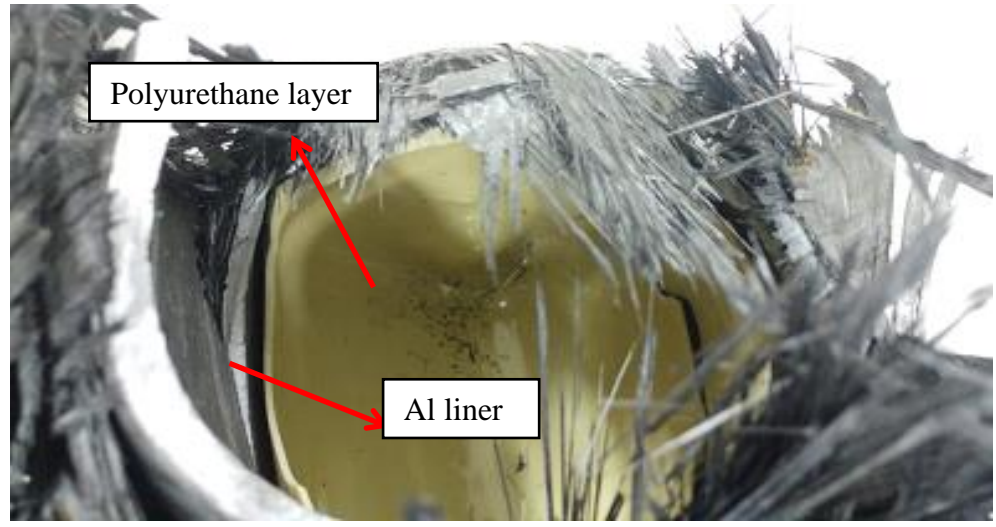
(d)

Figure 4.10. (a) Aluminum liner failure, (b) Composite tank front dome failure, (c) cylindrical failure, (d) Back dome failure

The polyurethane layer can be seen more clearly after failure in Figure 4.11. The inside walls of some composite tanks were covered by a polyurethane resin system to prevent leakage at elevated temperatures.



(a)



(b)

Figure 4.11. Polyurethane layer after failure (a) Top view, (b) Side view

The strain vs pressure graphs obtained for Al liner and some composite tanks and given below from Figure 4.12 to 4.22. As it can be seen from the graphs, the radial deformations are higher than axial deformations. For some tests, the accurate strain data cannot be obtained since the strain gauges located at the outermost section of the composite tanks and fiber breakage occurred near the strain gauge location which damages the strain gauge measurement.

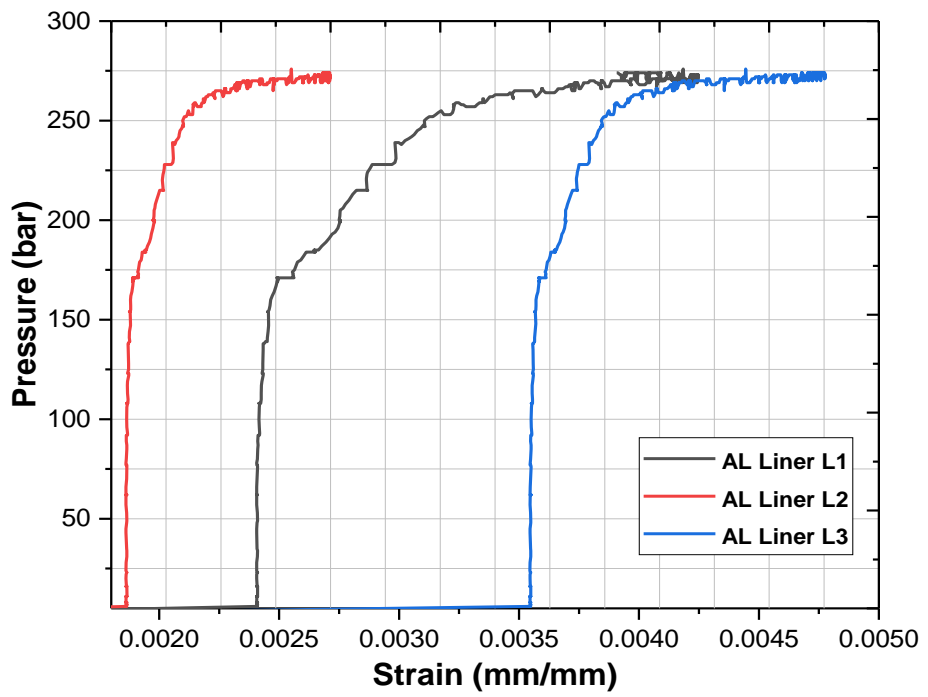


Figure 4.12. Local axial strain (L1, L2, and L3) vs. pressure values of Al Liner.

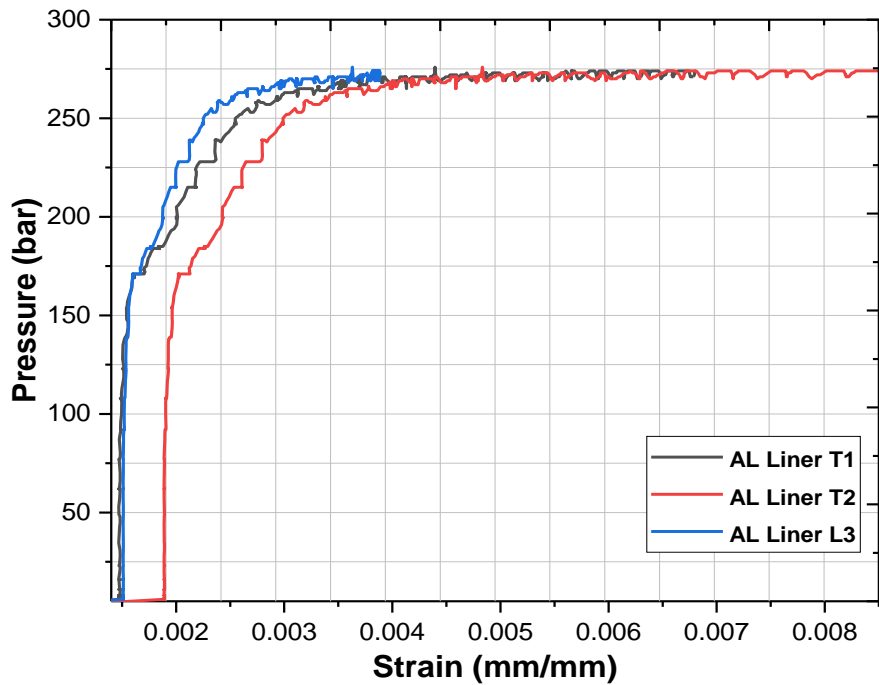


Figure 4.13. Local radial strain (T1, T2, and T3) vs. pressure values of Al Liner.

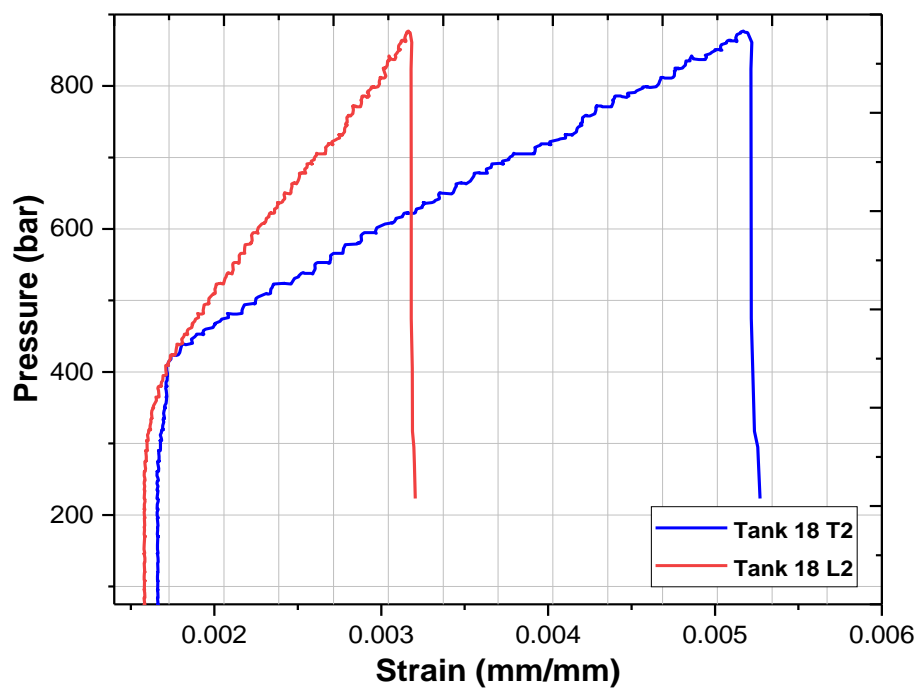


Figure 4.14. Axial and radial strain (L2 and T2) vs. pressure values of Tank 18

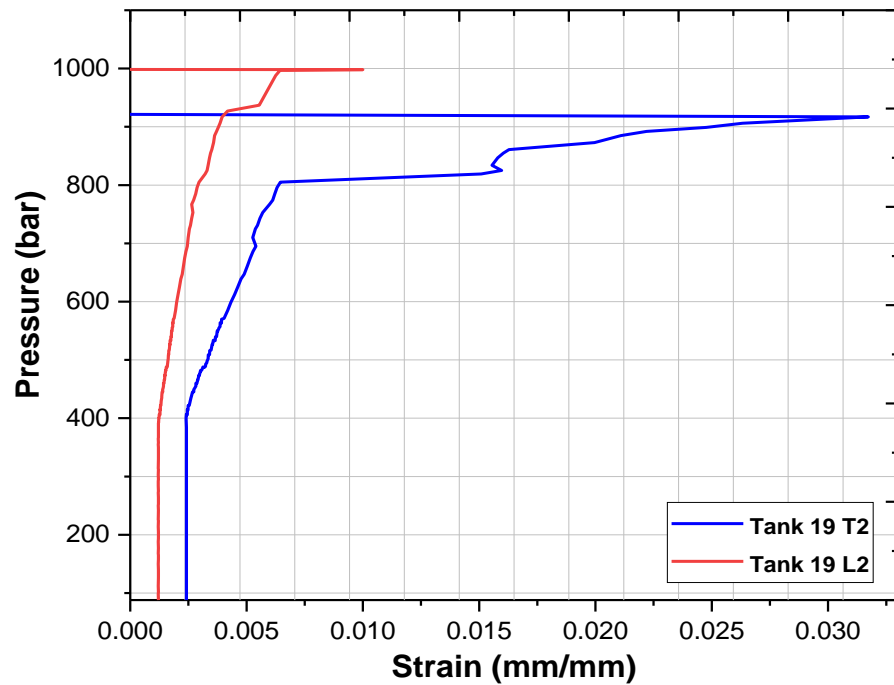


Figure 4.15. Axial and radial strain (L2 and T2) vs. pressure values of Tank 19

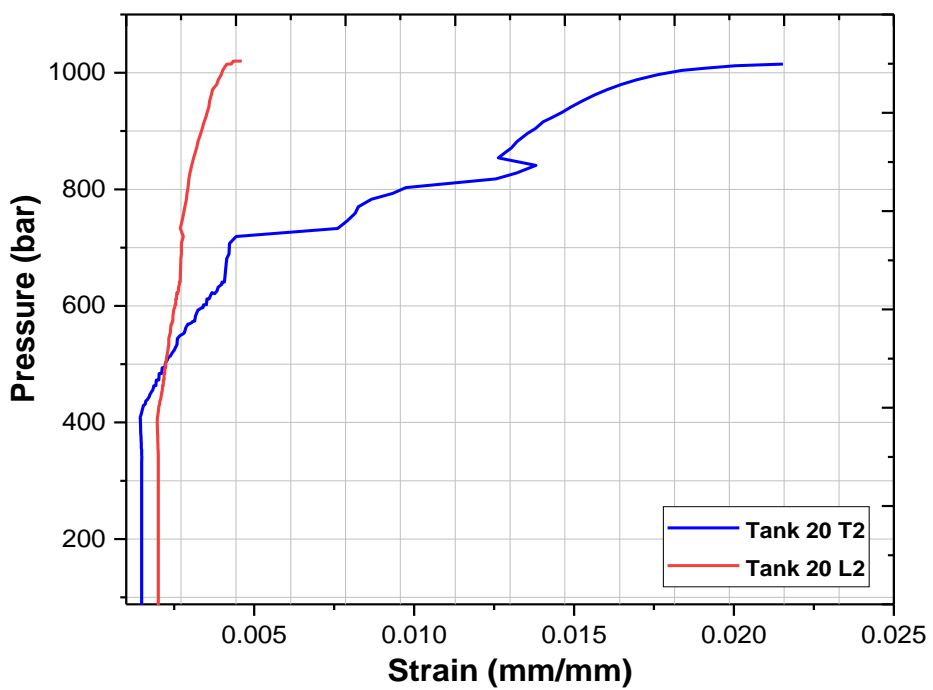


Figure 4.16. Axial and radial strain (L2 and T2) vs. pressure values of Tank 20

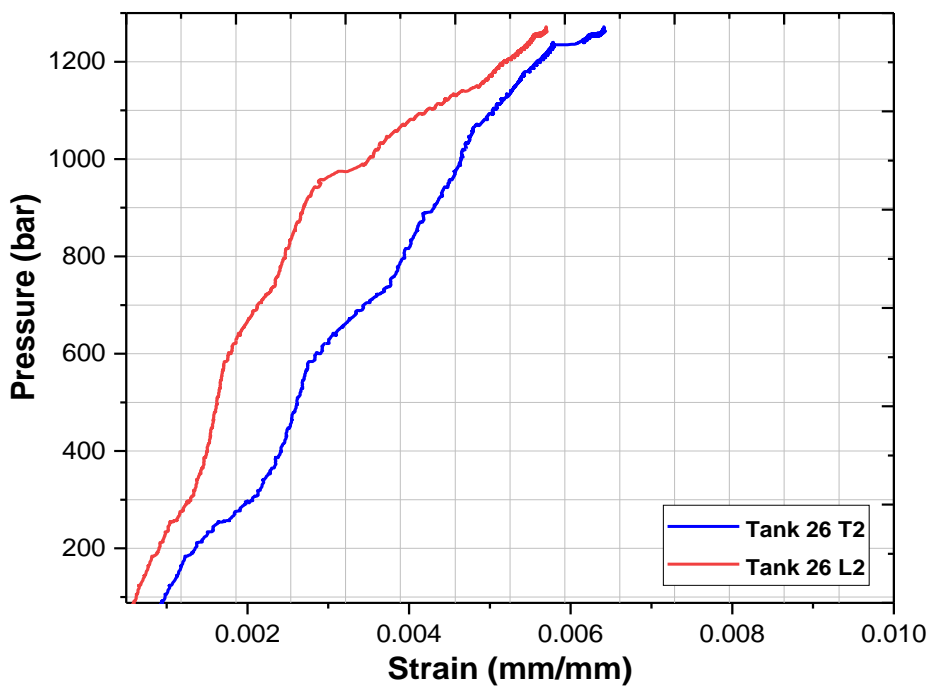


Figure 4.17. Axial and radial strain (L2 and T2) vs. pressure values of Tank 26

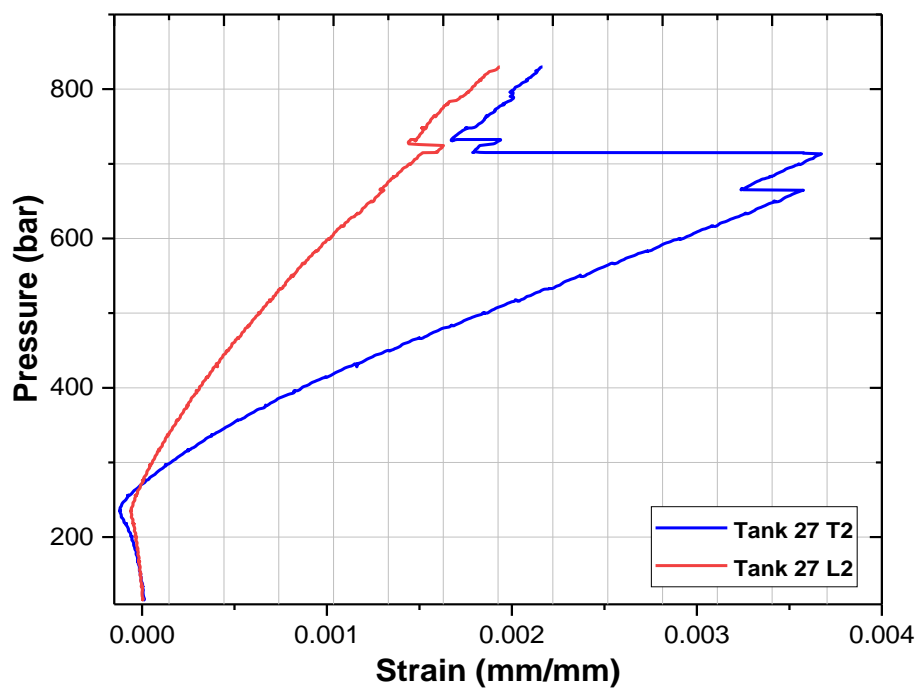


Figure 4.18. Axial and radial strain (L2 and T2) vs. pressure values of Tank 27

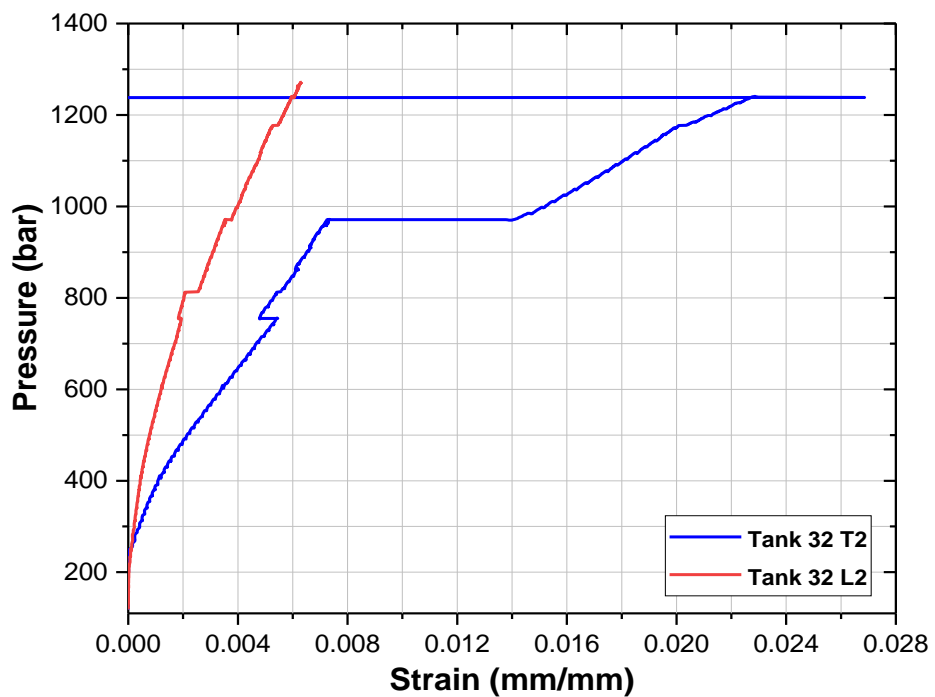


Figure 4.19. Axial and radial strain (L2 and T2) vs. pressure values of Tank 32

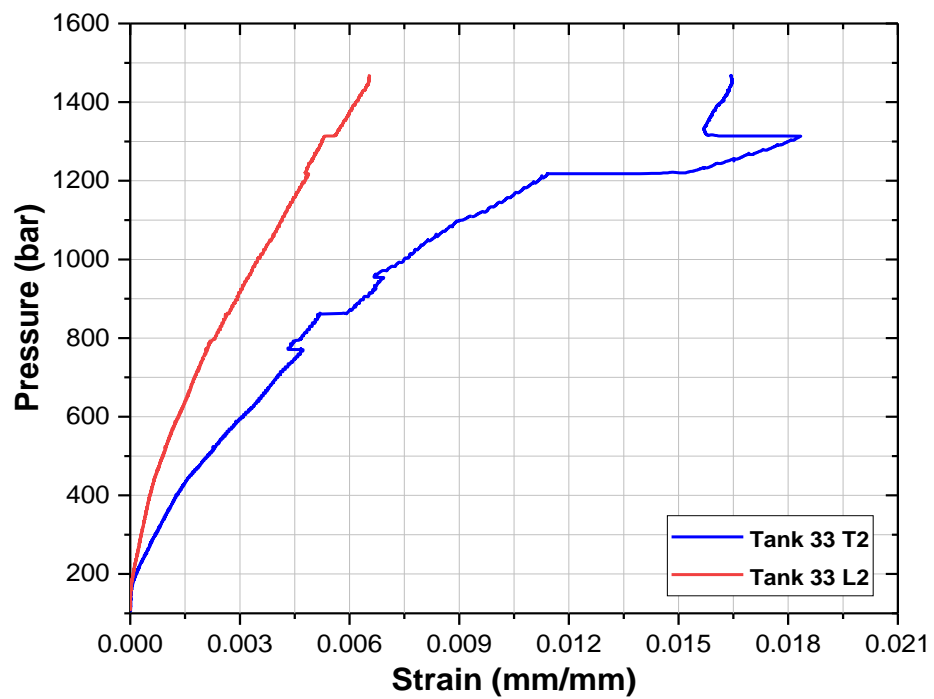


Figure 4.20. Axial and radial strain (L2 and T2) vs. pressure values of Tank 33

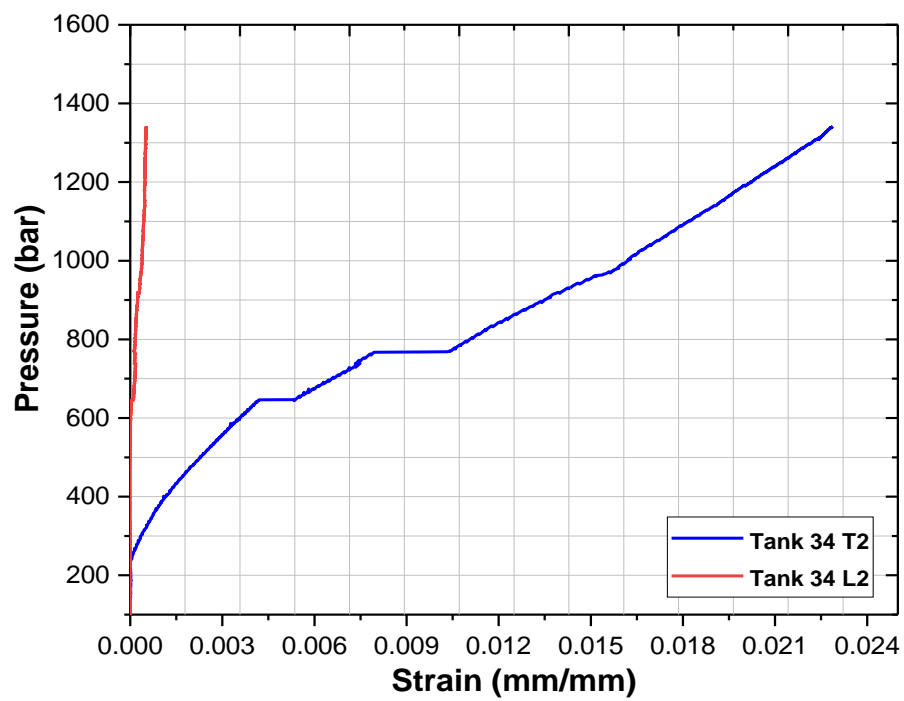


Figure 4.21. Axial and radial strain (L2 and T2) vs. pressure values of Tank 34

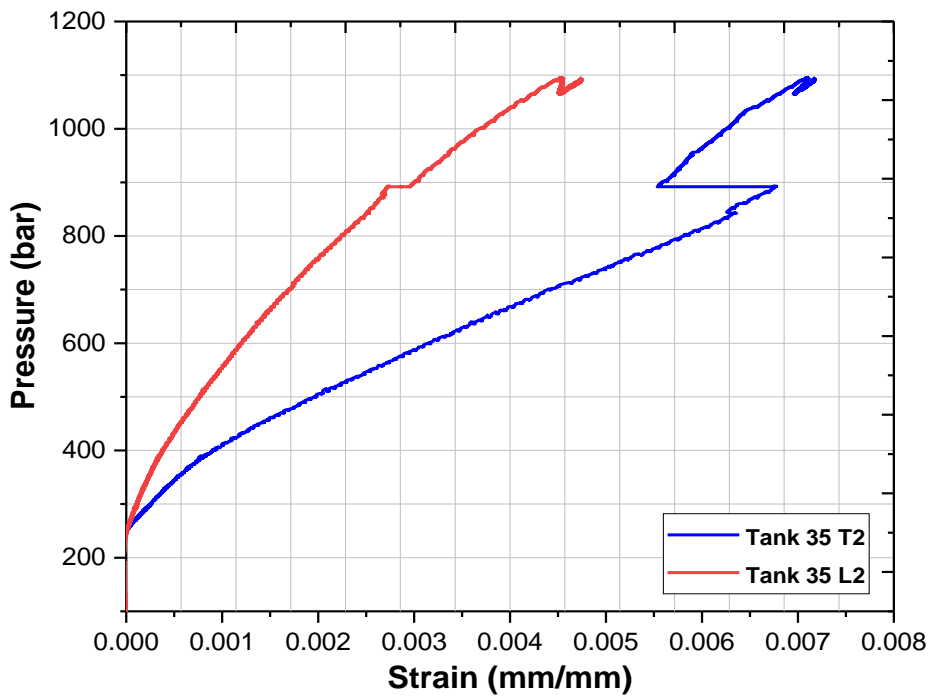


Figure 4.22. Axial and radial strain (L2 and T2) vs. pressure values of Tank 35

The composite tanks with aluminum liner not only have pressure advantage but also a significant mass advantage as compared to steel-based tanks. The steel liners have a burst pressure of 657 bar but the mass of them is 7500 gr. However, composite tanks with aluminum liner has a burst pressure of more than 1400 bar with a weight of 6498 gr. The composite tanks have a weight advantage of up to %13 percent and pressure advantage of % 113. Some weight and burst pressure comparisons are listed in Table 4.7.

Table 4.7. Mass comparisons of aluminum and steel-based tanks.

Tank	Burst Pressure (bar)	Mass (gr)
Al Liner	277	3253
Steel Tank	657	7500
Steel based Composite Tank (Tank 6)	1096	9519
Al-based Composite Tank (Tank 35)	1400+	6498

## CHAPTER 5

### EFFECT OF WINDING PARAMETERS ON THE PERFORMANCE OF COMPOSITE TANKS

#### 5.1. Manufacturing of Composite Tanks

The effect of filament winding parameters such as fiber tension and friction factor during winding on the burst pressure performance of composite tanks were investigated experimentally. These parameters are directly affecting the helical layer winding angle, winding pattern, amount of fiber usage, and coverage of the liner by composite section. First of all, a composite tank that has a friction factor value of 0.1 was manufactured as a reference value. 0.1 friction factor was selected according to software manufacturer suggestion. Then, to observe the effect of friction factor value on the burst pressure of the composite tank, 0.01 friction factor value was used which was the smallest obtained manufacturable value according to filament winding trials. To see the friction value effect, winding tension kept constant as 20 N value.

Besides, to investigate the effect of the winding tension, composite tanks with 10 N and 40 N winding tension was manufactured. 40 N is the maximum capacity of winding tensioner system and 10 N is the minimum manufacturable winding tension value.

All of the composite tanks manufactured for this specific study have 6 helical layers and 3 hoop layers. Carbon fiber filaments (Toray<sup>TM</sup> T700SC-12K-50C, 12 K) were used as the reinforcement material. 6061-T6 aluminum liners were used which are the same liners mentioned above sections. No doily layers were used because preliminary results showed that the failure occurred at the cylindrical section of the composite tanks.  $\pm 14^\circ$  helical layer winding angle was used and full coverage of aluminum liners was obtained. The details of the filament winding parameters were mentioned in Chapter 3. All manufactured composite tanks with different filament winding parameters are tabulated in Table 5.1

Table 5.1. Manufactured composite tanks with different winding properties

Tank Code	Layer Orientation	Winding Tension (N)	Friction Factor
1	$[\pm 14^\circ]_6 / [\pm 90^\circ]_3$	10	0.1
2	$[\pm 14^\circ]_6 / [\pm 90^\circ]_3$	40	0.1
3	$[\pm 14^\circ]_6 / [\pm 90^\circ]_3$	20	0.1
4	$[\pm 14^\circ]_6 / [\pm 90^\circ]_3$	20	0.01

The Friction factor value given as an input parameter of the CADWIND™ CAM software and the winding tension value of the fiber tensioner system can be seen in Figures 5.1 and 5.2 respectively.

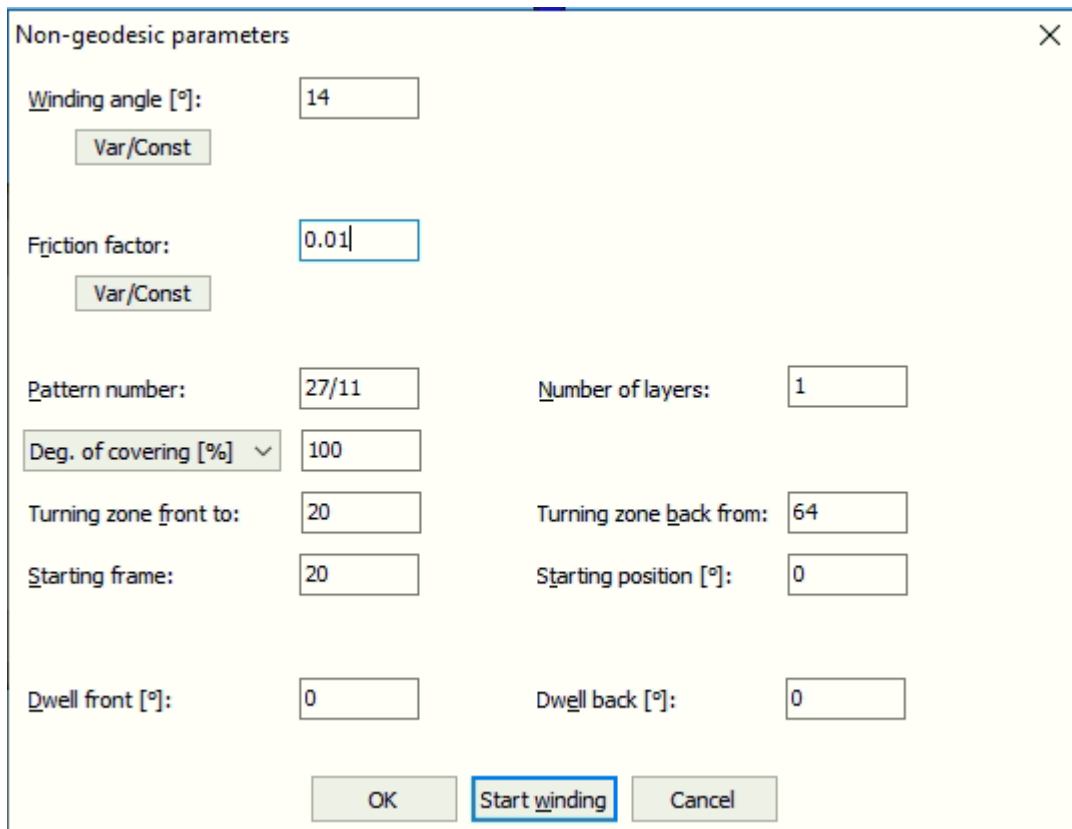


Figure 5.1. Defined Friction Factor Value

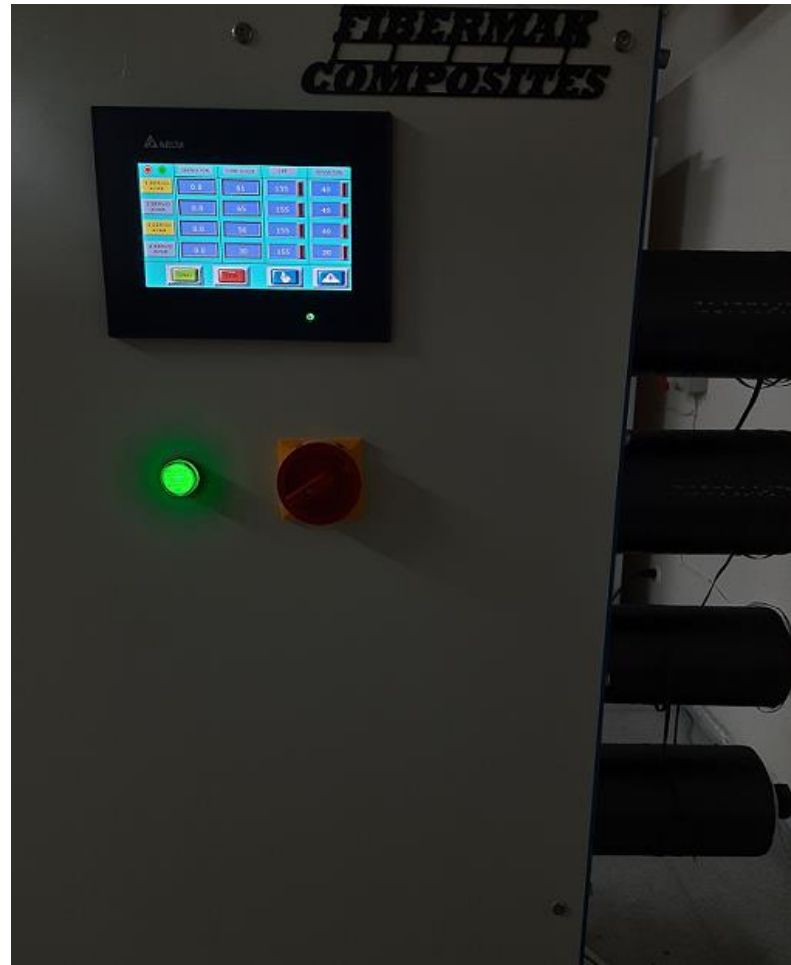


Figure 5.2. Fiber tensioner system

## 5.2. Results of Burst Pressure Test

The burst pressure test results of manufactured composite tanks are given in Table 5.2. The results showed that filament winding tension affects the burst pressure performance of the composite tanks significantly.

Table 5.2. Burst Pressure Results of Manufactured Composite Tanks

Tank Code	Layer Orientation	Winding Tension (N)	Friction Factor	Burst Pressure (Bar)
1	$[\pm 14^\circ]_6 / [\pm 90^\circ]_3$	10	0.1	765
2	$[\pm 14^\circ]_6 / [\pm 90^\circ]_3$	40	0.1	835
3	$[\pm 14^\circ]_6 / [\pm 90^\circ]_3$	20	0.1	763
4	$[\pm 14^\circ]_6 / [\pm 90^\circ]_3$	20	0.01	759

The burst pressure of a 10 N winding tension composite tank was found as a 765 bar. However, increasing the winding tension up to 40 N, the burst pressure of composite tank that manufactured with 40 N winding tension was found as an 835 bar (%9 increase). The burst pressure test results showed that the friction factor value did not affect the burst pressure results of composite tanks significantly. Since all the composite tanks failed from the cylindrical section, the friction factor could not affect the hoop winding. The friction factor was given as an input value for the software for only helical winding. The composite tanks after failure was given in Figure 5.3



(a)



(b)



(c)



(d)

Figure 5.3. Composite Tanks After Failure (a) Tank 1, (b) Tank 2, (c) Tank 3, (d)Tank 4

## CHAPTER 6

### CONCLUDING REMARKS

The large part of the energy needs of the world is supplied from fossil fuels nowadays. CO<sub>2</sub> and other greenhouse gases come from the burning of fossil fuels, cause global warming, and serious environmental pollution. Hydrogen is regarded as the new energy source for the next century due to zero greenhouse emission, high energy efficiency, and unlimited. To use this energy more widely and become an alternative to fossil fuels, hydrogen must be stored more compactly and safely. There are generally three ways to store hydrogen which are: (i) Storage in solid material, (ii) Storage as a cryogenic liquid, (iii) Compressed gaseous storage in a pressurized tank. Compressed gaseous storage in the pressurized tank technique is the most popular and effective way since the filling process is faster and more economical.

The high-pressure hydrogen storage tanks can be divided into four different categories according to their performance and cost. Type I: These types of tanks have all-metal construction, generally steel. They are cheap but heavy and not suitable for mobile applications. Type-II: These tanks have a metal liner but only the hoop section is overwrapped with the composite section. They are lighter than Type I tanks but more expansible. Type-III: They have also metal liner but all of the liner overwrapped with composite section. Type-IV: There are polymer liners in these types of tanks. They are lighter than Type-III tanks but heavier. In mobile applications, Type-III and Type-IV tanks are more practical. The working pressures of Type-III tanks are generally 350 bars, however, by storing hydrogen at 700 bars the same weight can be provided with lower volume. Therefore, it can be more suitable for the new generation of automobiles.

In this thesis, high-pressure composite tanks with Al liners were designed and manufactured by filament winding technique with various lay-up configurations and tested. The main objective of this study was to develop composite tanks with 700 bar working pressure and 1400 bar burst pressure. Furthermore, doily layers were incorporated into the front and end domes of the composite tanks to improve the burst pressure performance of the vessels manufactured with helical and hoop winding configurations. The winding simulations were completed using CADWIND™ CAM

software. The manufactured composite tanks were hydrostatically loaded with increasing internal pressure up to the burst pressure. During loading, the deformations over the tanks and liners were measured locally using strain gauges. Furthermore, the mechanical properties of the liners and the composite sections and the thermo-mechanical properties and the fiber mass fractions of composite sections were determined. To investigate the mechanical properties of composite sections, composite plates were manufactured by filament winding technique. Moreover, a preliminary study was carried out to investigate the effect of hybrid fiber usage on the burst pressure performance of steel liner based composite tanks. Glass and carbon fibers were used to reinforce the steel liners.

Before the filament winding process, winding simulations were conducted with CADWIND™ CAM software and filament winding parameters such as mandrel shape, fiber type, friction factor, number of rovings, winding patterns, etc. were given to the software as input values. After then winding simulations were carried out and G-codes were produced. These G-codes were adopted to the filament winding machine and winding started. During the manufacturing process for composite tanks, several manufacturing problems were solved such as fiber slippage, long manufacturing time, fiber and resin interactions, etc.

Especially for manufacturing Al liner based composite tanks, there were some problems with the quality of the aluminum liners. Since it is very hard to manufacture these aluminum liners some problems have occurred. First of all, some liners have micro-cracks so even if the composite tanks manufactured successfully, the burst pressure tests could not be performed because of these macro cracks. This problem was solved but the burst pressure test results were showed that the composite tanks were failed from the front dome sections. Therefore, doily layers were utilized. Doily layers provide extra strength at the dome sections and decrease the need for number helical layers which decreases the winding time and carbon fiber usage. Other advantages of doily layers are, they provide extra friction during the helical winding and decrease the risk of fiber slippage during the manufacturing. Especially, when the number of the helical layer increases, the thicknesses in the dome section increases significantly, so doily layers can be helpful about this problem.

For steel liner based composite tanks, the burst pressure test results showed that composite reinforcement increased the burst pressure performance of steel liner up to 25% percent. However, it is observed that hybridization has no significant effect on the burst pressure performance of composite tanks. This can be explained by the stiffness

difference between the carbon and glass filaments. All the tanks and liners failed from the cylindrical section.

For Al liner based composite tanks, the experimental measurements led to the following conclusions; with composite tanks containing  $\pm 14^\circ$  helical and hoop wounded composite plies, without any doily layer a burst pressure up to about 1050 bar can be achievable. However, for composite tanks manufactured without using any doily layers, there is no significant effect of increasing the number of the helical and hoop plies wounded over the tank to further increase the burst pressure values above some limit point. The failure observed at the front dome region explains the limited effect of the helical and hoop layer numbers on the burst pressure level. The addition of doily layers at the front and end dome sections improved the burst pressure performance of the composite tanks significantly and the 1400 bar critical pressure value was reached. In this case, a desired safe burst mode that is expected to occur in the mid-region of the composite tanks was successfully obtained. The failure location is also an important parameter for composite pressure tanks. The failure must have occurred at the cylindrical section which is called as “safe failure”. Otherwise, fragments can be spread out from the composite tank and the weak portions of the composite pressure tanks can be reinforced locally by utilizing the doily layers. There were no published studies in the literature about the effects of doily layers on the burst pressure performance of the composite tanks experimentally.

During the burst tests for Al liner based composite tanks, it was observed that at the elevated pressure some composite tanks had leaking problems. To solve this problem an innovative solution was found. The inside walls of the aluminum liner were coated with a polyurethane-based resin system after a composite tank was manufactured. Polyurethane resin system obtained and covered the inside of the composite tank. Then the tank was rotated until the resin system was cured inside the tank. Then the inside of the composite pressure tank was observed to control if the resin system distributes homogeneously by using snake cam. The results showed that after the polyurethane resin system was utilized there is no leaking problem even if above 1400 bar pressure values.

Besides, a special study was also carried out, the effect of winding parameters on the burst pressure performance of composite tanks was investigated experimentally. The effect of winding tension during the manufacturing process and effect of friction factor values used during simulation and winding process was investigated individually. The results showed that increasing winding tension during the manufacturing of a composite

tank increases the burst pressure performance of composite tanks significantly. However, the burst pressure test results showed that friction factor value has no effects on the burst pressure results of composite tanks. Since all the composite tanks failed from the cylindrical section, the friction factor could not affect the hoop winding. The friction factor was given as an input value for the software for only helical winding.

The above understandings may be useful for practical applications and future developments of composite tanks for high-pressure gaseous storage such as hydrogen.

## 6.1. Future Studies

Since there are important milestones in technologies for the use of hydrogen energy and developed products are in usage such as hydrogen is used as an energy source for public and personal transportation, in hospitals, public buildings and remote areas from settlements, hydrogen should be stored safely and compactly. It is understood from this study composite tanks can be a solution for this storage problem such as more than 1400 bar pressure values were obtained.

There is a solid knowledge of these composite tanks topic and some commercial products can be obtained in the market. However, there are some problems with the manufacturing of these composite tanks such as testing, costs, fiber and resin type, recyclability, production quantity, slippage problem, etc. These studies and investigations can be carried out to increase the usage of composite tanks for high-pressure gaseous applications:

- The liner material and the shape of the liner is directly affecting the filament winding manufacturing of composite tanks. Therefore, a liner which is suitable for helical winding can be developed the variety of helical winding angle can be obtained. Also, a polymeric liner can be manufactured with identical dimensions according to the aluminum liner and the effect of the liner type on the performance of the composite tanks can be investigated.
- In filament winding process friction factor between fibers-liner and fibers-fibers has great importance. This friction factor determines the winding angle of helical layers and when the friction factor increases, the variety

of winding angles also increases. Filament winding with towpregs offers a higher friction factor as compared to wet winding. These towpregs have higher friction factor value as indicated in the CADWIND™ CAM software user's manual and the slippage problem during the filament winding can be decreased significantly. Furthermore, since towpregs are resin pre-impregnated fibers, there will be no resin bath during manufacturing and the process can be faster.

- Burst pressure tests are applied to composite tanks but since these composite tanks are critical for the automotive industry and re-filling of these composite tanks are another design problem, fatigue tests can be applied to manufactured composite tanks.
- Thermoset resin materials were used to manufacture the composite tanks but thermoplastic resin can be used as a matrix material to obtain recyclable composite tanks. Besides, thermoplastic resin can decrease the slippage problem during filament winding.
- In the manufacturing composite tank, there are serious thickness variations for one helical layer. Especially in the back dome and front sections, thickness values are increasing up to 20 times compared to the cylindrical section. Therefore, a finite element model can be developed including these thickness and angle variations, and featuring a simple progressive failure model for the composite section.
- Filament winding parameters such as roving bandwidth, fiber volume fractions, friction factor, and winding tension are directly affecting the burst pressure performance of the composite tanks. Therefore, a parametric study can be carried out to optimize these parameters carbon fiber and resin usage, winding time, and weight of the composite tanks can be decreased.

## REFERENCES

- (1) Ellerman, D.; and Marcantonini, C. *The Cost of Abating CO<sub>2</sub> Emissions by Renewable Energy Incentives in Germany*. MIT CEEPR Working Paper, (2013).
- (2) Oyakhire, O. "Hydrogen untapped energy?", Institution of Gas Engineers and Managers, Report. [http://www.igem.org.uk/media/251537/IGEM\\_Hydrogen\\_%20Report\\_FINAL-v2013.pdf](http://www.igem.org.uk/media/251537/IGEM_Hydrogen_%20Report_FINAL-v2013.pdf) (accessed Jun 10, 2019).
- (3) Zheng, J.; Liu, X.; Xu, P.; Liu, P.; Zhao, Y.; Yang, J. Development of High Pressure Gaseous Hydrogen Storage Technologies. *Int. J. Hydrogen Energy* (2012), 37 (1), 1048–1057. <https://doi.org/10.1016/j.ijhydene.2011.02.125>.
- (4) Ghouaoula, A.; Hocine, A.; Chapelle, D.; Karaachira, F.; Boubakar, M. L. Analytical Prediction of Damage in the Composite Part of a Type-3 Hydrogen Storage Vessel. *Mech. Compos. Mater.* (2012), 48 (1), 77–88.
- (5) Red C. Pressure vessels for alternative fuels 2014-2023. Compos World, (2014).
- (6) Ichikawa, T.; Hanada, N.; Isobe, S.; Leng, H.; Fujii, H. Composite Materials Based on Light Elements for Hydrogen Storage. *Mater. Trans.* (2005), 46 (1), 1–14. <https://doi.org/10.2320/matertrans.46.1>.
- (7) Clyne, T. W.; Hull, D. *An Introduction to Composite Materials*; (2019). <https://doi.org/10.1017/9781139050586>.
- (8) Naslain, R. R.; Pomeroy, M. Ceramic Matrix Composites: Matrices and Processing. In *Reference Module in Materials Science and Materials Engineering*; (2016). <https://doi.org/10.1016/b978-0-12-803581-8.02317-1>.
- (9) Qin, Q. H. Introduction to the Composite and Its Toughening Mechanisms. In *Toughening Mechanisms in Composite Materials*; (2015). <https://doi.org/10.1016/B978-1-78242-279-2.00001-9>.
- (10) Tsai, S.; *Introduction to composite materials*; Routledge; (2018).
- (11) Ehrlich, H.; Janussen, D.; Simon, P.; Bazhenov, V. V.; Shapkin, N. P.; Erler, C.; Mertig, M.; Born, R.; Heinemann, S.; Hanke, T.; Worch, H.; Vournakis, J. N. Nanostructural Organization of Naturally Occurring Composites-Part II: Silica-Chitin-Based Biocomposites. *J. Nanomater.* (2008). <https://doi.org/10.1155/2008/670235>.
- (12) Johnson, Todd. "History of Composites." ThoughtCo, Aug. 1, 2018, [thoughtco.com/history-of-composites-820404](http://thoughtco.com/history-of-composites-820404) (accessed date: Nov 12, 2019).
- (13) Rajak, D. K.; Pagar, D. D.; Kumar, R.; Pruncu, C. I. Recent Progress of Reinforcement Materials: A Comprehensive Overview of Composite Materials. J.

- Mater. Res. Technol. (2019). <https://doi.org/10.1016/j.jmrt.2019.09.068>.  
<https://doi.org/10.1016/j.ijhydene.2016.03.178>.
- (14) Ray, B. C. Temperature Effect during Humid Ageing on Interfaces of Glass and Carbon Fibers Reinforced Epoxy Composites. *J. Colloid Interface Sci.* (2006). <https://doi.org/10.1016/j.jcis.2005.12.023>.
- (15) Xu, Y.; Chung, D. D. L.; Mroz, C. Thermally Conducting Aluminum Nitride Polymer-Matrix Composites. *Compos. - Part A Appl. Sci. Manuf.* (2001). [https://doi.org/10.1016/S1359-835X\(01\)00023-9](https://doi.org/10.1016/S1359-835X(01)00023-9).
- (16) Davim, J. P.; Reis, P. Study of Delamination in Drilling Carbon Fiber Reinforced Plastics (CFRP) Using Design Experiments. *Compos. Struct.* (2003). [https://doi.org/10.1016/S0263-8223\(02\)00257-X](https://doi.org/10.1016/S0263-8223(02)00257-X).
- (17) Mazumdar, S. K. *Composites Manufacturing: Materials, Product, and Process Engineering*; (2001).
- (18) Thoppul, S. D.; Finegan, J.; Gibson, R. F. Mechanics of Mechanically Fastened Joints in Polymer-Matrix Composite Structures - A Review. *Composites Science and Technology*. (2009). <https://doi.org/10.1016/j.compscitech.2008.09.037>.
- (19) Li, J.; Laghari, R. A. A Review on Machining and Optimization of Particle-Reinforced Metal Matrix Composites. *International Journal of Advanced Manufacturing Technology*. (2019). <https://doi.org/10.1007/s00170-018-2837-5>.
- (20) Metal Matrix Composites, <https://materion.com/products/metal-matrix-composites> (accessed date: Jan 31, 2020).
- (21) Porsche ceramic brake rotor, part of display for 300th anniversary of porcelain, <https://www.autoblog.com/2008/03/14/porsche-ceramic-brake-rotor-part-of-display-for-300th-anniversa/> (accessed date: Jan 31, 2020).
- (22) Carbon Fiber Composite Tubes, <https://www.carbon-light.com/products/carbon-fiber-tubes/> (accessed date: Jan 31, 2020).
- (23) Husić, S.; Javni, I.; Petrović, Z. S. Thermal and Mechanical Properties of Glass Reinforced Soy-Based Pol Yurethane Composites. *Compos. Sci. Technol.* (2005). <https://doi.org/10.1016/j.compscitech.2004.05.020>.
- (24) Rezaei, F.; Yunus, R.; Ibrahim, N. A. Effect of Fiber Length on Thermomechanical Properties of Short Carbon Fiber Reinforced Polypropylene Composites. *Mater. Des.* (2009). <https://doi.org/10.1016/j.matdes.2008.05.005>.
- (25) Gan, Y. X.; Solomon, D.; Reinbolt, M. Friction Stir Processing of Particle Reinforced Composite Materials. *Materials (Basel)*. (2010). <https://doi.org/10.3390/ma3010329>.
- (26) Aditya Narayan, D.; Ganapathi, M.; Pradyumna, B.; Haboussi, M. Investigation of Thermo-Elastic Buckling of Variable Stiffness Laminated Composite Shells Using Finite Element Approach Based on Higher-Order Theory. *Compos. Struct.* (2019). <https://doi.org/10.1016/j.compstruct.2018.12.012>.

- (27) Davim, J. P.; Reis, P.; António, C. C. Experimental Study of Drilling Glass Fiber Reinforced Plastics (GFRP) Manufactured by Hand Lay-Up. *Compos. Sci. Technol.* (2004). [https://doi.org/10.1016/S0266-3538\(03\)00253-7](https://doi.org/10.1016/S0266-3538(03)00253-7).
- (28) Al-Qureshi, H. A. Automobile Leaf Springs from Composite Materials. *Journal of Materials Processing Technology*; (2001). [https://doi.org/10.1016/S0924-0136\(01\)00863-9](https://doi.org/10.1016/S0924-0136(01)00863-9).
- (29) Hand Lay-up technique <https://www.eppcomposites.com/hand-layup-process.html> (accessed date: Jan 31, 2020).
- (30) Krishnamurthy, T. N.; Muralidhar Idkan. Fabrication of low cost filament winding machine. *International Journal of Recent Trends in Electrical & Electronics Engg.* (2014). 4(1), 30-39.
- (31) Quanjin, M.; Rejab, M. R. M.; Idris, M. S.; Zhang, B.; Kumar, N. M. Filament Winding Technique: SWOT Analysis and Applied Favorable Factors. *Journal of Mechanical Engineering*. (2019).
- (32) Goren, A.; Atas, C. Manufacturing of Polymer Matrix Composites Using Vacuum Assisted Resin Infusion Molding. *Arch. Mater. Sci. Eng.* (2008).
- (33) Vacuum infusion process <http://www.altropol.de/en/vakuuminfusion/> (accessed date: Feb 2, 2020).
- (34) Rouison, D.; Sain, M.; Couturier, M. Resin Transfer Molding of Natural Fiber Reinforced Composites: Cure Simulation. *Compos. Sci. Technol.* (2004). <https://doi.org/10.1016/j.compscitech.2003.06.001>.
- (35) The resin transfer molding <https://technicalmarvel.wordpress.com/2017/09/05/hprt/> (accessed date: Feb 3, 2020).
- (36) Akil, H. M.; De Rosa, I. M.; Santulli, C.; Sarasini, F. Flexural Behaviour of Pultruded Jute/Glass and Kenaf/Glass Hybrid Composites Monitored Using Acoustic Emission. *Mater. Sci. Eng. A* (2010). <https://doi.org/10.1016/j.msea.2010.01.028>.
- (37) Pultrusion <http://www.cyccomposites.net/sale-8445996-e-glass-fiberglass-single-end-roving-for-pultrusion.html> (accessed date: Feb 3, 2020).
- (38) Wittemann, F.; Maertens, R.; Bernath, A.; Hohberg, M.; Kärger, L.; Henning, F. Simulation of Reinforced Reactive Injection Molding with the Finite Volume Method. *J. Compos. Sci.* (2018). <https://doi.org/10.3390/jcs2010005>.
- (39) Sánchez, M.; Rams, J.; Ureña, A. Fabrication of Aluminium Composites Reinforced with Carbon Fibres by a Centrifugal Infiltration Process. *Compos. Part A Appl. Sci. Manuf.* (2010). <https://doi.org/10.1016/j.compositesa.2010.07.014>.
- (40) Bader, M. G. Selection of Composite Materials and Manufacturing Routes for Cost-Effective Performance. *Compos. - Part A Appl. Sci. Manuf.* (2002). [https://doi.org/10.1016/S1359-835X\(02\)00044-1](https://doi.org/10.1016/S1359-835X(02)00044-1).

- (41) Hu, C.; Sun, Z.; Xiao, Y.; Qin, Q. Recent Patents in Additive Manufacturing of Continuous Fiber Reinforced Composites. *Recent Patents Mech. Eng.* (2019). <https://doi.org/10.2174/2212797612666190117131659>.
- (42) Uyyuru, R. K.; Surappa, M. K.; Brusethaug, S. Tribological Behavior of Al-Si-SiCp Composites/Automobile Brake Pad System under Dry Sliding Conditions. *Tribol. Int.* (2007). <https://doi.org/10.1016/j.triboint.2005.10.012>.
- (43) Kong, C.; Lee, H.; Park, H. Design and Manufacturing of Automobile Hood Using Natural Composite Structure. *Compos. Part B Eng.* (2016). <https://doi.org/10.1016/j.compositesb.2015.12.033>.
- (44) The Carbon-Fiber Future: It's About More Than Speed (Op-Ed) <https://www.livescience.com/53995-carbon-fiber-may-finally-be-coming-to-cars-everywhere.html> (accessed date: Feb 3, 2020).
- (45) Alarifi, I. M. Investigation the Conductivity of Carbon Fibercomposites Focusing on Measurement Techniquesunder Dynamic and Static Loads. *Journal of Materials Research and Technology.* (2019). <https://doi.org/10.1016/j.jmrt.2019.08.019>.
- (46) Basri, E. I.; Sultan, M. T. H.; Faizal, M.; Basri, A. A.; Abas, M. F.; Majid, M. S. A.; Mandeep, J. S.; Ahmad, K. A. Performance Analysis of Composite Ply Orientation in Aeronautical Application of Unmanned Aerial Vehicle (UAV) NACA4415 Wing. *J. Mater. Res. Technol.* (2019). <https://doi.org/10.1016/j.jmrt.2019.06.044>.
- (47) What is MSE? <https://mse.skule.ca/guide/> (accessed date: Feb 3, 2020).
- (48) Young, Y. L. Fluid-Structure Interaction Analysis of Flexible Composite Marine Propellers. *J. Fluids Struct.* (2008). <https://doi.org/10.1016/j.jfluidstructs.2007.12.010>.
- (49) Composite solutions for ship propeller blades <https://www.airborne.com/composites-marine/> (accessed date: Feb 3, 2020).
- (50) Mahdavi, H. R.; Rahimi, G. H.; Farrokhabadi, A. Failure Analysis of ( $\pm 55^\circ$ )9 Filament-Wound GRE Pipes Using Acoustic Emission Technique. *Eng. Fail. Anal.* (2016). <https://doi.org/10.1016/j.engfailanal.2015.12.004>.
- (51) Composite manufacturing <http://compositesmanufacturingmagazine.com/2019/02/guerrilla-gravity-is-using-its-patent-pending-revved-carbon-technology-to-build-carbon-fiber-bicycle-frames/> (accessed date: Feb 3, 2020).
- (52) Rusman, N. A. A.; Dahari, M. A Review on the Current Progress of Metal Hydrides Material for Solid-State Hydrogen Storage Applications. *International Journal of Hydrogen Energy.* (2016). <https://doi.org/10.1016/j.ijhydene.2016.05.244>.
- (53) Staffell, I.; Scamman, D.; Velazquez Abad, A.; Balcombe, P.; Dodds, P. E.; Ekins,

- P.; Shah, N.; Ward, K. R. The Role of Hydrogen and Fuel Cells in the Global Energy System. *Energy and Environmental Science*. (2019). <https://doi.org/10.1039/c8ee01157e>.
- (54) Dodds, P. E.; Ekins, P. A Portfolio of Powertrains for the UK: An Energy Systems Analysis. In *International Journal of Hydrogen Energy*; (2014). <https://doi.org/10.1016/j.ijhydene.2014.06.128>.
- (55) Pollet, B. G.; Staffell, I.; Shang, J. L. Current Status of Hybrid, Battery and Fuel Cell Electric Vehicles: From Electrochemistry to Market Prospects. *Electrochimica Acta*. (2012). <https://doi.org/10.1016/j.electacta.2012.03.172>.
- (56) Fuel Cell Vehicles- Automobiles <https://www.fuelcellstore.com/blog-section/fuel-cell-vehicles-automobiles> (accessed date: Feb 4, 2020).
- (57) Hua, T.; Ahluwalia, R.; Eudy, L.; Singer, G.; Jermer, B.; Asselin-Miller, N.; Wessel, S.; Patterson, T.; Marcinkoski, J. Status of Hydrogen Fuel Cell Electric Buses Worldwide. *Journal of Power Sources*. (2014). <https://doi.org/10.1016/j.jpowsour.2014.06.055>.
- (58) Fuel Cell Buses, Utility Vehicles and Scooters <https://www.fuelcellstore.com/blog-section/fuel-cell-buses-utility-vehicles-scooters> (accessed date: Feb 4, 2020).
- (59) Hwang, H. T.; Varma, A. Hydrogen Storage for Fuel Cell Vehicles. *Current Opinion in Chemical Engineering*. (2014). <https://doi.org/10.1016/j.coche.2014.04.004>.
- (60) Kalanidhi, A. Boil-off in Long-Term Stored Liquid Hydrogen. *Int. J. Hydrogen Energy* (1988). [https://doi.org/10.1016/0360-3199\(88\)90055-9](https://doi.org/10.1016/0360-3199(88)90055-9).
- (61) Ahluwalia, R. K.; Hua, T. Q.; Peng, J. K.; Lasher, S.; McKenney, K.; Sinha, J.; Gardiner, M. Technical Assessment of Cryo-Compressed Hydrogen Storage Tank Systems for Automotive Applications. *Int. J. Hydrogen Energy* (2010). <https://doi.org/10.1016/j.ijhydene.2010.02.074>.
- (62) Principi, G.; Agresti, F.; Maddalena, A.; Lo Russo, S. The Problem of Solid State Hydrogen Storage. *Energy* (2009). <https://doi.org/10.1016/j.energy.2008.08.027>.
- (63) Umegaki, T.; Yan, J. M.; Zhang, X. B.; Shioyama, H.; Kuriyama, N.; Xu, Q. Boron- and Nitrogen-Based Chemical Hydrogen Storage Materials. *International Journal of Hydrogen Energy*. (2009). <https://doi.org/10.1016/j.ijhydene.2009.01.002>.
- (64) Bunsell, A. R. Composite Pressure Vessels Supply an Answer to Transport Problems. *Reinf. Plast.* (2006). [https://doi.org/10.1016/S0034-3617\(06\)70914-6](https://doi.org/10.1016/S0034-3617(06)70914-6).
- (65) Jorgensen, S. W. Hydrogen Storage Tanks for Vehicles: Recent Progress and Current Status. *Curr. Opin. Solid State Mater. Sci.* (2011). <https://doi.org/10.1016/j.cossms.2010.09.004>.

- (66) Carbon Fiber Composite Material Cost Challenges for Compressed Hydrogen Storage Onboard Fuel Cell Electric Vehicles [https://www.energy.gov/sites/prod/files/2017/07/f35/fcto\\_webinarslides\\_carbon\\_fiber\\_composite\\_challenges\\_072517.pdf](https://www.energy.gov/sites/prod/files/2017/07/f35/fcto_webinarslides_carbon_fiber_composite_challenges_072517.pdf) (accessed date: Feb 4, 2020).
- (67) Chapelle, D.; Perreux, D. Optimal Design of a Type 3 Hydrogen Vessel: Part i - Analytic Modelling of the Cylindrical Section. *Int. J. Hydrogen Energy* (2006). <https://doi.org/10.1016/j.ijhydene.2005.06.012>.
- (68) Fowler, C. P.; Orifici, A. C.; Wang, C. H. A Review of Toroidal Composite Pressure Vessel Optimisation and Damage Tolerant Design for High Pressure Gaseous Fuel Storage. *International Journal of Hydrogen Energy*. (2016). <https://doi.org/10.1016/j.ijhydene.2016.10.039>.
- (69) Ghouaoula, A.; Hocine, A.; Chapelle, D.; Karaachira, F.; Boubakar, M. L. Analytical Prediction of Damage in the Composite Part of a Type-3 Hydrogen Storage Vessel. *Mech. Compos. Mater.* (2012). <https://doi.org/10.1007/s11029-012-9253-y>.
- (70) Sorrentino, L.; Anamateros, E.; Bellini, C.; Carrino, L.; Corcione, G.; Leone, A.; Paris, G. Robotic Filament Winding: An Innovative Technology to Manufacture Complex Shape Structural Parts. *Compos. Struct.* (2019). <https://doi.org/10.1016/j.compstruct.2019.04.055>.
- (71) ISO. ISO/TS 15869:2009 Gaseous Hydrogen and Hydrogen Blends \ Land Vehicle Fuel Tanks. (2009).
- (72) Shao, Y.; Betti, A.; Carvelli, V.; Fujii, T.; Okubo, K.; Shibata, O.; Fujita, Y. High Pressure Strength of Carbon Fibre Reinforced Vinylester and Epoxy Vessels. *Compos. Struct.* (2016). <https://doi.org/10.1016/j.compstruct.2015.12.053>.
- (73) Shivamurthy, B.; Prabhuswamy M.S.; Design, Fabrication, and Testing of Epoxy/Glass-Reinforced Pressure Vessel for High-Pressure Gas Storage. *Journal of Reinforced Plastics and Composites* (2010). doi:[10.1177/0731684409351169](https://doi.org/10.1177/0731684409351169).
- (74) Harada, S.; Arai, Y.; Araki, W.; Iijima, T.; Kurosawa, A.; Ohbuchi, T.; Sasaki, N. A Simplified Method for Predicting Burst Pressure of Type III Filament-Wound CFRP Composite Vessels Considering the Inhomogeneity of Fiber Packing. *Compos. Struct.* (2018). <https://doi.org/10.1016/j.compstruct.2018.02.011>.
- (75) Zu, L.; Xu, H.; Wang, H.; Zhang, B.; Zi, B. Design and Analysis of Filament-Wound Composite Pressure Vessels Based on Non-Geodesic Winding. *Compos. Struct.* (2019). <https://doi.org/10.1016/j.compstruct.2018.09.007>.
- (76) Hocine, A.; Chapelle, D.; Boubakar, M. L.; Benamar, A.; Bezazi, A. Experimental and Analytical Investigation of the Cylindrical Part of a Metallic Vessel Reinforced by Filament Winding While Submitted to Internal Pressure. *International Journal of Pressure Vessels and Piping*. (2009). <https://doi.org/10.1016/j.ijpvp.2009.06.002>.
- (77) Cohen, D. Influence of Filament Winding Parameters on Composite Vessel Quality and Strength. *Compos. Part A Appl. Sci. Manuf.* (1997).

[https://doi.org/10.1016/S1359-835X\(97\)00073-0](https://doi.org/10.1016/S1359-835X(97)00073-0).

- (78) Cohen, D.; Mantell, S. C.; Zhao, L. The Effect of Fiber Volume Fraction on Filament Wound Composite Pressure Vessel Strength. *Compos. Part B Engineering* (2001). [https://doi.org/10.1016/S1359-8368\(01\)00009-9](https://doi.org/10.1016/S1359-8368(01)00009-9).
- (79) Nimdum, P.; Patamaprohm, B.; Renard, J.; Villalonga, S. Experimental Method and Numerical Simulation Demonstrate Non-Linear Axial Behaviour in Composite Filament Wound Pressure Vessel Due to Thermal Expansion Effect. *Int. J. Hydrogen Energy* (2015). <https://doi.org/10.1016/j.ijhydene.2015.05.068>.
- (80) Hwang, T. K.; Hong, C. S.; Kim, C. G. Size Effect on the Fiber Strength of Composite Pressure Vessels. *Compos. Struct.* (2003). [https://doi.org/10.1016/S0263-8223\(02\)00250-7](https://doi.org/10.1016/S0263-8223(02)00250-7).
- (81) Hwang, T. K.; Park, J. B.; Kim, H. G. Evaluation of Fiber Material Properties in Filament-Wound Composite Pressure Vessels. *Compos. Part A Appl. Sci. Manuf.* (2012). <https://doi.org/10.1016/j.compositesa.2012.04.005>.
- (82) Wang, D.; Liao, B.; Hua, Z.; Gu, C.; Xu, P. Experimental Analysis on Residual Performance of Used 70 MPa Type IV Composite Pressure Vessels. *J. Fail. Anal. Prev.* (2019). <https://doi.org/10.1007/s11668-019-00581-6>.
- (83) Frias, C.; Faria, H.; Frazão, O.; Vieira, P.; Marques, A. T. Manufacturing and Testing Composite Overwrapped Pressure Vessels with Embedded Sensors. *Mater. Des.* (2010). <https://doi.org/10.1016/j.matdes.2010.03.022>.
- (84) Perillo, G.; Grytten, F.; Sørboe, S.; Delhaye, V. Numerical/Experimental Impact Events on Filament Wound Composite Pressure Vessel. *Compos. Part B Eng.* (2015). <https://doi.org/10.1016/j.compositesb.2014.10.030>.
- (85) Zu, L.; Xu, H.; Zhang, Q.; Jia, X.; Zhang, B.; Li, D. Design of Filament-Wound Spherical Pressure Vessels Based on Non-Geodesic Trajectories. *Compos. Struct.* (2019). <https://doi.org/10.1016/j.compstruct.2019.03.045>.
- (86) Zu, L.; Xu, H.; Jia, X.; Zhang, Q.; Wang, H.; Zhang, B. Winding Path Design Based on Mandrel Profile Updates of Composite Pressure Vessels. *Compos. Struct.* (2020). <https://doi.org/10.1016/j.compstruct.2019.111766>.
- (87) Zheng, C. X.; Wang, L.; Li, R.; Wei, Z. X.; Zhou, W. W. Fatigue Test of Carbon Epoxy Composite High Pressure Hydrogen Storage Vessel under Hydrogen Environment. *J. Zhejiang Univ. Sci. A* (2013). <https://doi.org/10.1631/jzus.A1200297>.
- (88) Bai, H.; Yang, B.; Hui, H.; Yang, Y.; Yu, Q.; Zhou, Z.; Xian, P. Experimental and Numerical Investigation of the Strain Response of the Filament Wound Pressure Vessels Subjected to Pressurization Test. *Polym. Compos.* (2019). <https://doi.org/10.1002/pc.25304>.
- (89) Venkateshwar Reddy, C.; Ramesh Babu, P.; Ramnarayanan, R.; Das, D. Mechanical Characterization of Unidirectional Carbon and Glass/Epoxy Reinforced Composites for High Strength Applications. In *Materials Today*:

*Proceedings*; (2017). <https://doi.org/10.1016/j.matpr.2017.02.201>.

- (90) Almeida Júnior, J. H. S.; Staudigel, C.; Caetano, G. L. P.; Amico, S. C. Engineering Properties of Carbon/Epoxy Filament Wound Unidirectional Composites. In *16th European Conference on Composite Materials, ECCM 2014*;(2014).
- (91) Hamed, A. F.; Hamdan, M. M.; Sahari, B. B.; Sapuan, S. M. Experimental Characterization of Filament Wound Glass/Epoxy and Carbon/Epoxy Composite Materials. *J. Eng. Appl. Sci.* (2008).
- (92) Chen, W.; Yu, Y.; Li, P.; Wang, C.; Zhou, T.; Yang, X. Effect of New Epoxy Matrix for T800 Carbon Fiber/Epoxy Filament Wound Composites. *Compos. Sci. Technol.* (2007). <https://doi.org/10.1016/j.compscitech.2007.01.026>.
- (93) Roh, H. S.; Hua, T. Q.; Ahluwalia, R. K. Optimization of Carbon Fiber Usage in Type 4 Hydrogen Storage Tanks for Fuel Cell Automobiles. *International Journal of Hydrogen Energy*; (2013). <https://doi.org/10.1016/j.ijhydene.2013.07.016>.
- (94) Musthak, M.; Madar Valli, P.; Rao, S. N. Prediction of Transverse Directional Strains and Stresses of Filament Wound Composite Pressure Vessel by Using Higher Order Shear Deformation Theories. *Int. J. Compos. Mater.* (2016). <https://doi.org/10.5923/j.cmaterials.20160603.03>.
- (95) Hua, T. Q.; Roh, H. S.; Ahluwalia, R. K. Performance Assessment of 700-Bar Compressed Hydrogen Storage for Light Duty Fuel Cell Vehicles. *Int. J. Hydrogen Energy* (2017). <https://doi.org/10.1016/j.ijhydene.2017.08.123>.
- (96) Kumar, S. S.; Kumari, A. S. Design and Failure Analysis of Geodesic Dome of a Composite Pressure Vessel. *Int. J. Eng. Technol.* (2012).
- (97) Madhavi, M.; Venkat, R. Predicting Structural Behavior of Filament Wound Composite Pressure Vessel Using Three Dimensional Shell Analysis. *J. Inst. Eng. Ser. C* (2014). <https://doi.org/10.1007/s40032-014-0094-4>.
- (98) ASTM International. ASTM E8/E8M-16a - Standard Test Methods for Tension Testing of Metallic Materials. (2016). [https://doi.org/10.1520/E0008\\_E0008M-16A](https://doi.org/10.1520/E0008_E0008M-16A).
- (99) Materials SA. CADWIND V9 User Manual. Material SA: Brussels.

## APPENDIX A

### PRODUCED G-CODES FOR FILAMENT WINDING

#### Helical Layer G-Codes for Steel Liner Based Composite Tanks

```
;increment the line numbers (the block numbers after 'N') by 2
;Created by CADWIND
;15.12.2017 10:48:27
;File name: C:\Users\workstation\Desktop\15_12_deneme2

;goto pattern start point

;G01=linear interpolation
;G90=absolute positioning
;X0=position cross-carriage first in zero position to avoid
collision
;F60=60mm/min
G01 G90 Y0 F10000

;go to the program start point
X677.447 B82.203 F10000

;last position cross-carriage to avoid collision
Y-148.000

;Pause and wait for fibre attachment
M0

;switch to G91=relative positioning. G64 for smooth movement
G91 G64 F50000

;load Variable #60 with the number of cycles
#60=372

;mark this point of the program with a label
N1

;program data
;all the positions of the first cycle
A12.0000 X77.4897 ;F30357.59
A4.2995 X27.7636 ;F15178.79
A3.6069 Y-6.6170 B-0.5336 ;F8563.28
A2.4101 Y-4.7754 B-0.4324 ;F16856.85
A2.0283 Y-4.3810 B-0.4378 ;F16597.41
A2.8472 Y-7.3221 B-0.8373 ;F16185.30
A3.2339 Y-10.9172 B-1.7014 ;F15817.94
A4.7832 Y-11.6465 B-2.6999 ;F16584.44
A21.0826 Y-28.3514 B-10.2642 ;F11072.27
A83.3274 Y-5.1968 B-3.7588 ;F16599.69
A26.1615 Y17.0596 B10.9756 ;F7276.97
```

A8.8841 Y18.6268 B4.9016 ;F12810.83  
A5.0906 Y43.5210 B2.9135 ;F7567.81  
A2.7775 X-4.9604 B1.0566 ;F14775.99  
A1.1634 X-14.6295 B-1.1722 ;F27851.29  
A1.1799 X-12.5113 B-1.5513 ;F30361.85  
A0.7919 X-9.0701 B-1.9991 ;F30831.48  
A0.5786 X-7.1424 B-2.6661 ;F30972.05  
A0.5313 X-6.1237 B-3.8093 ;F20502.29  
A0.4884 X-5.4762 B-6.1663 ;F14469.45  
A0.3174 X-5.1974 B-12.0188 ;F11770.00  
A0.0083 X-10.9216 B-78.5648 ;F8177.89  
A0.4589 X-56.5140 B-58.5678 ;F3752.08  
A0.9389 X-10.0474 B0.2404 ;F17687.08  
A2.2227 X-31.3365 B-0.1347 ;F30075.62  
A7.2174 X-93.3533 B0.2260 ;F30089.62  
A12.9308 X-153.9942 B0.2381 ;F30105.63  
A22.6393 X-220.9155 B0.2233 ;F30157.13  
A5.9999 X-47.8112 B0.0598 ;F30235.27  
A6.0001 X-47.3082 B0.0605 ;F30240.34  
A1.0003 X-7.8871 B0.0101 ;F15304.69  
A8.1690 Y-12.7472 B1.0200 ;F8927.25  
A2.2071 Y-3.9703 B0.3891 ;F12918.54  
A81.7415 Y-32.4600 B6.9948 ;F10192.74  
A23.0368 Y49.1776 B-2.9615 ;F4147.21  
A11.8642 X0.9084 B-2.2009 ;F12212.90  
A3.2201 X43.6519 B1.0376 ;F15964.55  
A2.0688 X31.8615 B1.1866 ;F30083.85  
A1.3508 X23.7929 B1.3126 ;F30093.74  
A0.3707 X5.4127 B0.3387 ;F30129.24  
A1.3491 X16.9325 B1.2136 ;F30171.85  
A0.9268 X13.2982 B1.3179 ;F30219.17  
A0.6426 X10.5771 B1.3950 ;F30314.33  
A0.4490 X8.5105 B1.4476 ;F30471.71  
A0.6863 X10.1283 B2.1255 ;F30720.85  
A0.3336 X5.3261 B1.4552 ;F31156.43  
A0.5558 X7.4961 B2.5140 ;F31720.29  
A0.5688 X6.5766 B2.9116 ;F26762.11  
A0.5616 X5.8251 B3.4136 ;F21434.27  
A0.7867 X7.0887 B5.7747 ;F17162.88  
A0.6193 X5.0764 B5.7288 ;F14477.27  
A1.0226 X7.3582 B12.0810 ;F12678.54  
A0.5132 X1.9077 B4.5871 ;F11759.04  
A0.9180 X0.1286 B0.4190 ;F13307.01  
A5.0819 X4.2825 B11.6749 ;F12427.11  
A5.0713 X4.3205 B13.5745 ;F12030.62  
A5.0579 X4.3713 B14.2121 ;F11935.15  
A5.0412 X4.4346 B13.2109 ;F12114.77  
A5.0213 X4.5114 B11.1447 ;F12626.59  
A0.9502 X7.7071 B14.4935 ;F12252.54  
A0.2043 X23.0285 B21.7499 ;F15729.18  
A0.4740 X8.0658 B3.6882 ;F26007.64  
A0.3567 X5.3187 B1.8253 ;F31781.40  
A0.5484 X10.2506 B2.7126 ;F31074.34  
A0.4301 X6.6876 B1.2020 ;F30541.41  
A0.5979 X8.3223 B1.0644 ;F30321.43  
A0.8534 X10.7886 B0.9036 ;F30198.30

```

A1.2672 X14.7808 B0.7264 ;F30146.16
A38.7267 X311.2190 B0.7255 ;F30231.46

;jump to the begin of the first cycle until all cycles are done
;decrease Variable #60 by 1 and jump to N1 if greater then zero
#60=#60-1
IF[#60>0]GOTO1

N2 ; M30program end

;increment the line numbers (the block numbers after 'N') by 2
;Created by CADWIND
;19.12.2017 10:29:12
;File name: C:\Users\workstation\Desktop\combination

;goto pattern start point

;G01=linear interpolation
;G90=absolute positioning
;X0=position cross-carriage first in zero position to avoid
collision
;F60=60mm/min
G01 G90 Y0 F10000

;go to the program start point
X694.590 B82.203 F10000

;last position cross-carriage to avoid collision
Y-148.000

;Pause and wait for fibre attachment
;M0

;switch to G91=relative positioning. G64 for smooth movement
G91 G64 F50000

;load Variable #60 with the number of cycles
#70=1

;mark this point of the program with a label
N3

;program data
;all the positions of the first cycle
A11.9999 X60.2904 B-0.3357 ;F30588.91
A5.5975 X27.8201 B-0.1583 ;F15300.85
A3.7817 Y-4.3946 B-0.5681 ;F9941.99
A3.2109 Y-4.0737 B-0.5758 ;F19216.58
A2.8969 Y-3.9115 B-0.6128 ;F18813.11
A2.5489 Y-3.6998 B-0.6452 ;F18402.14
A3.9340 Y-6.5194 B-1.3480 ;F17791.82
A5.2951 Y-9.9640 B-2.7516 ;F17484.37
A7.7670 Y-9.7805 B-3.9965 ;F15083.41
A30.3845 Y-14.0605 B-11.3842 ;F9431.38
A47.0450 Y9.4653 B-2.6905 ;F19041.77
A14.9938 Y17.5848 B2.7133 ;F14885.86

```

A7.9485 Y19.4092 B2.0267 ;F16284.59  
A2.4455 Y9.9446 B0.7020 ;F7741.56  
A1.5874 X-13.9651 B-3.7191 ;F10554.96  
A0.7770 X-12.7777 B-4.9810 ;F22337.52  
A0.7801 X-13.9509 B-7.7579 ;F22248.84  
A0.4614 X-8.0791 B-6.2153 ;F17730.48  
A0.3370 X-5.9312 B-5.6851 ;F15620.69  
A0.3600 X-7.0177 B-8.3878 ;F14089.09  
A0.2371 X-6.1490 B-8.9523 ;F13105.32  
A1.5313 X-5.1868 B-8.8352 ;F12662.62  
A1.5109 X-5.0497 B-9.5608 ;F12332.50  
A1.4122 X-4.7775 B-9.4200 ;F12217.31  
A1.8185 X-6.2949 B-12.0708 ;F12288.58  
A1.4082 X-4.6075 B-7.7723 ;F12706.59  
A1.5613 X-5.3391 B-7.7969 ;F13266.94  
A1.8837 X-6.0300 B-6.9480 ;F14596.83  
A2.1963 X-6.6828 B-5.6550 ;F17237.31  
A2.4690 X-7.2851 B-4.3116 ;F22087.94  
A2.6772 X-7.8210 B-3.1524 ;F30310.28  
A3.5625 X-10.4201 B-2.6773 ;F32628.49  
A6.8460 X-17.0576 B-1.4510 ;F32426.59  
A2.3083 X-5.4340 B-0.1652 ;F32607.17  
A12.3763 X-26.4704 B-0.1527 ;F33117.58  
A7.1451 X-11.9324 B0.6243 ;F35002.43  
A5.4746 X-8.1808 B0.4801 ;F36140.84  
A5.4293 X-7.3581 B0.4629 ;F37330.41  
A6.0000 X-7.1873 B0.6426 ;F39171.54  
A6.0000 X-6.9715 B0.6588 ;F39682.18  
A6.0000 X-6.7636 B0.6742 ;F40214.64  
A6.0000 X-6.5542 B0.6913 ;F40794.77  
A6.0000 X-6.3484 B0.7086 ;F41413.91  
A6.0000 X-6.1461 B0.7262 ;F42074.22  
A6.0001 X-5.9467 B0.7442 ;F42782.47  
A5.9988 X-5.7526 B0.7613 ;F43524.87  
A6.0011 X-5.5512 B0.7836 ;F44381.54  
A6.0001 X-5.3623 B0.8017 ;F45243.02  
A5.9999 X-5.1726 B0.8217 ;F46191.32  
A6.0000 X-4.9848 B0.8424 ;F47219.51  
A6.0000 X-4.7996 B0.8635 ;F48328.31  
A6.0000 X-4.6162 B0.8852 ;F49532.88  
A5.9999 X-4.4348 B0.9075 ;F50842.99  
A6.0001 X-4.2558 B0.9302 ;F52268.33  
A6.0000 X-4.0782 B0.9535 ;F53825.60  
A5.9987 X-3.9060 B0.9750 ;F55486.56  
A6.0013 X-3.7251 B1.0039 ;F57457.19  
A6.0000 X-3.5564 B1.0263 ;F59469.93  
A6.0002 X-3.3861 B1.0514 ;F61748.71  
A5.9998 X-3.2157 B1.0776 ;F62030.75  
A6.0000 X-3.0483 B1.1035 ;F61378.23  
A6.0000 X-2.8818 B1.1301 ;F60762.96  
A6.0000 X-2.7165 B1.1570 ;F60184.53  
A6.0000 X-2.5526 B1.1841 ;F59643.79  
A6.0001 X-2.3895 B1.2117 ;F58567.35  
A5.9999 X-2.2275 B1.2394 ;F56806.30  
A6.0000 X-2.0668 B1.2671 ;F55156.29  
A6.0000 X-1.9067 B1.2950 ;F53603.28

```

A6.0000 X-1.7475 B1.3230 ;F52145.62
A6.0000 X-1.5890 B1.3508 ;F50785.24
A6.0000 X-1.4315 B1.3782 ;F49529.94
A6.0000 X-1.2742 B1.4057 ;F48346.56
A6.0000 X-1.1177 B1.4325 ;F47263.87
A6.0001 X-0.9617 B1.4589 ;F46263.57
A6.0000 X-0.8062 B1.4845 ;F45348.79
A6.0000 X-0.6509 B1.5093 ;F44514.60
A6.0000 X-0.4957 B1.5336 ;F43752.18
A6.0000 X-0.3411 B1.5564 ;F43077.08
A6.0000 X-0.1865 B1.5781 ;F42477.07
A6.0000 X-0.0318 B1.5987 ;F41948.26
A6.0000 X0.1225 B1.6174 ;F41502.68
A6.0000 X0.2773 B1.6350 ;F41119.26
A6.0000 X0.4318 B1.6504 ;F40818.56
A6.0000 X0.5868 B1.6643 ;F40584.40
A6.0000 X0.7419 B1.6761 ;F40424.88
A6.0000 X0.8974 B1.6859 ;F40336.05
A6.0000 X1.0532 B1.6936 ;F40320.65
A6.0000 X1.2095 B1.6991 ;F40377.14
A6.0000 X1.3665 B1.7024 ;F40503.80
A6.0000 X1.5238 B1.7033 ;F40709.99
A6.0000 X1.6820 B1.7022 ;F40985.54
A6.0000 X1.8408 B1.6987 ;F40084.39
A6.0000 X2.0006 B1.6930 ;F28579.79
A6.0000 X1.5588 B1.0526 ;F16129.07
A6.0000 X0.6588 B-0.0002 ;F26347.67
A6.0000 X0.6589 ;F37212.83
A6.0000 X0.6589 ;F48078.04
A437.9999 X48.0995 ;F54324.67
A318.0000 X34.9217 ;F54324.69
A821.9999 X90.2691 B0.0002 ;F54324.68
A492.0000 X54.0294 B-0.0003 ;F54324.68
A6.0000 X0.6591 B0.0003 ;F54324.94
A6.3723 X0.4037 B-0.3073 ;F54169.35
A6.0366 X0.6333 B0.0044 ;F54297.72
A6.0366 X0.6326 B0.0041 ;F54297.06
A12.0730 X1.2645 B0.0089 ;F54295.62
A6.0364 X0.6317 B0.0044 ;F49440.00
A6.0364 X0.6313 B0.0044 ;F38580.16
A6.0363 X0.6305 B0.0041 ;F27720.95
A6.0364 X0.6304 B0.0044 ;F16862.44

;jump to the begin of the first cycle until all cycles are done
;decrease Variable #60 by 1 and jump to N1 if greater then zero
#70=#70-1
IF[#70>0]GOTO3

```

N4 ;M30 program end

```

;increment the line numbers (the block numbers after 'N') by 2
;Created by CADWIND
;18.12.2017 16:02:51
;File name: C:\Users\workstation\Desktop\celikhoopdeneme6

```

```

;goto pattern start point

;G01=linear interpolation
;G90=absolute positioning
;X0=position cross-carriage first in zero position to avoid
collison
;F60=60mm/min
G01 G90 F10000 ;Y0

;go to the program start point
X693.000 B0.000 F10000

;last position cross-carriage to avoid collision
Y-148.049

;Pause and wait for fibre attachment
;M0

;switch to G91=relative positioning. G64 for smooth movement
G91 G64 F50000

;load Variable #60 with the number of cycles
#80=4

;mark this point of the program with a label
N5

;program data
;all the positions of the first cycle
A30.0000 B0.4307 ;F54005.55
A37080.0000 X-356.0000 ;F54002.41
A60.0000 B-0.8613 ;F54006.39
A37080.0000 X356.0000 ;F54002.40
A30.0000 B0.4307 ;F54006.40

;jump to the begin of the first cycle until all cycles are done
;decrease Variable #60 by 1 and jump to N1 if greater then zero
#80=#80-1
IF[#80>0]GOTO5

N6 M30 ;program end

```

### **Helical Layer G-Codes for Aluminum Liner Based Composite Tanks**

```

;increment the line numbers (the block numbers after 'N') by 2
;Created by CADWIND
;3.07.2018 09:46:28
;File name:
C:\Users\workstation\Desktop\al_liner_helical14_row9.cnc

;goto pattern start point

;G01=linear interpolation

```

```

;G90=absolute positioning
;X0=position cross-carriage first in zero position to avoid
collison
;F60=60mm/min
G01 G90 Y0 F10000

;go to the program start point
X374.760 B80.817 F10000

;last position cross-carriage to avoid collision
Y-134.000

;Pause and wait for fibre attachment
M0

;switch to G91=relative positioning. G64 for smooth movement
G91 G64 F50000

;load Variable #60 with the number of cycles
#60=49

;mark this point of the program with a label
N1

;program data
;all the positions of the first cycle
A3.1738 X45.9840 B1.9809 ;F30099.13
A4.9569 X45.7457 B0.0244 ;F30175.61
A8.4327 X72.1147 B-0.1529 ;F30204.48
A17.4732 X126.9395 B-0.3298 ;F30282.98
A13.7172 X74.3290 B-0.2427 ;F30506.75
A4.5000 X20.1228 B-0.0632 ;F23055.82
A3.1316 X14.0039 B-0.0440 ;F7685.28
A-4.0588 B0.4282 ;F5428.77
A13.9674 Y-12.5481 B-1.5787 ;F7284.74
A2.7357 Y-3.6799 B-0.3916 ;F15446.40
A2.4487 Y-3.8607 B-0.3898 ;F17827.09
A2.1849 Y-3.8854 B-0.3897 ;F17274.70
A3.7905 Y-7.2351 B-0.8124 ;F17017.44
A2.9381 Y-6.3679 B-0.8270 ;F16634.16
A2.0297 Y-5.2883 B-0.7845 ;F16220.25
A16.6672 Y-32.9379 B-8.3176 ;F9505.49
A96.3731 Y-6.2482 B-3.9293 ;F11973.37
A24.9089 Y82.0515 B11.4192 ;F3953.59
A5.4480 X-6.3328 B2.3584 ;F9937.48
A1.3869 X-18.2116 B-1.5493 ;F22394.64
A1.1027 X-13.1797 B-1.6443 ;F30336.63
A0.6908 X-8.8133 B-1.6446 ;F30608.10
A0.5078 X-6.8566 B-1.7910 ;F31085.86
A0.3923 X-5.5626 B-1.9694 ;F31895.29
A0.3578 X-5.2709 B-2.5256 ;F25040.47
A0.5154 X-7.3089 B-5.2282 ;F18593.58
A0.4144 X-6.1807 B-7.5103 ;F13999.71
A0.3267 X-5.0045 B-10.3125 ;F12009.43
A0.2962 X-5.0730 B-17.9099 ;F11226.29
A0.0702 X-56.8941 B-109.3814 ;F6801.50

```

```

A1.6712 X-21.5037 B-0.7517 ;F18204.38
A9.1227 X-96.2876 B-0.0444 ;F30134.32
A4.0797 X-301.5800 B0.7354 ;F30263.86
A4.5001 X-21.9815 B0.0579 ;F30622.42
A4.5001 X-21.8071 B0.0583 ;F22974.21
A1.1661 X-5.6513 B0.0151 ;F7658.04
A-2.6846 B-0.2676 ;F5425.04
A13.7945 Y-14.1855 B1.4860 ;F7767.56
A2.6734 Y-3.6492 B0.3701 ;F9168.07
A-2.6734 B-0.3701 ;F5451.51
A7.5620 Y-7.0292 B1.1672 ;F7419.62
A4.1869 Y-6.5572 B0.659 ;F14945.88
A3.3773 Y-5.9165 B0.9129 ;F17426.30
A6.3160 Y-11.3987 B2.0903 ;F17368.03
A2.4309 Y-16.5854 B3.6830 ;F14279.39
A21.3906 Y-12.1895 B4.4320 ;F7695.87
A31.7375 Y8.3029 B1.5006 ;F14832.15
A28.9042 B-4.0110 ;F17060.21
A19.7982 Y24.3490 B-5.5030 ;F9813.86
A9.8251 Y44.8594 B-3.3440 ;F7698.11
A2.1124 X22.7214 B1.0753 ;F15081.40
A0.5708 X28.3825 B3.3047 ;F30208.66
A0.5171 X25.7856 B5.6570 ;F21130.31
A0.0248 X20.9616 B10.0429 ;F6248.88
A1.8788 X-16.7915 B-3.0744 ;F7670.72
A3.1685 X4.8760 B3.4950 ;F5241.29
A3.1816 X4.8265 B4.4360 ;F13305.31
A3.1908 X4.7893 B5.7239 ;F15314.97
A3.1963 X4.7646 B7.4742 ;F13615.05
A3.1976 X4.7512 B9.7476 ;F12526.07
A3.1952 X4.7493 B12.3519 ;F11903.34
A3.1892 X4.7586 B14.5429 ;F11607.62
A3.1792 X4.7783 B15.1859 ;F11545.63
A3.1657 X4.8093 B13.8585 ;F11694.99
A3.1480 X4.8507 B11.3896 ;F12112.28
A3.1266 X4.9026 B8.8547 ;F12920.37
A3.1010 X4.9649 B6.7708 ;F14276.55
A3.0711 X5.0377 B5.2033 ;F16328.35
A3.0366 X5.1205 B4.0556 ;F19182.24
A2.9977 X5.2141 B3.2157 ;F22905.08
A2.9535 X5.3170 B2.5928 ;F27541.13
A2.9043 X5.4299 B2.1236 ;F33126.48
A1.9662 X7.5647 B2.4862 ;F29670.22
A2.1420 X5.7577 B1.4254 ;F15898.58
A-3.8347 X35.9375 B8.4865 ;F29276.05

```

```

;jump to the begin of the first cycle until all cycles are done
;decrease Variable #60 by 1 and jump to N1 if greater then zero
#60=#60-1
IF[#60>0]GOTO1

```

```
N2 M30 ;program end
```

## G-Codes for Composite Plate Manufacturing

```
;increment the line numbers (the block numbers after 'N') by 2
;Created by CADWIND
;15.05.2018 09:46:47
;File name: C:\Users\workstation\Desktop\plaka_deneme_v2.PPR

;goto pattern start point

;G01=linear interpolation
;G90=absolute positioning
;X0=position cross-carriage first in zero position to avoid
collison
;F60=60mm/min
G01 G90 Y0 F10000

;go to the program start point
X149.358 B0.127 F10000

;last position cross-carriage to avoid collision
Y-22.500

;Pause and wait for fibre attachment
M0

;switch to G91=relative positioning. G64 for smooth movement
G91 G64 F50000

;load Variable #60 with the number of cycles
#60=1

;mark this point of the program with a label
N1

;program data
;all the positions of the first cycle
A603.0000 X3.3488 ;F54000.86
A369.0001 X2.0492 ;F54000.87
A603.0000 X3.3488 ;F54000.88
A369.0000 X2.0493 ;F54000.87
A962.9999 X5.3480 ;F54000.89
A387.0000 X2.1492 ;F54000.88
A369.0000 X2.0492 ;F54000.67
A603.0000 X3.3487 ;F53999.60
A3582.0000 X19.8923 ;F53999.60
A3789.0000 X21.0419 ;F53999.60
A549.0000 X3.0488 ;F53999.60
A963.0000 X5.3479 ;F53999.60
A1467.0000 X8.1468 ;F53999.60
A531.0000 X2.9489 ;F53999.60
A441.0000 X2.4492 ;F53999.60
A99.0000 X0.5498 ;F53999.60
A873.0000 X4.8485 ;F53999.60
A963.0000 X5.3484 ;F53999.60
```

A666.0000 X3.6989 ;F53999.60  
A657.0000 X3.6488 ;F53999.60  
A63.0000 X0.3498 ;F53999.60  
A801.0000 X4.4488 ;F53999.60  
A927.0000 X5.1485 ;F53999.60  
A657.0000 X3.6489 ;F53999.60  
A198.0000 X1.0995 ;F53999.60  
A117.0000 X0.6499 ;F53999.60  
A477.0000 X2.6492 ;F53999.60  
A99.0000 X0.5498 ;F53999.60  
A387.0000 X2.1493 ;F53999.60  
A207.0000 X1.1496 ;F53999.60  
A1494.0000 X8.2973 ;F53999.60  
A261.0000 X1.4495 ;F53999.60  
A441.0000 X2.4492 ;F53999.60  
A657.0000 X3.6488 ;F53999.60  
A1143.0000 X6.3480 ;F53999.60  
A603.0000 X3.3491 ;F53999.60  
A927.0000 X5.1485 ;F53999.60  
A1314.0000 X7.2978 ;F54006.02  
A279.0000 X1.5495 ;F54009.90  
A639.0000 X3.5490 ;F54009.90  
A531.0000 X2.9491 ;F54009.90  
A261.0000 X1.4496 ;F54009.90  
A1017.0000 X5.6482 ;F54009.90  
A441.0000 X2.4492 ;F54009.90  
A171.0000 X0.9497 ;F54009.90  
A99.0000 X0.5498 ;F54009.90  
A387.0000 X2.1493 ;F54009.90  
A171.0000 X0.9497 ;F54009.90  
A2565.0000 X14.2457 ;F54009.90  
A153.0000 X0.8497 ;F54009.90  
A306.0000 X1.6994 ;F54009.90  
A261.0000 X1.4496 ;F54009.90  
A711.0000 X3.9488 ;F54009.90  
A171.0000 X0.9497 ;F54009.90  
A207.0000 X1.1496 ;F54009.90  
A18864.0000 X104.7741 ;F54009.90  
A9.0000 X0.0500 ;F54009.91  
A9.0000 X-0.5053 B-0.2556 ;F54115.82  
A18756.0000 X-104.1745 ;F53990.11  
A279.0000 X-1.5495 ;F53989.30  
A333.0000 X-1.8495 ;F53989.30  
A117.0000 X-0.6498 ;F53989.30  
A1413.0000 X-7.8477 ;F53989.30  
A333.0000 X-1.8494 ;F53989.30  
A63.0000 X-0.3499 ;F53989.30  
A153.0000 X-0.8497 ;F53989.30  
A531.0000 X-2.9490 ;F53989.30  
A333.0000 X-1.8494 ;F53989.30  
A117.0000 X-0.6497 ;F53989.30  
A153.0000 X-0.8497 ;F53989.30  
A261.0000 X-1.4495 ;F53989.30  
A153.0000 X-0.8498 ;F53989.30  
A63.0000 X-0.3499 ;F53989.30  
A1467.0000 X-8.1477 ;F53989.30

```

A261.0000 X-1.4496 ;F53989.30
A2655.0000 X-14.7458 ;F53989.30
A441.0000 X-2.4492 ;F53989.30
A261.0000 X-1.4496 ;F53989.30
A117.0000 X-0.6498 ;F53989.30
A639.0000 X-3.5490 ;F53989.30
A306.0000 X-1.6994 ;F53989.30
A477.0000 X-2.6492 ;F53989.30
A369.0000 X-2.0494 ;F53989.30
A117.0000 X-0.6498 ;F53989.30
A603.0000 X-3.3490 ;F53989.30
A63.0000 X-0.3499 ;F53989.29
A711.0000 X-3.9489 ;F53989.30
A531.0000 X-2.9492 ;F53989.30
A441.0000 X-2.4494 ;F53989.30
A261.0000 X-1.4496 ;F53989.30
A117.0000 X-0.6498 ;F53989.30
A621.0000 X-3.4491 ;F53989.30
A279.0000 X-1.5495 ;F53989.30
A261.0000 X-1.4496 ;F53989.30
A153.0000 X-0.8497 ;F53989.30
A774.0000 X-4.2987 ;F53989.30
A522.0000 X-2.8991 ;F53989.30
A711.0000 X-3.9487 ;F53989.30
A558.0000 X-3.0990 ;F53989.30
A117.0000 X-0.6498 ;F53989.30
A63.0000 X-0.3499 ;F53989.30
A153.0000 X-0.8497 ;F53989.30
A261.0000 X-1.4496 ;F53989.30
A99.0000 X-0.5498 ;F53989.30
A1251.0000 X-6.9478 ;F53989.30
A531.0000 X-2.9492 ;F53989.30
A261.0000 X-1.4495 ;F53989.30
A153.0000 X-0.8498 ;F53989.30
A747.0000 X-4.1488 ;F53989.30
A261.0000 X-1.4496 ;F53989.30
A369.0000 X-2.0494 ;F53989.30
A63.0000 X-0.3499 ;F53989.29
A4122.0000 X-22.8915 ;F53989.30
A981.0000 X-5.4479 ;F53989.30
A333.0000 X-1.8493 ;F53989.30
A2763.0000 X-15.3441 ;F53989.30
A261.0000 X-1.4494 ;F53989.30
A1314.0000 X-7.2973 ;F53989.30
A153.0000 X-0.8497 ;F53989.30
A2502.0000 X-13.8949 ;F53989.30
A279.0000 X-1.5495 ;F53989.30
A3042.0000 X-16.8939 ;F53989.30
A9.0000 X-0.0500 ;F53989.28

```

```

;jump to the begin of the first cycle until all cycles are done
;decrease Variable #60 by 1 and jump to N1 if greater then zero
#60=#60-1
IF[#60>0]GOTO1

```

```
N2 M30 ;program end
```

# VITA

Osman KARTAV

03.06.1989, Denizli/Turkey

## **EDUCATION**

- **Ph.D.** in English, 2020, Mechanical Engineering, İzmir Institute of Technology.
- **M.Sc.** in English, 2014, Mechanical Engineering, İzmir Institute of Technology.
- **B.Sc.** in English, 2007, Mechanical Engineering, İzmir Institute of Technology.

## **PUBLICATIONS**

### **Journal Articles**

S. Kangal, **O. Kartav**, M. Tanoğlu, H. Seçil Artem, E. Aktaş, Investigation of interlayer hybridization effect on burst pressure performance of composite overwrapped pressure vessels with load-sharing metallic liner, Journal of Composite Materials, First Published August 27, 2019 (doi: [10.1177/0021998319870588](https://doi.org/10.1177/0021998319870588))

A.Yılmaz, **O. Kartav**, K. Yüksel, Design and analysis of a novel fiber optic sensing system for process monitoring of composite materials, 25th Signal Processing and Communications Applications Conference (SIU), May 17

### **Selected Conference Papers**

**O. Kartav**, S. Kangal, M. Tanoğlu, H. Seçil Artem, E. Aktaş, Development and Modeling of Type-III Composite Overwrapped Pressure Vessels for Hydrogen Storage, International porous and powder materials symposium and exhibition, PPM2019, October 2019

**O. Kartav**, S. Kangal, M. Tanoğlu, H. Seçil Artem, E. Aktaş, Investigation Of Hybrid Ply Effect On Burst Pressure Performance Of Composite Overwrapped Pressure Vessels, 4. International Ege Composite Materials Symposium 2018, September 2018

S. Kangal, **O. Kartav**, M. Tanoğlu, Development of Composite High Pressure Vessels for Hydrogen Storage, 9<sup>th</sup> International Automotive Technologies Congress (OTEKON 2018), May 2018, Bursa, Turkey

**O. Kartav**, Z. Ay, M. Tanoğlu, Tensile And Impact Behaviours Of Short Glass/Carbon Fiber Reinforced Hybrid Polyamide Composites, 5 th International Polymeric Composites, November 2017